MODULATION OF ADENO-ASSOCIATED VIRUS TRANSDUCTION BY THE PROMYELOCYTIC LEUKEMIA PROTEIN, ARSENIC TRIOXIDE, AND PROTEASOME INHIBITORS

Angela Marie Mitchell

A dissertation submitted to the faculty at the University of North Carolina at Chapel Hill in partial fulfillment of the requirements for the degree of Doctor of Philosophy in the Department of Microbiology and Immunology in the School of Medicine.

Chapel Hill
2013

Approved by:

R. Jude Samulski

Mark T. Heise

Aravind Asokan

Tal Kafri

Lishan Su

ABSTRACT

Angela Marie Mitchell: Modulation of adeno-associated virus transduction by the promyelocytic leukemia protein, arsenic trioxide, and proteasome inhibitors
(Under the direction of R. Jude Samulski)

Adeno-associated virus (AAV) has been developed as a gene therapy vector and has been utilized in over 100 clinical trials, which demonstrate increasing efficacy. However, the efficacy of systemic applications is often hampered by low transgene expression at lower doses or loss of transgene expression over time at higher doses. Therefore, mechanisms are needed to increase rAAV transduction efficiency without increasing viral dose.

The promyelocytic leukemic protein (PML) is a known cell-intrinsic antiviral factor, which has not been examined in the context of rAAV. Using PML knockout mice, we determined that PML inhibits rAAV transduction up to 50-fold in a serotype-independent manner and at several doses. Mechanistically, this transduction inhibition occurred at the level of second-strand DNA synthesis and not at earlier transduction steps. We further demonstrated human PML inhibited rAAV transduction, mostly through the actions of PML isoform II. This effect was extended to rAAV and wild type AAV production and replication. These data demonstrate PML inhibits rAAV transduction and suggest that PML may be an important target for efforts to enhance rAAV transduction.

Moreover, various cell stressors enhance rAAV transduction through diverse mechanisms. We examined the effect of arsenic trioxide (As_2O_3), a chemotherapeutic agent approved for use in humans, on rAAV transduction. As_2O_3 treatment caused a dose dependent

increase in rAAV transduction *in vitro*, in cell lines from several cell type and species origins. This transduction increase was due to reaction oxygen species dependent stabilization of rAAV virions at the perinuclear region. As_2O_3 increased transduction *in vivo* with several rAAV serotypes. Therefore, As_2O_3 treatment and the dependent mechanisms are promising avenues to enhancing rAAV transduction.

Finally, we investigated whether proteasome inhibition was sufficient to enhance rAAV transduction, as previous work demonstrating proteasome inhibitors enhance rAAV transduction was conducted with non-specific proteasome inhibitors. Using carfilzomib, we determined that proteasome inhibition was sufficient to enhance rAAV transduction and that this was the mechanism through which other proteasome inhibitors act. In addition, we determined that the proteasome inhibitors caused increased efficiency in a late step in rAAV transduction. These data further elucidate the mechanism by which proteasome inhibitors enhance rAAV transduction.

To my family for their support

ACKNOWLEDGEMENTS

First, I would like to thank my mentor, Jude Samulski, for his help and support during my graduate career. His help in training me to be an independent scientist has been invaluable. I would also like to thank my committee members, Mark Heise, Aravind Asokan, Tal Kafri, and Lishan Su, for their time and help throughout my time at UNC. They have been very open and available for questions and I greatly value their support. In addition, I would like to thank all of the current and former members of the Samulski lab for their suggestions, support, and friendship. In particular, I would like to thank Karen Hogan, without whom the lab could not run. I would also like to thank Chengwen Li who is always willing to look at data and offer suggestions and Matthew Hirsch for his insightful analyses. In addition, I would like to thank Sarah Nicolson and Jayme Warischalk who have made their journeys through the Samulski lab with me and have been available for support through all the trials of graduate school. The Samulski lab is part of the larger family of the UNC Gene Therapy Center and I would like to thank everyone in the GTC for the support, help, and fun. Finally, I would like to thank all of my family: my parents, grandparents, aunts, uncles, cousins, and my cousins' children. I cannot thank them enough for their love and support.

I would like to thank Sophia Shih and Swati Yadav for technical assistance with titering vectors and Pier Paolo Pandolfi (Beth Israel Deaconess Cancer Center) and Peter Hemmerich (Leibniz Institute for Age Research) for their kind gift of reagents necessary for experiments in this dissertation. In addition, this dissertation utilized equipment and software from the UNC

Flow Cytometry Core, UNC Small Animal Imagining Facility, UNC Microscopy Services Laboratory, and UNC Animal Clinical Chemistry Core.

This work was supported by National Institutes of Health grants 1R01AI080726 and 5R01DK084033 (to C.L. and R.J.S.), 5U54AR056953 and 5R01AI072176 (to R.J.S.), as well as a fellowship 5T32-AI007419 (to A.M.M.).

TABLE OF CONTENTS

LIST OF FIGURES

LIST OF ABBREVIATIONS

AAP	Assembly activating protein
AAV	Adeno-associated virus
AAV2	AAV serotype 2 (other serotypes denoted in similar manner)
Ad	Adenovirus
Ad-DBP	Ad DNA binding protein
ALT	Alanine amino transferase
As_2O_3	Arsenic trioxide
AST	Aspartate aminotransferase
DHE	Dihydroethidium
EBV	Epstein Barr virus
F.IX	Factor IX
HCMV	Human cytomegalovirus
HFF hTERT	Human foreskin fibroblast immortalized with telomerase
HIV	Human immunodeficiency virus
HSV	Herpes simplex virus
i.p.	intraperitoneal
LCA	Leber's congenital amaurosis
LPL	Lipoprotein lipase
LPLD	Lipoprotein lipase deficiency
MFI	Median fluorescence intensity
MTOC	Microtubule organizing center

MVM	Minute virus of mice
NAC	N-acetyl-L-cysteine
PCNA	Proliferating cell nuclear antigen
PI	Proteasome inhibitor
PML	Promyelocytic leukemia protein
PMLI	PML isoform I (other isoforms denoted in similar manner)
$PML^{-/-}$	PML knockout mouse
$PML^{+/+}$	Wild-type mouse
PMSF	Phenylmethane sulfonylfluoride
rAAV	Recombinant AAV vector
RFC	Replication factor C
ROS	Reactive oxygen species
RPA	Replication protein A
RPE65	Retinal pigment epithelium-specific protein 65 kDa
scAAV	self-complementary AAV
ssAAV	single-stranded AAV
TR	Terminal repeat
TRIM	Tripartite motif
Vg	Vector genome
Vg/cell	Vector genomes per cell
VLDL	Very low-density lipoprotein
VZV	Varicella zoster virus

CHAPTER 1

Introduction

AAV Biology

Adeno-associated virus (AAV) is a small single-stranded DNA virus of the parvovirus family. AAV was first discovered as a contaminant of adenovirus (Ad) stocks (1) and later determined to be dependent upon Ad for replication, leading to its classification as a dependovirus. This classification in the dependovirus genus separates AAV from the other members of the parvovirus subfamily, the autonomous parvovirus and erythrovirus genera (2). Although the majority of the population is seropositive for AAV (3), to date, no pathogenicity has been linked to AAV (4). AAV's 4.7 kb genome encodes two genes, *Rep* and *Cap*, flanked by inverted terminal repeats (TR) (**Fig. 1.1**), which are the only viral elements required in *cis* for genome packaging (5). The *Rep* gene encodes four non-structural proteins, Rep78, Rep68, Rep52, and Rep40, using two promoters and alternative splicing. These proteins function to control viral transcription, nick the genome to allow completion of genome replication, integrate the genome in a site-specific manner, and package the genome into the capsid (6, 7). Specifically, Rep78 and Rep68 possess DNA binding and endonuclease activities responsible for TR nicking during DNA replication, while Rep52 and Rep40 have ATP-dependent helicase activity and are thought to be responsible for packaging of the genome into the capsid (2). The *Cap* gene encodes the three viral capsid proteins, VP1, VP2, and VP3, as well as a non-structural protein involved in packaging called the assembly activating protein (AAP) through alternative

start sites and alternative splicing (2, 8). The capsid proteins share their C-terminal domain, the VP3 common region, and differ in their N-terminal domains. The unique regions of VP1 and VP2 are denoted as VP1u and VP1/2 common region, respectively, and have motifs including punitive nuclear localization signals and a phospholipase domain (9, 10). AAP is responsible for targeting of the capsid proteins to the nucleolus and assembling them into the T=1 icosahedral capsid (8). VP1, VP2, and VP3 assemble in a ratio of 1:1:10 and thus capsids contain five copies of VP1, five copies of VP2, and fifty copies of VP3 surrounding the positive- or negative-sense viral genome (11).

Although there are numerous serotypes of AAV, the majority of AAV's life cycle has been elucidated based on the archetypical AAV serotype, AAV2 (**Fig. 1.2**). AAV initially contacts cells through binding to primary receptor consisting of a sugar moiety, such as heparan sulfate or sialic acid, and then to a secondary receptor, such as an integrin or a growth factor receptor (12). The virus enters the cell via receptor-mediated endocytosis (13) and traffics through the endolysosomal pathway to the microtubule-organizing center (MTOC) where the virus accumulates before and after endosomal escape (14). The majority of the virus is maintained at the MTOC; however, a small proportion of virus continues on its transduction pathway by trafficking intact to the nucleus where the viral genome can be uncoated (15). As AAV is a single-stranded DNA virus, before transcription, the genome is converted into a double-stranded form either through second-strand DNA synthesis by cellular replication factors (16) (**Fig. 1.3A**) or, perhaps, through annealing of positive-sense and negative-sense genomes (17). In the absence of a helper virus, viral transcription is repressed by the Rep proteins (18) and AAV genomes persist episomally in a circular, concatemerized form (19). The Rep proteins can also mediate the site-specific integration of the AAV2 genome into the AAVS1 integration site

on chromosome 19 (20, 21). The AAV genomes persist until replication is activated by the presence of a helper virus.

Although AAV was first discovered in association with Ad (1), several other viruses are also able to provide helper functions for AAV, including herpes simplex virus (HSV) (22), human papillomavirus (HPV) (23), and vaccinia (24). Furthermore, conditions of cellular stress, including treatment with hydroxyurea or UV light in the presence of oncogenes, have been demonstrated to substitute for AAV helper virus functions (25, 26). AAV helper viruses increase the efficiency of or are necessary for a number of steps in AAV life cycle. The helper viruses increase the efficiency of nuclear transport of AAV (27), facilitate second-strand DNA synthesis (16), encourage genome circularization (28), release Rep repression of the viral p5 promoter (29), increase the efficiency of mRNA splicing, transport, and translation (30-32), allow genome replication (33, 34), and provide a means of cell escape (35). Therefore, in the presence of a helper virus, AAV genomes are replicated by cellular DNA replication machinery such as DNA polymerase δ, proliferating cell nuclear antigen (PCNA), replication factor C (RFC), and replication protein A (RPA) (**Fig. 1.3A**) with the assistance of helper virus proteins such as Ad DNA binding protein (Ad-DBP) (36, 37). AAV DNA replication proceeds through a strand displacement mechanism illustrated in **Fig. 1.3B**, wherein the terminal repeat acts to prime leading strand synthesis for DNA molecule (2). Rep then acts to break the strands in the TR nicking stem, separating the strands and allowing the TR to be replicated. This genome form, a double-stranded monomer, is the major form of replicative AAV DNA. Alternatively, if Rep fails to nick the TR before the DNA replication machinery begins to synthesize another DNA strand, a double-stranded dimer molecule can be formed, representing the minor replicative form of AAV DNA. Newly synthesized genomes are packaged into the newly assembled viral capsid,

presumably in the nucleolus, with the aid of Rep and AAP (8) and the virions are released from the cell by helper virus cell lysis, completing AAV's lifecycle.

Although the majority of AAV biology has been generated using AAV2, many different serotypes of AAV have been isolated from the tissues of a broad range of animal species and show between 49% and 99% identity in capsid amino acid sequence (38). These serotypes can have markedly different tissue tropisms; for instance, AAV1 is largely muscle-tropic, while AAV2 is liver-tropic and AAV9 is systemic (39). Capsid structures are available for many of the serotypes (11, 40-46), allowing the influence of various capsid regions on the steps of the viral lifecycle to be elucidated.

rAAV Vector Biology

Due to many advantageous facets of AAV biology, AAV has been developed as a vector for gene delivery. AAV's lack of known pathogenesis is suggestive of safety for AAV-mediated gene delivery. In addition, AAV is relatively non-inflammatory, precluding the cytokine storms that have been observed with some other gene delivery methods (47). AAV can infect both dividing and non-dividing cells (48), which makes it a good choice for delivery to terminally differentiated target cells, as well as targets that are more amenable to transduction. Furthermore, AAV DNA can persist episomally in cells for long time periods, especially in cells with slow rates of cell division, making it well suited for delivery of genes for long-term expression (3, 49). Finally, AAV2 genomes can be packaged into capsids from different serotypes, a process known as transencapsidation (50, 51). The wide variety of AAV serotypes available for packaging allows vectors with a large range of tropisms and differing transduction properties. These factors make rAAV a highly promising gene therapy vector.

To produce an AAV virus-like particle or vector (rAAV), the viral genes can be completely removed from the vector genome and supplied in *trans* with the TRs being the only viral elements required in *cis* (5). A transgene cassette is then substituted for the viral genes and the vector is produced through a triple transfection method with an Ad helper plasmid minimizing the risk of wild-type virus production (52). Through this method, the same transgene cassette can be packaged into the capsids of various AAV serotypes, allowing comparisons between the serotypes. In addition, self-complementary rAAV genomes can be produced which contain a mutation in the Rep nicking element in one TR, producing an rAAV genome which can self-anneal avoiding the rate-limiting step of second-strand DNA synthesis and increasing transduction kinetics and efficiency (**Fig. 1.2**) (53, 54). These features make rAAV highly amenable as a gene therapy vector.

rAAV is thought to undergo the same transduction steps and intracellular trafficking as wild-type AAV in the absence of a helper virus through the step of second-strand DNA synthesis. However, due to the lack of Rep protein in rAAV transduction, rAAV cannot integrate in a site-specific manner and so only low-level (<0.5%), illegitimate integration occurs (55-57). The vast majority of genomes persist episomally as head-to-tail concatemers (58). The illegitimate integration occurs due to interactions between the host DNA and the TRs leading to integration of the vector genome and a small deletion of host DNA (59). This integration can occur throughout the genomes although ribosomal DNA repeats, genes, initiation sites, CpG islands, and palindromic sequences appear to be hotspots for integration (57, 59). Some studies have suggested an increased risk of oncogenesis from rAAV integration (57); however, others have reported no increased risk and any effects appear to be transgene and promoter specific (55,

56). Therefore, this low level of illegitimate integration has not prevented the utilization of rAAV to delivery genes for clinical gene therapy applications.

Clinical Successes with rAAV

Given AAV's many advantages as a gene delivery vector, over 100 clinical trials to date are utilizing or have utilized rAAV for gene therapy purposes (http://www.abedia.com/wiley). The results of these trials strongly demonstrate that rAAV-mediated gene delivery is a very safe method for delivering transgenes in the clinic (4). In addition, recent clinical trials, especially in restricted transduction sites, have begun to demonstrate successes in reaching their efficacy goals. Of the trials conducted, several stand out including trials leading to the licensing of the first commercial gene therapy product in Europe (60), trials for the treatment of retinal disease (61), trials for the treatment of CNS diseases (62), and trials for congestive heart failure (63). Two of these applications are discussed in more detail below.

Glybera®, a commercial gene therapy product. Glybera®, gene therapy product marketed to treat lipoprotein lipase deficiency (LPLD), was approved for commercial use in Europe in November of 2012 and is seeking approval in other markets. LPLD, caused by loss of function mutations in the lipoprotein lipase (LPL) gene or its functional partners, is an orphan disease affecting approximately one in five hundred thousand to one in one million people, although certain geographical regions such as eastern Canada exhibit higher rates of disease (60). LPL is produced by muscle cells and adipocytes and secreted into circulation where it binds to the luminal surface of blood vessels (60). After a meal, LPL is responsible for clearing triglycerides from chylomicrons, whereas LPL affects triglycerides in very low-density lipoprotein (VLDL) during fasting. In patients with LPLD, the triglycerides are not effectively

cleared from the plasma, leading to plasma triglyceride levels 10 to 100-fold higher than normal. These high levels of triglycerides lead to complications including acute and chronic pancreatitis (60). As the serum half-life of LPL is very short prohibiting enzyme replacement therapy, the only treatment available for LPLD prior to Glybera® was dietary management to enact an extremely low fat diet, which was often not effective.

The lack of effective treatments for LPLD led to the development of AAV-mediated gene addition approaches to target LPLD resulting from mutations in LPL. Early LPLD gene therapy studies in animal models were conducted with Ad vectors and demonstrated proof-of-principle that delivery of LPL could led to decreases in serum triglyceride levels and disease symptoms; however, the highly inflammatory response to Ad vectors led to short-term transgene expression and immune responses directed against the transgene (64, 65). Therefore, further studies were conducted with rAAV1, which is a muscle-tropic serotype of AAV. These studies also utilized a naturally occurring gain of function mutant of LPL, LPL^{S447X}, which is present in approximately 20% of the human population and results in low plasma triglyceride levels and reduced risk of cardiovascular disease (66). Preclinical studies in LPL deficient mice demonstrated that intramuscular injection of rAAV1- LPL^{S447X} resulted in decreased plasma triglyceride levels and disease symptoms lasting more than one year, suggesting that this approach led to long-term disease improvements (67). Further preclinical studies in a feline LPLD model also demonstrate improvements although the treatment was limited by an antibody response to the human LPL transgene expressed (68). Given these promising preclinical results, clinical trials were initiated to determine whether the treatment would be safe and effective in humans.

Due to the low prevalence of LPLD, the first clinical trial examining the effect of rAAV1- LPL^{S447X} treated four patients each with a low and a high dose of rAAV1- LPL^{S447X}

using 40 to 60 simultaneous intramuscular injections (69). Most importantly, this study resulted in no serious adverse events. In addition, it demonstrated a significant but transient decrease in plasma triglyceride levels, thought to be limited by an immune response. A larger dose escalation study conducted with 14 patients and utilizing immunosuppression for 12 weeks after treatment demonstrated significant decreases in plasma triglyceride levels that were, however, still transient, suggesting that the short-term nature of the decrease was not due to an immune response (70). Nevertheless, signs of clinical improvement, including a decrease in incidences of pancreatitis, changes in the patients' tolerance for certain food, and changes in the profile of lipids present in the blood out to two years following treatment, as well as long-term muscle expression of the LPL^{S447X} transgene, suggested that plasma triglyceride levels might not be an appropriate biomarker of successful treatment and that treatment with rAAV1- LPL^{S447X} had the capacity to improve patient outcomes. Therefore, a third clinical study was conducted looking for the effects of treatment with rAAV1- LPL^{S447X} on abdominal pain, pancreatitis, and chylomicron plasma clearance.

This third clinical trial enrolled five patients and demonstrated that rAAV1- LPL^{S447X} treatment resulted in an improvement of chylomicron metabolism (71). In addition, the patients reported increased energy, increased ability to eat, decreased abdominal pain, and decreased incidence of pancreatitis through two years post-treatment. A retrospective study of 22 of the 27 patients treated previously determined that treatment resulted in decreased incidence of pancreatitis, severity of pancreatitis, and hospitalization (60). Taken together, these studies present good evidence that rAAV-mediated gene transfer can be effective in treating clinical disease. Based on these finding, rAAV1- LPL^{S447X} (Glybera®) was recently approved for

commercial use in Europe, representing a great success for both AAV-mediated gene delivery and gene therapy in general.

Retinal targeted AAV gene therapy. Thus far, mutations in approximately 200 genes have been linked to inherited retinal diseases, including Bardet-Biedl syndrome, chorioretinal atrophy, cone dystrophy, cone-rod dystrophy, congenital stationary night blindness, Leber's congenital amaurosis (LCA), macular degeneration, and retinitis pigmentosa (https://sph.uth.edu/retnet/home.htm). These retinal diseases are an especially attractive target for AAV-mediated gene therapy. The small site of delivery and restricted numbers of cells to transduce allow very small doses of rAAV to be effective in expressing transgenes (72). Moreover, the site of transduction is reached by relatively easy surgery and the specific cells transduced can be tailored by subretinal or intravitreal injection to target different retinal cell layers (73). In addition, subretinal injections lead to immune privilege, avoiding immune responses to the transgene or the vector (74). Furthermore, various rAAV serotypes are capable of targeting different cell types in the retina allowing customization of delivery (75). Finally, non-invasive technologies, such as tomography and electroretinography, allow efficacy outcomes to be easily evaluated (72). For all of these reasons, AAV-mediated gene therapy for retinal disease is a promising avenue of investigation.

Preclinical investigations of rAAV-mediated gene addition have been conducted in animal models with deficiencies in at least ten different genes related to retinal diseases including retinitis pigmentosa, LCA, and rod monochromacy (75). The vast majority of these studies demonstrated long-term improvements in the retinal degeneration. Of these diseases, LCA caused by mutations in *RPE65* (retinal pigment epithelium-specific protein 65 kDa) has recently been the focus of several very successful clinical trials for rAAV-mediated gene

delivery (72, 76-78). LCA, an early onset form of retinal degeneration, accounts for about 5% of retinal disease and is the leading cause of childhood blindness (75). Mutations leading to this disease have been identified in 14 genes to date (https://sph.uth.edu/retnet/home.htm); however, mutations to *RPE65* account for approximately 6 to 16% of LCA cases (75). RPE65 is an enzyme responsible for converting the all-*trans*-retinal formed when photoreceptors signal to 11-*cis*-retinal, allowing photoreceptors to signal again (79). Three clinical trials delivering *RPE65* using an rAAV2 vector were initiated based on very promising small and large animal models and reported their results in 2008 (80-82). All of these trials demonstrated the safety of the treatment and the two trials utilizing strong promoters demonstrated improvements in various measures of visual function including nystagmus, visual fields, dark-adapted perimetry, and mobility at low luminance (81, 82). In total, these trials treated 30 patients and have now reported lasting improvements through three years post-treatment (78). In addition, a follow up study treated the contralateral eye in three patients, demonstrating safety and efficacy with re-administration via the subretinal injection (83). Based in part on these results, eight clinical trials utilizing rAAV to treat retinal diseases have been initiated since 2008 for indications including age-related macular degeneration, choroderaemia, and a phase III trial for LCA (http://www.abedia.com/wiley), exemplifying the promise of rAAV-mediated gene therapy.

Systemic Transduction

The large number of clinical studies utilizing rAAV and their increasing success at reaching efficacy goals demonstrate an exciting proof-of-principle for rAAV mediated gene therapy. However, issues with low levels of transgene expression or loss of transgene expression over time have been observed repeatedly in clinical systemic gene therapy, hampering the

efficacy of these approaches. These findings are exemplified by the results garnered from trials to treat hemophilia B, one of the earliest targets of rAAV-mediated gene therapy. Hemophilia B is an X-linked monogenetic disease caused by loss of function mutations to the factor IX (F.IX) gene affecting approximately 1 in 25 000 males (84). Hemophilia B can be characterized by the percentage of normal F.IX activity possessed by the patient (84). Patients with mild disease (5% to 30% activity) usually only have bleeding episodes in response to major trauma or surgery and are often diagnosed as adults. Patients with moderate disease (1% to 5% activity) generally have bleeding episodes after injury and relatively few spontaneous episodes. The majority of hemophilia B patients have severe disease (less than 1% activity) and experience frequent spontaneous bleeding into muscle tissue and joints, leading to long-term tissue damage. Hemophilia B is generally treated with injections of exogenous F.IX; however, this treatment is extremely expensive and often not feasible for those in developing countries (84). In addition, 2% to 4% of patients treated with exogenous F.IX develop inhibitory antibodies, necessitating more complicated treatments (84). For these reasons, hemophilia B is considered a good target for rAAV-mediated gene therapy.

Given hemophilia B's strength as a target for gene therapy, four clinical trials have utilized rAAV to deliver F.IX to the liver (85-88), while one trial used rAAV to delivery F.IX to the muscle (89, 90). In most of these trials, no serious adverse events related to the vector were reported. Here, we will focus on the liver directed gene therapy approaches. The early clinical trials utilized rAAV2 as this was the first serotype developed and approved for clinical use. The results of a dose escalation trial treating 7 patients with severe hemophilia at a range of rAAV2-F.IX doses from 8×10^{10} vector genomes (vg)/kg to 2×10^{12} vg/kg were published in 2006 (86). At the lower vector doses, very little increase in F.IX levels was observed after treatment with

rAAV2-F.IX, suggesting that the dose was not high enough to allow for successful transduction. At the high dose, F.IX levels initially reached moderate or even mild hemophilia levels in the first 5 weeks post-transduction; however, after this time, the levels of F.IX decreased, returning to baseline by 10 weeks post-transduction. This decrease in transduction was thought to be the result of an immune response and correlated with a small increase in liver enzyme levels in one patient. Although the trial did not reach efficacy goals, the results demonstrated the safety of the treatment and encouraged further investigations.

A later clinical trial tried to improve these results by altering the vector used to deliver the *F.IX* gene (88). Specifically, the trial utilized a rAAV8 vector, which has much higher transduction efficiency in the liver than rAAV2, a self-complementary genome that avoids the rate-limiting step of second-strand DNA synthesis, and a codon-optimized version of the *F.IX* gene. The trial treated six patients with severe hemophilia with doses of scAAV2/8-F.IX ranging from 2×10^{11} vector genomes (vg)/kg to 2×10^{12} vg/kg. The patients in the low and moderate dose groups demonstrated F.IX levels at 1-4% of normal moving them from severe to moderate disease and decreasing their reliance on exogenous F.IX infusions. The patients in the high dose group demonstrated F.IX levels in the range of mild disease early after treatment (7-12%); however, these patients exhibited increased liver enzyme levels that were treated with prednisone and, for one patient, were reported as an adverse event. Subsequently, the F.IX levels of the patient who had a large spike in liver enzyme levels dropped to 3% of normal levels, returning to moderate disease. Although every effort was made to optimize the vector and delivery with current technology, the levels of F.IX found in this trial were still not high enough to move the majority of the patients to mild disease. This pattern of either too little transgene expression or, at higher vector doses, loss of transgene expression over time has been repeatedly observed in trials

for other systemic gene therapy applications utilizing rAAV as well. Furthermore, it is clear that even the clinical successes with rAAV would benefit from higher transgene expression in order to improve the level of efficacy observed. Given all of these data, strategies are needed to increase the level of transgene expression without increasing vector dose.

Enhancement of rAAV Transduction

As clinical studies with rAAV have repeatedly demonstrated the need for increased transgene expression from rAAV vectors, several approaches have been undertaken in order to increase the efficiency of rAAV transduction. These approaches include random mutagenesis and directed evolution approaches to identify vectors that have high transduction potential in specific targets, understanding limiting steps in AAV biology and altering rAAV to avoid these barriers, and pharmacologically altering the environment of the cell in order to improve the efficiency of transduction. These approaches will be discussed in more detail below.

Directed evolution of rAAV capsids. Directed evolution is a library-based approach that has been utilized to optimize rAAV capsids for specific applications and to identify capsids that can escape specific barriers to transduction (91). Although several early directed evolution approaches utilized only error prone PCR to generate capsid libraries (92, 93), in more recent approaches, an assortment of different AAV *Cap* genes are mixed and partially digested with DNase (94-97). The resulting gene fragments are then reassembled by error prone PCR, resulting in a library of *Cap* genes, which are chimeras of several AAV serotypes and contain an array of point mutations. These *Cap* genes are subcloned into an AAV2 infectious clone (pSSV9) and used to produce a library of AAV viruses. A selective pressure of choice can then be applied to the library in order to select for capsid that possess advantages in the given situation. With

specific alterations, this approach has been applied both *in vitro* and *in vivo* to isolate capsids that are efficient in transducing certain cell types (95, 96), evading neutralizing antibody responses (92), targeting tissues of interest and detargeting other tissues (94), and increasing efficiency for specific disease models (94). Three examples of successful directed evolution approaches are detailed below.

The first rAAV directed evolution approach utilizing libraries that re-assort *Cap* genes from different AAV serotypes attempted to isolate rAAV capsids that could infect a hamster melanoma cell line, CS1, generally refractory to rAAV transduction (96). The authors created a library of several million clones and allowed five rounds of replication on CS1 cells in the presence of Ad, resulting in the recovery of a single clone named AAV1829. This clone was a chimera of AAV serotypes consisting of the N-terminus of AAV1, followed by a short region of AAV8, a long section of AAV2, and the C-terminus of AAV9 and shared heparan binding ability with AAV2. This clone demonstrated increased transduction compared to the parental serotypes on CS1 cells and several murine melanoma cell lines and equal transduction to rAAV2 on human melanoma cell lines. When tested *in vivo*, this clone demonstrated lower transduction of the liver and muscle and a switch in brain transduction from neuronal tropism to neural progenitor cell tropism. These results demonstrated that a library of AAV clones from several AAV serotypes can be generated and used to isolate clones that perform better than the parental serotype. However, they also demonstrate a potential pitfall of the directed evolution approach: isolation of the selected variable. In this case, instead of a widely applicable melanoma-tropic vector, the clone isolated was improved only in rodent derive cell lines. Therefore, care must be taken in specifically identifying the selection variable and determining how to avoid selection for other variables.

Another study, demonstrating the breadth of libraries applicable to directed evolution, selected for AAV clones that could successfully transduce primary human astrocytes, as these cells are important targets for gene therapy but are generally poorly transduced by rAAV (95). Three libraries were generated in this study and then combined before four rounds of selection on the primary astrocytes: AAV2 *Cap* with random mutagenesis, a shuffled capsid library as described above, and a peptide display library based on AAV2. This approach isolated several clones containing point mutations to AAV2 *Cap*, as well as several chimeric clones that were more efficient at transducing astrocytes than rAAV2. When tested *in vivo*, the isolated clones demonstrated a 3 to 5-fold higher percentage of astrocytes transduced than rAAV2. In addition, with sub-retinal injection, one of the clones demonstrated increased tropism for Müller glia. Interestingly, despite the large number of clones in the initial libraries, an attempt to select the libraries separately through five rounds of selection resulted in no improvements over rAAV2's transduction. These results demonstrate that directed evolution approaches are capable of identifying rAAV clones that transduce specific cell types more efficiently than the parental rAAV serotypes; however, they also suggest that the results of the directed evolution can vary widely from trial to trial and that beneficial clones can sometimes be lost during cycling.

The approach of directed evolution has been taken farther and applied to *in vivo* selection experiments. Specifically, a chimeric library was used to select for clones which could cross the blood brain barrier in areas of seizure induced damage and transduce the damaged areas in order to create a vector selective for the damaged tissue (94). Since coinfection with Ad is not appropriate in this selection, the clones were recovered from each round of selection through PCR and then packaged as for the initial library production; therefore, this selection method isolates clones that can enter the cells of interest, but does not necessarily select for the capacity

to transduce cells successfully. Consequently, a variety of isolated clones were screened for efficient transduction. Two clones were isolated that exhibited the desired pattern of transduction of the damaged regions of the brain following seizures. In addition, these clones exhibited decreased transduction of many peripheral organs compared to the parental serotypes, suggesting that the biopanning experiment not only placed positive pressure on transduction of neurons in the damaged areas of the brain but also exhibited negative selection for transduction of peripheral organs. Therefore, given the lack of replication during the cycling, this *in vivo* selection approach can be very useful for isolating tissue specific clones as long as care is taken to screen multiple clones. Furthermore, clones isolated in this type of *in vivo* selection experiment are likely to be specific for the specific disease model utilized and may not be capable of being generalized to other models.

The results of these studies demonstrate that directed evolution is a viable and very useful approach for isolating capsids that are efficient in a specific cell type, tissue, or disease model. However, several limitations to the approach constrain its utility for widespread enhancement of transduction including isolation of the correct selective pressure, variation in results between experiments, and specificity to the species or disease model tested. In addition, it would be hoped that directed evolution would lead to the isolation and characterization of specific motifs on AAV capsids that make the capsids more efficient in certain cell types or situations. Thus far, few efforts to link these capsid changes to the virus biology have been successful. Therefore, although directed evolution is very efficient for generating specific transduction enhancement, more specifically targeted approaches are needed to increase rAAV transduction in a wide range of tissues and situations.

Engineering of rAAV to alter or avoid limiting steps in transduction. An alternative approach to the library-based directed evolution is to understand specific steps in the rAAV transduction pathway that are inefficient and alter rAAV to increase its efficiency at these steps or avoid these steps entirely. For this approach, rAAV's transduction pathway needs to be understood and then strategies devised to alter specific steps. Two examples of this strategy being successfully employed are the development of self-complementary rAAV and the transfer of receptor binding domains between rAAV serotypes. The generation of self-complementary AAV began with the observation that rAAV2 transduction was significantly enhanced by co-infection with Ad (16). This was an interesting observation given that many of the helper functions described for Ad at the time, such as activation of viral promoters or promotion of viral mRNAs splicing (29-32), were not applicable to the transduction of rAAV. The authors determined that the effect of Ad was mediated by the Ad E4Orf6 protein and observed increased double-stranded rAAV genomes despite equal amounts of uncoated DNA, suggesting that Ad enhanced rAAV second-strand DNA synthesis (16). As this enhancement of second-strand synthesis led to transduction levels orders of magnitude higher, the authors concluded that second-strand DNA synthesis is the rate-limiting step in rAAV transduction. This conclusion was further collaborated by *in vivo* experiments demonstrating that rAAV DNA was present in the nucleus of a high percentage of hepatocytes, most of which demonstrate no transgene expression, and that this expression could be rescued by co-infection with Ad (98).

From these data, it was later hypothesized that, if a genome that could become double-stranded without DNA synthesis could be packaged, the transduction of the rAAV would be greatly increased. The first approach undertaken was to create a rAAV genome that was slightly smaller than half the packaging capacity of rAAV capsids (54). In this case, a significant portion

of genomes packed should be single-stranded dimers consisting of a two copies of the transgene in opposite orientations with TRs present on both ends as well as in between the transgene cassettes. When released from the capsid, this self-complementary molecule can fold back on itself to form a double-stranded hairpin molecule. In fact, when these particle were isolated based on their density, they demonstrated 20-fold higher transduction than a comparable transgene cassette packaged in single-stranded form and a reprieve from reliance on DNA synthesis for transgene expression. In addition, when the vectors were utilized *in vivo*, the authors demonstrated both increased kinetics of transgene expression and increased steady state levels of transduction. These results demonstrated that self-complementary vectors had greatly increased transgene expression through avoidance of the rate-limiting step in rAAV transduction of second-strand DNA synthesis. The self-complementary rAAV technology was then further improved by deleting the D element of one TR, and so removing the Rep nicking stem, forcing a self-complementary molecule to be packaged (53). This mutation led to a much higher percentage of self-complementary genomes packaged and greater ease in self-complementary AAV production. Self-complementary vectors allowed for transduction in the mouse liver, brain, and muscle much higher than that of single-stranded rAAV. Therefore, the development of self-complementary rAAV is a compelling example of knowledge of rAAV biology leading to improvements in rAAV that circumvent limiting steps in transduction.

Another example of advances in the understanding of rAAV biology leading to altered vectors with differential transduction is the transfer of primary receptor binding footprints between capsids of different serotypes. The first instance was carried out with AAV1 and AAV6, two very closely related serotypes of AAV (99). Only six surface exposed amino acids differ between AAV1 and AAV6; yet, rAAV6 exhibits binding to heparan sulfate, although this

binding is not essential for transduction, and strong liver transduction, while rAAV1 does not bind heparan sulfate and has weak liver transduction. Swapping of each amino acid between rAAV1 and rAAV6 followed by heparan affinity column experiments demonstrated that altering single amino acid, 531 (rAAV1 E531K, rAAV6 K531E), could both remove heparan binding ability from rAAV6 and confer heparan binding ability to rAAV1 (99). In addition, the authors demonstrated that a comparable mutation in a different serotype of AAV, rAAV8 E533K, could also confer heparan binding. The heparan binding mutant of rAAV1 demonstrated greatly increased transduction in both a human-derived liver cell line and in the liver *in vivo*. These data demonstrate that understanding of the receptors utilized by AAV and their binding location on the AAV capsid can lead to alterations and enhancement of transduction.

Similarly, the identification of AAV9's receptor as N-linked galactose (100) and the discovery of the binding footprint of galactose on the AAV9 capsid (101), allowed for the transfer of the galactose binding domain to AAV2, generating a capsid that can bind heparan sulfate and galactose (102). As the binding domain for heparan sulfate and galactose are present at separate sites on the AAV capsid, the authors were able to mutate the rAAV2 capsid in order to confer galactose binding (102). This new capsid, called rAAV2G9, could utilize both heparan sulfate and galactose for cell entry, and was only inhibited when neither were available. In addition, this capsid, while remaining primarily liver-tropic, exhibited increased transduction in the heart, muscle, and kidney, as well as the liver. Moreover, the authors transferred the same galactose-binding domain into a chimeric variant of AAV2, AAV2i8, which does not bind heparan (102). This vector, rAAV2i8G9, demonstrated greatly increased transduction across a wide range of tissues. These results exemplify the process through which understanding of rAAV

biology can lead to improvements in the efficiency of transduction. Therefore, elucidation of rAAV biology is a useful strategy leading to improvements in rAAV transduction.

Pharmacological approaches to enhance rAAV transduction and elucidate AAV biology. A third approach to enhancing rAAV transduction is to utilize pharmacological agents to alter the cellular milieu and so enhance rAAV transduction. Many pharmacological agents, specifically chemotherapeutics that cause cellular stress, have been observed to enhance rAAV transduction in a serotype independent manner. These stressors include DNA damaging agents, such as radiation (UV, gamma, X-ray), tritiated thymidine, and cisplatinum (16, 103), DNA synthesis inhibitors, such as aphidicolin and hydroxyurea (16, 104), topoisomerase inhibitors, such as etoposide and camptothecin (104), and proteasomal inhibitors, such as MG132, LLnL, and bortezomib (105-109). Some pharmacological treatments have also been derived that affect rAAV in a serotype-specific manner. For instance, treatment of cells with neuraminidase to remove sialic acid moieties results in inhibited rAAV1 transduction, which utilizes sialic acid as its primary receptor, has no effect on rAAV2 transduction, which utilizes heparan sulfate as its primary receptor, and results in enhanced rAAV9 transduction, which utilizes galactose as its primary receptor (100). Therefore, while some treatments target universal steps in rAAV transduction, others target specific transduction steps that differ between serotypes.

In addition to simply enhancing rAAV transduction, the changes in the transduction pathway of rAAV in the presence of these pharmacological agents can also lead to advances in the understanding of rAAV biology. For instance, a study examining the effects of hydroxyurea and proteasome inhibitors, as well as several siRNA treatments, demonstrated the importance of trafficking of rAAV capsids between the nucleolus and the nucleoplasm for successful transduction (107). This study determined that treatment of cells with a proteasome inhibitor,

MG132, resulted in increased nucleolar accumulation of rAAV virions, whereas treatment with hydroxyurea resulted in increased localization of virions to the nucleoplasm. The drugs both enhance transduction and co-treatment with the two drugs results in a synergistic increase in transduction. These data led the authors to hypothesize that virions entering the nucleus stably accumulate in the nucleolus and then move to the nucleoplasm where uncoating of the genome can occur. This hypothesis, derived from changes occurring due to pharmacological treatments, can now be further investigated to elucidate the details of the nuclear steps in rAAV transduction. Therefore, pharmacological agents are useful tools not only for enhancing rAAV transduction, but also for revealing rAAV biology.

Dissertation Objectives

In summary, rAAV is an important gene delivery vector for clinical applications and has recently demonstrated success in reaching efficacy goals, especially in restricted sites such as the retina; however, low levels of transgene expression and loss of transgene expression over time have hampered many clinical systemic gene delivery efforts. These results led to the need to enhance rAAV transduction without increasing vector dose. The goal of this dissertation is to identify methods by which rAAV transduction, specifically *in vivo* transduction, can be increased. Towards this aim, we have undertaken several approaches: we have identified a cellular restriction factor that inhibits rAAV transduction, we have identified a chemotherapeutic approved for use in humans that enhances rAAV transduction, and we have explored the mechanisms by which a known class of pharmacological agents enhances rAAV transduction. Thus, of the approaches for enhancing rAAV transduction discussed above, we pursued gaining greater knowledge of the limiting steps in rAAV transduction as well as utilizing pharmacological agents to modify the cellular environment and determining how these agents

affect rAAV biology. The results of these approaches are detailed in Chapters 2, 3, and 4, while the final chapter will discuss the implications and future directions of these discoveries in the broader context of rAAV biology and applications towards clinical gene therapy.

Specifically, Chapter 2 will answer the question does the promyelocytic leukemia protein (PML) inhibit rAAV transduction. PML is a tripartite motif protein that has been demonstrated to play many cellular roles including as a cell-intrinsic antiviral defense factor. PML can inhibit both RNA and DNA viruses through many varied mechanisms (110-114) and the importance of PML can be demonstrated by the wide variety of viruses that encode factors that block or modify PML activities (115, 116). Despite the wide range of viruses inhibited by PML, including AAV's traditional helper viruses HSV and Ad (115, 116), the functional role of PML in the transduction and replication of parvoviruses has not been examined, although a possible role is suggested by the partial temporal colocalization of PML with the replication centers of both AAV (117) and minute virus of mice (MVM) (118). In this chapter, we utilized PML knockout mice, as well as knockdown and overexpression studies in human cells, to determine that PML inhibits rAAV second-strand synthesis leading to up to 50-fold inhibition of transduction *in vivo*. We also determined that human PML isoform II was mainly responsible for this effect and that the effect could be extended both to the production of rAAV and to the replication of wild-type AAV. These results will have implications for the enhancement of rAAV transduction and possibly for the replication other parvoviruses.

Chapter 3 will answer the question does arsenic trioxide (As_2O_3) enhance the transduction of rAAV. As discussed above, many cellular stressors including chemotherapeutic agents have been demonstrated to enhance rAAV transduction (16, 103-105). We utilized As_2O_3, which is a chemotherapeutic agent approved for the treatment of acute promyelocytic leukemia

(119) and is under evaluation for the treatment of many other types of leukemia (120, 121). This compound affects many different cellular pathways including inducing reactive oxygen species formation, inhibiting BCL-2 and NFκB activation, decreasing mitochondrial membrane potential, changing histone acetylation patterns and, at high doses and with long treatments, degrading PML and inducing cell-intrinsic apoptosis (122). We determined that As_2O_3 treatment caused a dose-dependent increase in rAAV transduction in a number of human and non-human cell lines through stabilization of perinuclear accumulations of rAAV virions. In addition, we determined that this effect was mediated by reactive oxygen species and that As_2O_3 treatment led to up to 10-fold enhancement of rAAV transduction *in vivo*. These results will have implications for the pharmacological enhancement of rAAV transduction.

In chapter 4, we will answer the question of whether proteasome inhibition is sufficient for the enhancement of rAAV transduction and examine the mechanisms of proteasome inhibitor effects on rAAV transduction. Although many groups have demonstrated that proteasome inhibitors can enhance the transduction of rAAV (105, 107, 109), these proteasome inhibitors also inhibit other proteases, such as serine and cysteine proteases, which have very different cellular roles (123). These off-target effects have led to the widely held hypothesis that proteasome inhibitors act on rAAV transduction not through inhibition of the proteasome but through their effects on other proteases. In addition, whether the effect of these drugs is through prevention of rAAV virion degradation or through alterations in the trafficking of capsids is not clear from the current data. In this chapter, we utilized a very specific proteasome inhibitor, carfilzomib, to determine that proteasome inhibition is sufficient for the enhancement of rAAV transduction, that other proteasome inhibitors also act through this mechanism, and that the effects of proteasome inhibition occur through positive changes in late steps in transduction.

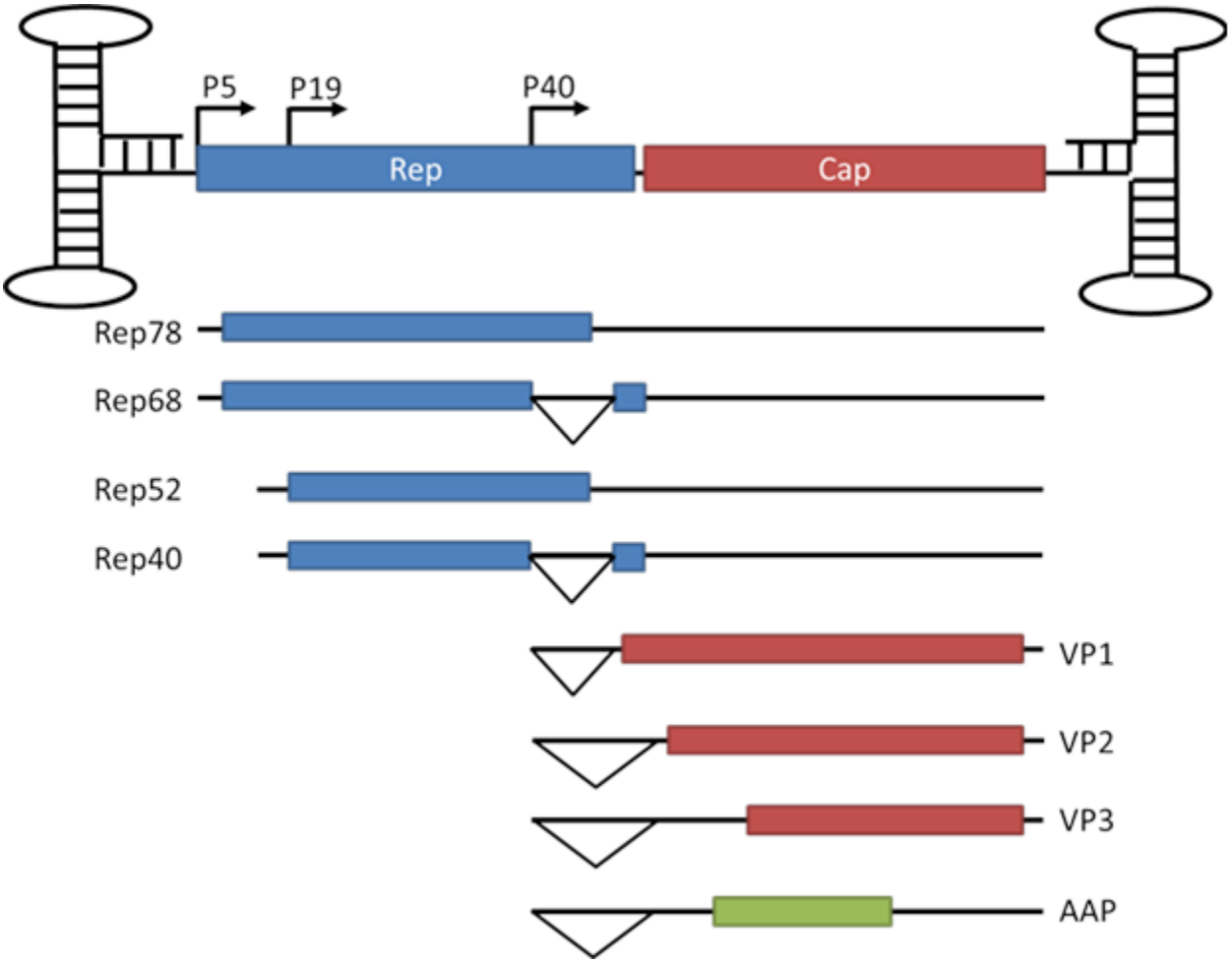

Figure 1.1: AAV2 genome organization. The AAV genome consists of a positive-sense or negative-sense single-stranded 4.7 kb DNA molecule encoding two genes, *Rep* and *Cap*, flanked by inverted terminal repeats (TRs) necessary for genome packaging and replication. There are three promoters: the p5 promoter and p19 promoters, which are responsible for *Rep* transcription, and the p40 promoter, which is responsible for *Cap* translation. The Rep78 protein is translated from an mRNA beginning at the p5 promoter. The Rep68 mRNA begins at the same promoter but is spliced at the 3' region of the coding sequence. The Rep52 and Rep40 mRNAs begin at the p19 promoter and differ in their 3' splicing. VP1 is translated off a minor splice variant of the mRNA encoded from the p40 promoter, while VP2, VP3, and AAP are translated from the major splice variant. VP2 and AAP levels are modulated by initiation from non-canonical start codons.

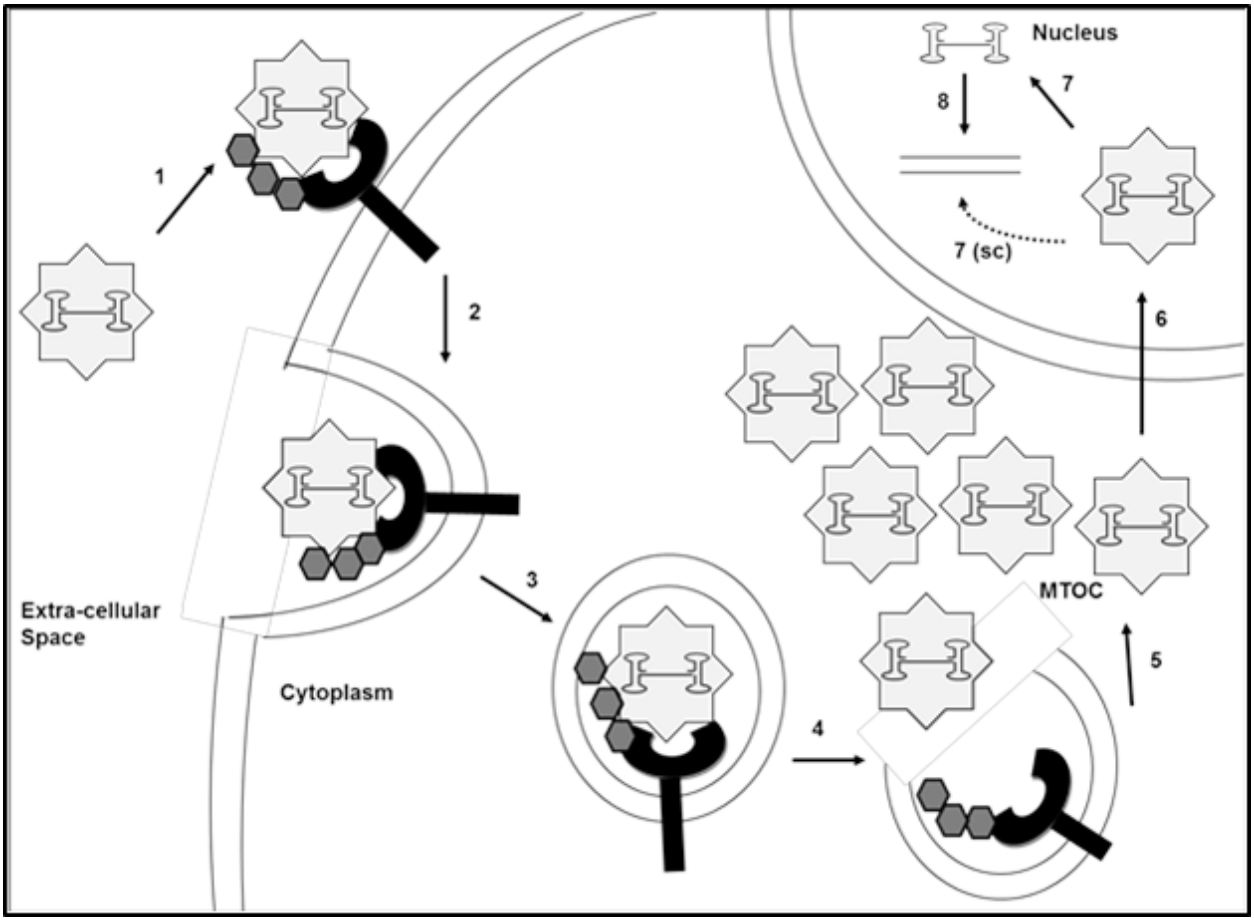

Figure 1.2: The transduction pathway of AAV. AAV first binds to cells through interaction with its primary and secondary receptors (1) and then enters the cell through receptor-mediated endocytosis (2). AAV traffics through the endolysosomal pathway (3) toward the MTOC where it escapes from the endosome (4). The virions are then retained at the MTOC (5). A portion of the virions escapes from the MTOC and traffic to the nucleus (6) where the genome is released from the capsid (7). The genome is then converted to a transcriptionally functional double-stranded form (8). Self-complementary AAV genomes contain a mutated TR, which cannot be resolved during genome replication and leads to the packaging of a molecule containing two copies of the genome in opposite orientations. When these genomes are released, they can self-anneal avoiding the necessity for second-strand DNA synthesis (7(sc)). In the absence of helper virus functions, the remainder of the AAV lifecycle (i.e. genome replication, assembly, cell escape) cannot proceed.

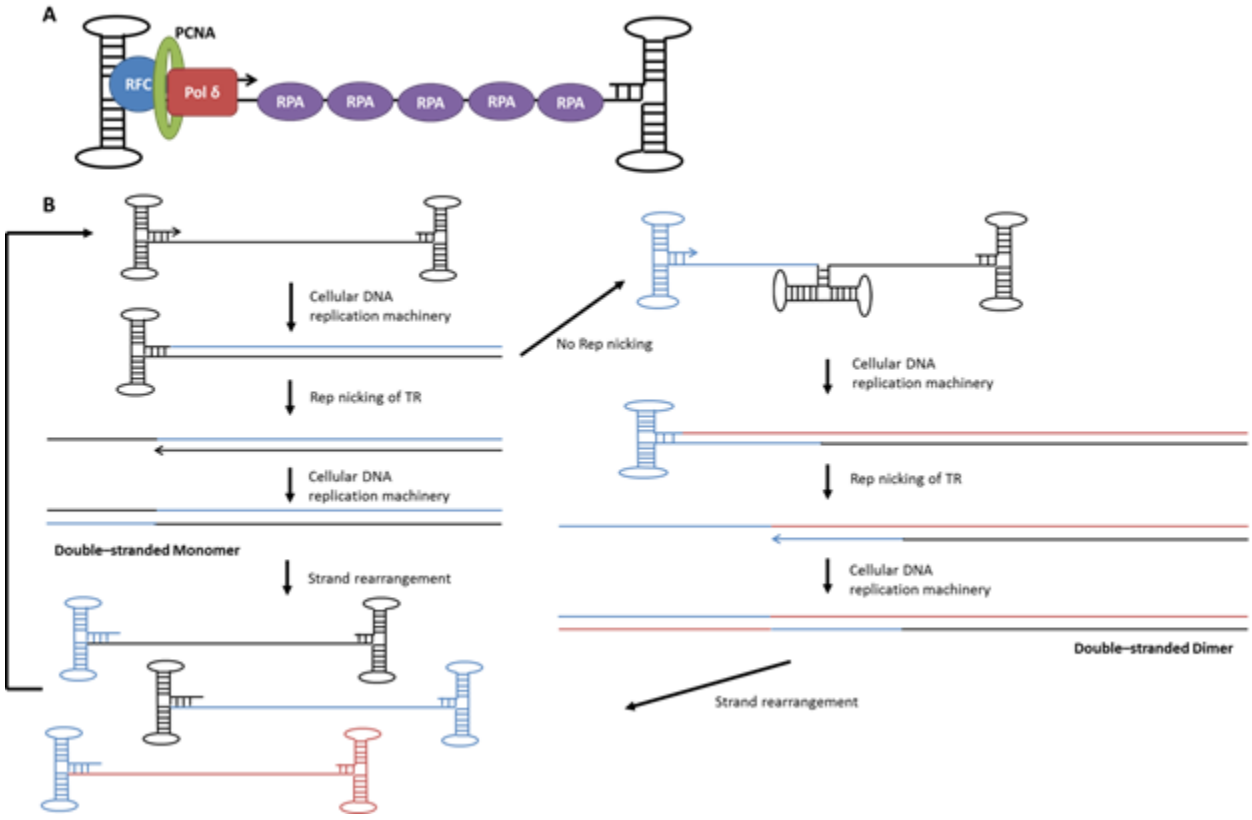

Figure 1.3: AAV genome replication factors and pathway. (A) Several cellular replication factors have been demonstrated to be involved in AAV DNA replication, which requires only leading strand DNA synthesis. These factors include DNA polymerase δ, PCNA, which encourages processitivity, RFC, which loads PCNA onto the DNA, and RPA, which is a single-stranded DNA binding protein. **(B)** AAV DNA replication occurs through a strand displacement mechanism. DNA synthesis is self-primed by the terminal repeat and then proceeds to end of the DNA molecule. The terminal repeat is then cleaved at the nicking stem by the Rep proteins and the TR is copied, forming a double-stranded monomer. The strands then separate and refold allowing replication of the new strands to begin from the terminal repeats. Alternatively, if Rep fails to cleave the nicking stem prior to synthesis of a new strand, a double-stranded dimer molecule can form which is eventually resolved by Rep nicking.

CHAPTER 2

The promyelocytic leukemia protein is a cell-intrinsic defense inhibiting parvovirus DNA replication[1]

Summary

The promyelocytic leukemia protein (PML) is a viral restriction factor inhibiting processes from uncoating to transcription to cell survival. Here, we investigated PML's effect on adeno-associated virus (AAV), a parvovirus used for gene delivery. Although dependovirus (AAV) and autonomous parvovirus (MVM) replication centers can colocalize with PML, PML's functional effect on parvoviruses is unknown. We determined PML knockout enhances rAAV2 transduction up to 56-fold at a range of vector doses in both male and female mice. PML inhibited several rAAV serotypes, suggesting a conserved mechanism, and organ specificity correlated with PML expression. Mechanistically, PML inhibited rAAV second-strand DNA synthesis, precluding inhibition of self-complementary rAAV. We confirmed the effect of human PML on rAAV transduction through knockdown experiments and linked the highest level of inhibition to PML isoform II. PMLII overexpression resulted in inhibition of second-strand synthesis, vector production, and genome replication. Moreover, PMLII inhibited wild-type AAV2 production and infectivity. Our data demonstrate PMLII inhibits AAV second-strand

[1]Adapted for this dissertation from: **Mitchell A.M., Hirsch M.L, Li C., and R.J. Samulski**. Posted November 6th, 2013. The promyelocytic leukemia protein is a cell-intrinsic defense inhibiting parvovirus DNA replication. J Virol. doi:10.1128/JVI.02922-13.

synthesis and replication, processes necessary for all parvoviruses, suggesting implications for both general parvovirus replication and AAV-mediated gene delivery.

Introduction

Adeno-associated virus (AAV) is a helper-dependent member of the *Parvoviridae* family, which, in addition to AAV, contains other viruses of clinical and veterinary importance such as B19 parvovirus, human bocavirus, and canine parvovirus. AAV consists of an icosahedral capsid surrounding a single-stranded DNA genome encoding two genes, *Rep* and *Cap*, and has been developed as a gene delivery vector for gene therapy applications. For use as a vector or virus-like particle (rAAV), the viral genes can be removed and replaced with a transgene cassette, the terminal repeats being the viral only elements required in *cis* (5). Although clinical rAAV-mediated gene therapy has demonstrated increasing success in reaching efficacy goals, especially in restricted sites such as the eye (124), low transgene expression or loss of expression over time have repeatedly compromised the efficacy in other clinical trials (86, 88). Therefore, efforts to increase the efficiency of rAAV transduction without increasing vector dose are imperative.

AAV's replication pathway involves receptor-mediated endocytosis, trafficking to the perinuclear region, nuclear entry, uncoating, and second-strand DNA synthesis, followed by either gene expression or persistence of episomal DNA (Reviewed in (4)). As AAV evolved to infect cells in the presence of a helper virus, it relies on these viruses, traditionally adenovirus (Ad) or herpes simplex virus (HSV), for various processes in its infection pathway. AAV helper virus functions span from increasing efficiency of intracellular viral trafficking (125) to inducing AAV gene expression (29) to allowing cell escape (35). When examining AAV biology, rAAV can be utilized to study the steps in AAV production prior to replication, as it undergoes the

same transduction steps as wild-type AAV through second-stand synthesis but cannot proceed with replication, making AAV a good model for studying the initial transduction of parvoviruses without the later steps of replication occluding the results.

The AAV helper viruses Ad and HSV share the ability to modify or degrade the promyelocytic leukemia protein (PML). PML is a member of the tripartite motif (TRIM) family of proteins, which play a key role in both cell intrinsic and immune host responses against viruses (Reviewed in (126)). The antiviral mechanisms of TRIM proteins range from TRIM5α which directly binds to incoming HIV-1 capsids preventing uncoating (127) to TRIM21, an intracellular antibody receptor, which causes proteasome-mediated degradation of antibody bound virions (128) to regulation of pattern recognition receptor signaling by at least eight different TRIMs (Reviewed in (129)). PML (TRIM19), specifically, is an interferon responsive protein involved in a wide variety of cellular processes including apoptosis, differentiation, and antiviral defense. Various isoforms of PML are present in the cytoplasm, nucleoplasm, and PML bodies (130). PML bodies, punctate nuclear structures formed by a lattice of PML protein, act as organizing centers for protein modifications and as depots for storage of key cellular proteins (131). PML inhibits the infection of many RNA and DNA viruses through a variety of diverse mechanisms. These mechanisms include inhibition of vesicular stomatitis virus and human foamy virus transcription by PML isoform III (110, 113), sequestration of HSV ICPO in the cytoplasm by PMLIb (111), sequestration of varicella-zoster viral capsids in a cage of PMLIV (114), and activation of p53 and induction of apoptosis by PMLIII in response to poliovirus (112). These mechanisms illustrate the breadth of viral families affected by PML and the range of mechanisms by which they are affected.

To avoid PML antiviral activity, many viruses encode PML modifying proteins. For instance, Ad E4Orf3 binds directly to PMLII and causes its rearrangement from spherical PML bodies to track-like structures (116). Furthermore, HSV encodes ICP0, an E3 ligase, that causes proteasomal degradation of PML (115). In a natural AAV infection, the PML modifying properties helper viruses may protect AAV from any potential inhibitory effects of PML. Moreover, not only have AAV replication centers been shown to colocalize with PML track-like structures in the presence of Ad (117), but the replication centers of an autonomous parvovirus, minute virus of mice (MVM), have also been demonstrated to colocalize with PML bodies during specific times in its replication cycle (118). However, the functional consequences of PML on parvovirus transduction and replication have not been examined. Therefore, we asked whether, in the absence of a helper virus, PML is capable of inhibiting rAAV transduction. To address this question, we utilized PML knockout mice, siRNA-mediated knockdown in human cells, and overexpression of PML isoforms. We demonstrated PML inhibits the transduction of rAAV both *in vivo* and in human cells in culture. This inhibition is due to the prevention of second-stand synthesis and the majority of inhibition can be traced to PML isoform II. PMLII can also inhibit the production of both rAAV and wild-type AAV and the infection of wild-type AAV. These data may lead to strategies for enhancing the efficiency of rAAV mediated gene therapy. In addition, these data may have implications for the other members of the parvovirus family.

Materials and Methods

Cell culture and virus production. HEK293, HeLa, and HuH7 cells were maintained in Dulbecco's modified Eagle medium supplemented with 10% fetal bovine serum, 100 U/ml

penicillin, and 100 g/ml streptomycin at 37°C with 5% CO_2. Adult mouse tail fibroblasts cultured in the media above supplemented with 1X MEM non-essential amino acids. AAV vectors were produced through cesium gradient purification as has been described (52). Self-complementary rAAV and corresponding control vectors were purified to yield pure virus as has been described (132). Wild-type AAV was produced as for rAAV except that the plasmid encoding AAV's genes and the transgene cassette plasmid were replaced with pSSV9. Virus and vectors were titered by qPCR (52).

Isolation of adult mouse tail fibroblasts. Adult tail snip fibroblasts were isolated using the protocol on the ENCODE Database entitled "Establishment and Propagation of Adult Mouse Fibroblast Cultures" (http://genome.ucsc.edu/ENCODE/protocols/cell/ mouse/Fibroblast_Stam_ protocol.pdf). Briefly, tail snips were clipped into Hank's Balanced Salt Solution (HBSS, Life Technologies) and minced with a razor blade. The tissue was then digested with collagenase Type XI-S at a final concentration of 1000 U/ml in HBSS for 30 minutes at 37°C. Tissue was washed once with HBSS, resuspended in 0.05% trypsin-EDTA (Life Technologies), and incubated at 37°C for 20 minutes. The tissue was then resuspended in complete growth media, pipetted to dissociate cells, and seeded in 35-mm plates with tissue clumps under glass coverslips. Media was changed every four days. When cells were subcultured, the cells were detached with 0.25% trypsin-EDTA (Life Technologies) and were seeded ratios of 1:2 to 1:4.

Animals and *in vivo* transduction assays. All animal experiments were conducted in accordance with the policies of the Institutional Animal Care and Use Committee at the University of North Carolina at Chapel Hill. Wild-type 129/SV and PML knockout 129/SV-*PML*^{tm1Ppp}mice (133) were a kind gift from Dr. Pier Paolo Pandolfi (Beth Israel Deaconess Cancer Center). Age and sex matched mice were treated with the indicated rAAV dose in PBS

by retro-orbital injection. Transduction from luciferase carrying vectors was assayed by live luciferase imaging (132). Transduction from GFP vectors was determined using a GFP ELISA kit (Cell Biolabs, Inc.). Briefly, livers were harvested at 7 days post-transduction and minced. A sample (approximately 50 mg) was lysed with RIPA buffer, homogenized with a Tissue-Tearor (BioSpec Products), and total protein concentration was determined using the Bio-Rad Protein Assay and BioRad SmartSpec Plus spectrophotometer. Equal amounts of protein were used to proceed with the GFP ELISA as per manufacturer's directions. A Bio-Rad iMark plate reader was used to determine absorbance and pg GFP per mg total protein was calculated.

Biodistribution experiments and PML expression analysis. Mice were treated with rAAV as for transduction experiments and the specified organs were harvested and frozen on day 14 post-transduction. The organs were minced and small samples were taken for luciferase assay and vector genome quantification. Luciferase samples were lysed in 2X passive lysis buffer (Promega) and homogenized with a TissueLyser (Qiagen) for 5 min at 40 Hz. The lysate was cleared by centrifugation and luciferase activity was assayed as per the manufacturer's instructions (Promega) using a Wallac1420 Victor2 plate reader. Protein levels were determined as for transduction assays. Vector genome copy number was determined by harvesting total DNA with a DNeasy Blood and Tissue Kit (Qiagen) and performing qPCR as has been described (132). For determination of *in vivo* PML expression, the indicated organs were harvested and 100 mg samples were immediately stored in RNA*later* (Qiagen) at 4°C. RNA was purified with TRIzol (Life Technologies) as per the manufacturer's instructions. cDNA was synthesized using a High Capacity cDNA Reverse Transcription Kit (Life Technologies) and transcript levels relative to GAPDH were determined by qPCR.

qPCR protocols and primers. To determine PML expression levels from cDNA made from mouse tissues and from human cells, qPCR assays were designed using the Universal Probe Library Assay Design Center (Roche). The amplicon was designed to be in the 5' region shared between PML isoforms. For mouse tissues, the primers and probe for PML were as follows: 5'-AGAGGAACCCTCCGAAGACT-3', 5'-ATTCCTCCTGTATGGCTTGC-3', and Mouse Universal Probe Library probe 76 (Roche). The primers and probe for mouse GAPDH were as follows: 5'-GGGTTCCTATAAATACGGACTGC-3', 5'-CCATTTTGTCTACGGGA CGA-3', and Mouse Universal Probe Library probe 52 (Roche). For human cells, the primers and probe for PML were as follows: 5'-TTCTGCTCCAACCCCAAC-3', 5'-CGCTGATGTCGC ACTTGA-3', and Human Universal Probe Library probe 5 (Roche). The primers and probe for human GAPDH were as follows: 5'-ATCACTGCCACCCAGAAGACT-3', 5'-ACACGGAAGG CCATGCCA-3', and Mouse Universal Probe Library probe 34 (Roche). The qPCR reactions were run with LightCycler 480 Probes Master mix (Roche) on the following program in the Roche LightCycler 480: 95°C 10 minutes, [95°C 10 s, 60°C 30 s, 72°C 1 s (acquisition)] 45 cycles, 40°C 30 minutes. Standard curves for each primer set were used to determine efficiency and calculate relative expression.

Entry, nuclear fractionation and DNase protection assays. Mice were treated as for transduction experiments and livers were harvested at the indicated time points and placed immediately on ice. Nuclear fractionation and DNase protection assays were performed as has been described (134) with slight modification. After mincing, small samples of liver tissue were taken and analyzed for total vector genome copy number as for biodistribution experiments. Ultracentrifugation through a sucrose cushion was performed for 20 minutes. Nuclear and DNase protected DNA was purified by DNeasy Blood and Tissue Kit with 5 µg salmon sperm DNA

(Life Technologies) added to DNase treated samples to act as a carrier. We determined the purity of isolated nuclei to be greater than 99.5% using the EnzChek acid phosphatase assay kit (Life Technologies).

siRNA and *in vitro* transduction assays. We used SMARTpool On-TARGETplus PML siRNA (Thermo Scientific) to knockdown human PML and On-TARGETplus Non-targeting Control Pool siRNA (Thermo Scientific as a negative control. HuH7 cells were seeded and transfected with DharmaFECT as per the manufacturer's instructions with slight modification. HuH7 cells were transfected with 25 nM siRNA 48 hours and 24 hours prior to transduction. At time of transduction, the media was changed to contain the indicated dose of rAAV and cells were incubated for 24 hours. Cells were harvested with 1X passive lysis buffer (Promega) and luciferase and protein assays were performed as above. Mouse fibroblasts were seeded 16 hours prior to transduction and the media was changed to contain rAAV at the indicated dose at the time of transduction. Transduction was assayed as for siRNA experiments 48 hours post-transduction.

PML isoform plasmid backbone control and PMLII cloning. To generate a pEGFP-C3 backbone plasmid not containing a PML construct, pEGFP-C3-PMLII was digested with BglII and BamHI (New England Biolabs) and the 4.7 kb band was gel purified (Qiagen). This band was self-ligated with T4-DNA ligase (New England Biolabs), transformed into XL10 gold ultracompetent cells (Agilent Technologies), and colonies were screened by digestion with AgeI and AvrII (New England Biolabs). To clone the PMLII sequence into the pTR-ss-CMV-EGFP backbone, pTR-ss-CMV-EGFP was digested with SalI (New England Biolabs) and then the ends were blunted with Klenow DNA polymerase (New England Biolabs). The DNA was purified with a PCR Purification Kit (Qiagen) to remove the enzymes and buffers. The DNA was then

digested with AgeI (New England Biolabs) and a 4.2 kb band containing the plasmid backbone without the EGFP gene was gel purified (Qiagen). For retrieval of the PMLII DNA, the pEGFP-C3-PMLII plasmid was PCR amplified with the primers 5'-AAACCGGTCCATGGAGCCTGC ACC-3' and 5'-CCCTTCTCTTGTAACCTTGGAATTC GC-3' and Illustria Hot Start Mix RTG (GE Healthcare). The PCR program was as follows: 95°C for 5 minutes, [95°C for 30 s, 60°C for 30 s, 72°C for 120 s] 30 cycles, 72°C for 5 minutes, 4°C ∞. The ends of the PCR product were blunted with Klenow polymerase, PCR purified, and then digested with AgeI. The 2.6 kb PCR product was then gel purified. The fragments were ligated with T4 DNA ligase, transformed into electrocompetent DH10B (Life Technologies), and colonies were picked based on sequence.

PML overexpression experiments. GFP-tagged overexpression constructs for PML isoforms I-VI were a kind gift from Dr. Peter Hemmerich (Leibniz Institute for Age Research). The backbone plasmid was used as a negative control. HeLa cells were transfection with PML plasmids in a 1:1 ratio with either pTR-CBA-Luc or salmon sperm DNA (Life Technologies). Briefly, HeLa cells were seeded in 24-well plates at 8×104 cells per well 24 hours prior to transfection. The cells were transfected with PEI Max (Polysciences, Inc) with a 1:1 ratio of the appropriate PML or backbone control plasmid (pEGFP-C3-PMLI, pEGFP-C3-PMLII, pEGFP-C1-PMLIII, pEGFP-C1-PMLIV, pEGFP-C1-PMLV, or pEGFP-C1-PMLVI, or pEGFP-C3) and either pTR-CBA-Luciferase or salmon sperm DNA (Life Technologies). Total amounts used per well were 0.5 µg total DNA and 3 µl PEI Max (1 mg/ml) in 50 µl OptiMEM (Life Technologies) added to 500 µl complete growth media. Transfection complexes were incubated 10 minutes then added to cells. Cells were incubated for 16 hours and then media was changed to remove transfection reagents. Cells were transduced at 24 hours post-transfection. Cells were transduced with 500 vg/cell rAAV2-CBA-Luc 24 hours post-transfection, incubated for 24 hours, and

assayed for transduction by luciferase assay. Luciferase values from transduction were normalized to those from transfection. For the self-complementary rAAV experiment, HeLa cells were seeded and transfected with pTR-CMV-PMLII or pTR-CMV-Luciferase and carrier DNA and transduced with indicated doses of single stranded or self-complementary rAAV2-CMV-EGFP 24 hours post-transfection. Transduction was assayed at 24 hours by flow cytometry (132).

Virus and vector production assays. For rAAV2 production experiments, HEK293 cells were seeded onto 15-cm plates at 1:3 24 hours prior to transfection (for 70% confluence at the time of transfection). For transfection, pXX680 (12 μg/plate), a pXR plasmid (10 μg/plate), and a pTR-CMV- plasmid encoding either PMLII or a reporter gene (6 μg/plate) were combined with 520 μl OptiMEM (Life Technologies) and 110 μl 1 mg/ml PEI Max (Polysciences, Inc). The complexes were incubated for 10 minutes at room temperature and then the total volume was added to the plates and cells were incubated for 48 hours to allow vector production. Cells were harvested, vector was purified as above, and vector was titered by qPCR. For rAAV2 and wildtype AAV protein level experiments and wildtype AAV production experiments, HEK293 cells were seed at 1:3 24 hours prior to transfection in 10-cm plates. For rAAV experiments, cells were transfected as before with 4.8 μg pXX680, 4 μg pXR2, and 2.4 μg of either pTR-CMV-Luciferase or pTR-CMV-PMLII in 208 μl OptiMEM and 44 μl PEI Max. For wildtype AAV2 experiments, cells were transfected as before with 4.8 μg pXX680, 4 μg pSSV9, and 2.4 μg of either pEGFP-C3 or pEGFP-C3-PMLII in 208 μl OptiMEM and 44 μl PEI Max. Cells were incubated for 48 hours to allow production. For wildtype AAV2 production, cells were harvested and DNase treated as for virus production and titers were measured by qPCR. Immunoblotting was performed as has been described (107) with slight modifications. 150 μg of protein were

loaded on 12% Mini-PROTEAN TGX precast polyacrylamide gels (Bio-Rad) and electrophoresed at 225V for 35 minutes in Tris/Glycine/SDS buffer (Bio-Rad). Proteins were transferred to a nitrocellulose membrane using an iBlot (Life Technologies) on P3 for 4 minutes. AAV capsid proteins were detected with B1 antibody, rep proteins with IF11 antibody, and actin with Abcam ab8226.

Replication and infection assays. For rAAV DNA replication assays, HEK293 cells were seeded at a 1:4 density into 10 cm plates 24 hours prior to transfection with PMLII or control plasmid. For transfection, 6 µg of pEGFP-C3 or pEGFP-PMLII were combined with 300 µl DMEM without FBS or antibiotics and 40 µl PEI Max (Polysciences, Inc) and incubated for 10 minutes at room temperature. The entire volume was added to the plate and cells were incubated for 6 hours. The media was then changed to remove the transfection reagents. Three days following transfection of the PML overexpression plasmid, or an eGFP expression plasmid, an additional transfection was performed to investigate rAAV replication. Three plasmids were used in this PEI transfection: i) the adenoviral helper plasmid XX680 (10ug), pXR2 (3ug) which supplies Rep2 and Cap2, and an AAV vector plasmid (3ug) pITR2-CBA-luc. Three days following the second transfection, HIRT DNA was isolated using modified protocol (135) and digested overnight with DpnI (New England Biolabs). Samples were separated on an alkaline gel, transferred to a nitrocellulose membrane (Amersham XL) and hybridization was performed with the product of a random primed labeling reaction (Roche) using the packaged transgenic DNA sequence as template (which also served as our size standard; (52)). Blots were exposed to film and DNA quantitation of the replication products was performed using ImageJ.

For wildtype AAV2 infection experiments, HEK293 cells were seeded at 1:3 in 10-cm plates 24 hours prior to transfection. The cells were transfected as before with 3 µg pEGFP-C3 or

pEGFP-C3-PMLII and 3 μg pXX680 or salmon sperm DNA in 300 μl OptiMEM and 40 μl PEI Max. Transfection cocktails were incubated 10 minutes at room temperature and the total volume was added to the plates. Media was changed to remove transfection reagents 6 hours post-transfection. At 24 hours post-transfection, the cells were concurrently seeded into 24-well plates at 1×10^5 cells/well and infected with the indicated dose of AAV2. Total DNA was harvested 48 hours post-transduction by DNeasy Blood and Tissue Kit and numbers of viral genomes per cell were analyzed by qPCR.

Data Analysis. We determined the statistical significance of all data using the non-parametric Kruskal-Wallis test and considered a p-value of less than 0.05 to be significant.

Results

PML knockout enhances rAAV2 transduction *in vivo*. During wild-type AAV's natural lifecycle, replicating AAV may be sheltered from the effect of PML by the PML modifying activity of its helper viruses. We hypothesized that PML may inhibit rAAV transduction in environments where helper viruses are not present. To test this hypothesis, we transduced wild-type ($PML^{+/+}$) and PML knockout (129/SV-PML^{tm1Ppp}, $PML^{-/-}$) mice with a range of rAAV2-luciferase doses and examined transduction by live imaging. Although we observed very low levels of transduction with 1×10^{10} vector genome (vg)/mouse, we observed expression of luciferase in the area of the liver at day 11 post-transduction in $PML^{-/-}$ mice whereas no expression was observable in $PML^{+/+}$ mice (**Fig. 2.1A & Fig. 2.2A**). At a five-fold higher dose of virus (5×10^{10} vg/mouse), we observed transduction at the site of injection in $PML^{+/+}$ mice, although liver expression was still low; however, liver and injection site expression was apparent in $PML^{-/-}$ mice (**Fig. 2.1B**). With 1×10^{11} vg/mouse, a commonly utilized

dose of AAV, similar transduction levels were observed in $PML^{+/+}$ mice as with 5×10^{10} vg/mouse; however, $PML^{-/-}$ mice demonstrated increasing levels of liver and injection site transduction (**Fig. 2.1C**). At a high dose of rAAV2 (5×10^{11} vg/mouse), we observed high levels of transduction in all mice, but more transduction in $PML^{-/-}$ mice (**Fig. 2.1D**). By quantifying the light output, we created doses curves for transduction (**Fig. 2.2B**) and observed significant enhancement of transduction in $PML^{-/-}$ mice as compared to $PML^{+/+}$ mice at all of the tested doses in either total transduction (**Fig. 2.1E**) or transduction in the area of the liver (**Fig. 2.1F**), demonstrating that knockout of PML can enhance rAAV2 transduction and suggesting that PML can inhibit rAAV2 transduction.

We performed the AAV dose experiment with female mice. As male mice have been demonstrated repeatedly to have higher liver transduction than female mice (136), we more thoroughly examined the effects of PML knockout in male and female mice to determine whether the higher transduction levels in male mice would override the effects of PML knockout. We transduced male and female $PML^{+/+}$ and $PML^{-/-}$ mice with 2×10^{11} vg/mouse rAAV2 and assayed transduction by live imaging. In female mice, quantification demonstrated significantly enhanced transduction in $PML^{-/-}$ mice at both 7 days and 12 days post-transduction (**Fig. 2.1G**). In fact, transduction was 28.2-fold higher at 7 days and 18.6-fold higher at 12 days post-transduction. In male mice, transduction was also significantly higher in $PML^{-/-}$ mice, 10.8-fold higher at 4 days and 56.4-fold higher at 11 days post-transduction (**Fig. 2.1H**). The increases in transduction are also evident visually (**Fig. 2.2C-D**). These data demonstrate that PML causes significant inhibition of rAAV2 transduction *in vivo* and that this effect can be observed in both male and female mice.

Effect of PML knockout is conserved among several rAAV serotypes. After determining that PML inhibited rAAV2 transduction *in vivo*, we examined the transduction of various serotypes of rAAV in $PML^{-/-}$ mice to determine whether the transduction pathway affected by PML is specific to rAAV2 or is conserved among rAAV serotypes. Therefore, we transduced $PML^{+/+}$ and $PML^{-/-}$ mice with 1×10^{11} vg/mouse rAAV6, rAAV8, or rAAV9 and assayed transduction by live luciferase imaging. At 7 days post-transduction, we observed enhanced rAAV6 transduction in the area of the liver in $PML^{-/-}$ mice (**Fig. 2.3A**) and quantified this enhancement at 15.0-fold (**Fig. 2.3B**). In addition, we observed higher transduction from rAAV8 (**Fig. 2.3C**) and quantitated this increase at 47.0-fold at 3 days post-transduction (**Fig. 2.3D**). With rAAV9, we observed increased transduction in $PML^{-/-}$ mice at day 7 post-transduction (**Fig. 2.3E**) and quantified this difference at 5.6-fold (**Fig. 2.3F**). Thus, these data demonstrate PML knockout can enhance transduction of a number of rAAV serotypes, suggesting PML inhibits a process in AAV transduction conserved between serotypes.

PML knockout enhances rAAV transduction in a manner correlating to PML expression. To investigate further the enhancement of rAAV transduction we observed in $PML^{-/-}$ mice, we determined in which organs transduction was enhanced by measuring transduction *ex vivo*. We transduced $PML^{-/-}$ and $PML^{+/+}$ mice with rAAV2, harvested organs at 14 days post-transduction, and measured luciferase activity and vector genome copy number. We observed significant increases in luciferase activity from the liver (22.6-fold) and the kidney (9.2-fold); however, we observed no increase in heart and lung and observed very little muscle transduction (**Fig. 2.4A**). In addition, we observed no differences in rAAV2 genome copy number in any of the organs tested (**Fig. 2.4B**). Although these data suggest there may be some organ specificity of the effect of PML on rAAV transduction, rAAV2's strong liver tropism occludes this conclusion.

Therefore, we investigated the effect of PML knockout on the biodistribution of rAAV9, a systemic vector.

As with rAAV2, we transduced $PML^{-/-}$ and $PML^{+/+}$ mice with rAAV9 and harvested tissues at 14 days post-transduction. Similarly to rAAV2, we observed significant increases in luciferase activity in the liver (3.9-fold), spleen (2.8-fold), and kidney (5.2-fold), and no significant increases in heart, lung, and muscle (**Fig. 2.4C**). In addition, the only significant changes in vector genome copy number observed were in the liver where copy number was 3.5-fold higher in $PML^{-/-}$ mice and the lung where copy number was 2-fold lower in $PML^{-/-}$ mice (**Fig. 2.4D**). To investigate the organ specificity further, we examined the expression of PML in the $PML^{+/+}$ mice by qRT-PCR. We observed the highest levels of PML expression in the liver and spleen, intermediate levels of expression in the kidney, low levels of expression in the heart and lung, and very low levels of expression in the muscle (**Fig. 2.4E**). Interestingly, we observed no increase in PML expression in the liver following rAAV2 transduction (**Fig. 2.5**), suggesting rAAV transduction does not induce PML transcription. As the levels of PML expression appear to correlate with the increases in rAAV9 transduction we observed (**Fig. 2.4C**), this suggests the organ specificity of rAAV transduction enhancement observed with PML knockout occurs based on varying PML expression levels. Furthermore, our genome copy number data (**Fig. 2.4B & 2.4D**) suggest changes in rAAV genome number are not necessary for PML's effect on rAAV transduction.

PML inhibits rAAV second-strand DNA synthesis. PML is present in both the cytoplasm and nucleoplasm of cells and additionally forms PML nuclear bodies that organize post-translational modification of many proteins (126); therefore, it is possible for PML to affect rAAV transduction directly or indirectly at many transduction steps. To determine the step in

rAAV transduction that PML knockout affects, we transduced $PML^{-/-}$ and $PML^{+/+}$ mice with rAAV2 and harvested liver tissue at several times post-transduction. We first asked whether the difference occurred in cell entry by determining the vector genome copy number at 1 day and 7 days post-transduction. We observed no difference in copy number between $PML^{+/+}$ and $PML^{-/-}$ mice at either time point (**Fig. 2.6A**), suggesting that the effect of PML occurs post-entry. This agrees with our biodistribution data, demonstrating no difference in rAAV2 vector genome copy number 14 days post-transduction (**Fig. 2.4B**). We next performed nuclear fractionation to determine levels of nuclear entry at these time points. At both 1 day and 7 days, we observed equal numbers of nuclear vector genomes in $PML^{+/+}$ and $PML^{-/-}$ mice (**Fig. 2.6B**), suggesting PML acts after rAAV2 nuclear entry. The next step in rAAV transduction after nuclear entry is uncoating of the vector genome; therefore, we assayed the numbers of uncoated genomes by performing a DNase protection assay on our nuclear fractions. We observed no difference in the numbers of unprotected (uncoated) genomes between $PML^{+/+}$ and $PML^{-/-}$ mice (**Fig. 2.6C**), suggesting PML acts after this transduction step on either second-strand DNA synthesis or transcription.

To access whether PML knockout affects second-strand DNA synthesis, we transduced $PML^{+/+}$ and $PML^{-/-}$ mice with self-complementary and single-stranded rAAV8-EGFP and determined transduction in harvested liver tissue at 7 days post-transduction. Self-complementary rAAV genomes do not require second-strand synthesis for transcription and so should be unaffected by inhibition of this step. As expected, with single-stranded rAAV8, we observed a 7.9-fold transduction enhancement in $PML^{-/-}$ mice; however, we observed no difference in transduction from self-complementary rAAV8 between $PML^{+/+}$ and $PML^{-/-}$ mice (**Fig. 2.7A**), suggesting PML inhibits rAAV second-strand DNA synthesis. To further

substantiate this conclusion, we treated fibroblasts from the $PML^{+/+}$ and $PML^{-/-}$ mice with a wide range of rAAV2 doses to determine whether there is a difference in the lower transduction threshold. We hypothesized that transduction increases with PML knockout might be greater at lower vector doses if PML affects second-strand synthesis as annealing of genomes could not compensate for lack of second-strand synthesis. In fact, we observed transduction in the 100 vg/cell group for $PML^{-/-}$ cells but did not observe transduction in the $PML^{+/+}$ cells until the 500 vg/cell group (**Fig. 2.7B**), demonstrating a lower threshold for transduction in $PML^{-/-}$ cells. These data also agree with our *in vivo* dosing data showing similar thresholding at our lowest rAAV2 dose (**Fig. 2.1A**). The differences in the threshold for transduction support our mechanism of PML inhibition of rAAV second-strand DNA synthesis. Taken together, our results demonstrate PML knockout enhances second-strand DNA synthesis of rAAV vectors, suggesting PML can inhibit this transduction step.

Human PML inhibits rAAV transduction through the actions of PMLII. Our data to this point demonstrate the effect of murine PML knockout on rAAV transduction. To confirm the validity of our results for human PML, we used siRNA to knockdown PML in HuH7 cells, a hepatocellular carcinoma cell line, and achieved 68% knockdown on an RNA level (**Fig. 2.9A**). We transduced cells with several doses of rAAV2-luciferase and determined knockdown approximately doubled rAAV2 transduction at all doses tested (**Fig. 2.8A**). Although this increase is less than that observed *in vivo*, it is similar to that achieved in primary fibroblasts harvested from the mice at the higher vector doses (**Fig. 2.7B**). Therefore, incomplete knockdown (**Fig. 2.9A**) and differences between the *in vitro* and *in vivo* environment likely account for the lesser effect of knockdown. Nevertheless, these data confirm human PML can inhibit rAAV transduction. Human PML has at least seven major isoforms and a number of

minor isoforms, all of which share their N-terminal domains and differ in their C-terminal domains (126). Of the major isoforms, isoforms I through VI are nuclear (130) and could possibly mediate the effect of PML on rAAV2 second-strand synthesis. We acquired plasmids expressing EGFP-tagged versions of these nuclear isoforms (137), expressed them in HeLa cells (**Fig. 2.9B**), and examined the effect of these isoforms on rAAV2 transduction. We determine that expression of five of the six isoforms (PMLI, PMLIII, PMLIV, PMLV, and PMLVI) resulted in an approximately 2-fold decrease in transduction, while expression of PMLII resulted in a 4.9-fold decrease in transduction (**Fig. 2.8B**). To confirm our *in vivo* mechanism, we then examined whether PMLII could inhibit self-complementary rAAV2 transduction. In fact, although we observed a significant decrease in the number of cells transduced with single-stranded rAAV2 after PMLII overexpression, we observed significantly less inhibition of self-complementary rAAV2 transduction (**Fig 2.8C**), confirming human PML isoform II is responsible for the inhibition of rAAV second-strand synthesis.

PMLII overexpression inhibits rAAV2 and wildtype AAV2 production and replication. All of our data thus far address the role of PML in rAAV transduction; however, given our second-strand synthesis mechanism we set out to determine whether PML plays a role in rAAV genome replication and virus production. We began by examining the effect of PMLII overexpression on virus production by encoding PMLII as a transgene for rAAV vectors. We determine the presence of the PMLII transgene resulted in a 6.8-fold decrease in the yield of vector (**Fig. 2.10A**). As the effect of PML on rAAV transduction was through second-stand synthesis, we hypothesized that PMLII inhibits rAAV production on the level of genome replication. Therefore, we performed a replication assay to determine whether the level of replicated DNA was lower in cells expressing PMLII than in cells expressing a control vector. In

fact, we observed slightly lower levels of the replicative monomer and dimer form of the vector genome in PMLII expressing cells (**Fig. 2.10B**), which quantified at 73% of the control value (**Fig. 2.10C**). We then examined whether PML could also inhibit the production of wild-type AAV by producing wild-type AAV2 from an infectious clone with or without PMLII overexpression and assaying the levels of virus produced. As with rAAV2, we observed a 6.5-fold decrease in wild-type AAV2 when PMLII was overexpressed (**Fig. 2.10D**), demonstrating PML also inhibits wild-type AAV2. We further investigated this production effect with both wild-type and recombinant AAV by examining levels of the rep and capsid proteins. We observed greatly reduced levels of all three capsid proteins, as well as the four Rep proteins, with PMLII overexpression (**Fig. 2.10E**), although the degree of decrease varied. These data demonstrate PML can inhibit the production of both recombinant and wild-type AAV on a protein level. As utilizing an infectious clone of AAV2 avoids the initial steps AAV's infectious pathway and introduces high levels of template for the viral genome, we then tested the effect of PMLII overexpression on the infection of wild-type AAV by transfecting cells with PMLII and the Ad helper plasmid, infecting with AAV2, and measuring viral genomes produced. At 48 hours post-infection, we observed large significant inhibition of AAV2 replication in the presence of PMLII (**Fig. 2.10F**), especially at low viral doses (60.1-fold at 1 vg/cell and 1207-fold at 0.1 vg/cell). We also observed significant inhibition of AAV2 infection by PMLII at earlier time points (**Fig. 2.11**), confirming PML's inhibitory role in AAV's lifecycle. Overall, our results demonstrate that PML can inhibit the transduction of rAAV vectors both human and murine contexts through the inhibition of second-strand DNA synthesis. Moreover, we traced this inhibition to human PMLII and expanded the effect to the production of recombinant and wild-type AAV and to wild-type AAV infectivity.

Discussion

In this study, we have examined the functional role of PML in the transduction of AAV and in AAV production and infection, in order to determine whether PML can inhibit AAV. We determined PML inhibits rAAV transduction *in vivo* in a manner that correlates with PML expression level and that is conserved among serotypes. Utilizing subcellular fractionation as well as self-complementary rAAV, we demonstrated that the inhibition of rAAV transduction by PML appeared to occur at the level of conversion of the single-stranded vector genome to a functional double-stranded form. In addition, we established that human PML, especially PMLII, could also inhibit rAAV2 transduction, production, and wild-type AAV2 infection. To our knowledge, these data represent the first time a functional role for PML in the transduction or replication of a parvovirus has been described.

Four pieces of data contribute to our conclusion that PML inhibits rAAV second-strand DNA synthesis: (1) Equal the numbers of vector genomes completed the pre-second-strand synthesis transduction steps of cell entry, nuclear entry, or uncoating *in vivo* in $PML^{+/+}$ and $PML^{-/-}$ mice. (2) Neither PML knockout *in vivo* nor PML knockdown in human cells had an effect on self-complementary rAAV transduction, which avoids second-strand synthesis by self-annealing. (3) Dose curves both *in vitro* and *in vivo* demonstrated a lower threshold rAAV dose required for successful transduction with $PML^{-/-}$, suggesting a greater effect of PML at low vector doses where possible annealing of vector genomes cannot compensate for a lack of second-strand synthesis. (4) Our rAAV DNA replication assay demonstrated a small but significant decrease in rAAV genome replication when PML is overexpressed. Taken together, these data provide strong evidence suggesting inhibition of rAAV second-strand DNA synthesis by PML.

Furthermore, although PML affects the replication of many viruses through sequestration of viral components (111, 114) or prevention of transcription (110, 113), we are not aware of any other studies demonstrating a PML effect specifically on genome replication. AAV genome replication relies on cellular replication machinery including DNA polymerase δ, replication factor C, proliferating cell nuclear antigen, and replication protein A (36, 37), although second-strand synthesis has not been directly examined. In the future, it will be interesting to investigate whether any of these factors are involved in PML's effect on rAAV second-strand synthesis. Moreover, as the same replication factors are involved in MVM DNA replication (138) and PML overexpression greatly inhibited AAV2 replication, it will be interesting to determine whether PML plays a role on the second-strand synthesis and DNA replication of other parvoviruses.

In addition to investigating the role of PML in rAAV transduction *in vivo*, we examined the effect of human PML on AAV in order to eliminate the possibility that the PML effects were specific to mouse and determined human PML could also inhibit rAAV transduction. Furthermore, given PML acted at a nuclear step in transduction, we examined the six major nuclear human PML isoforms and elucidated their effect on rAAV. We determined overexpression of five of the isoforms (I, III, IV, V, VI) caused a 2-fold decrease in rAAV2 transduction, while PMLII caused a 5-fold decrease in transduction. Two possible hypotheses could explain the partial effect of several isoforms and full effect of one isoform: (1) PML proteins contain two domains important for rAAV transduction inhibition, one in the shared exons (1-7a) and one in the unique region of PMLII; or (2) the effect on rAAV transduction is unique to PMLII and overexpression of other isoforms draws more endogenous PMLII into PML bodies (137), where rAAV effects might occur. Further studies will determine which of these

hypotheses is correct. Nevertheless, our data clearly demonstrate that PMLII, and specifically its unique region, is important for rAAV transduction inhibition.

The unique region of PMLII consists of the majority of exon 7b and spans from amino acid 571 to 824, the C-terminus (**Fig. 2.12**). Interestingly, while PMLI and PMLII are the most abundant PML isoforms, the majority of known PMLII functions are interactions with AAV's helper viruses Ad and HSV. Specifically, Ad E4Orf3 binds within amino acids 645 to 674 of PMLII and rearranges it to form tract-like structures (116). In addition, the conserved region 3 on Ad E1A-13S interacts with PMLII and may enhance viral and cellular transcription (139). Furthermore, HSV has two distinct mechanisms to decrease PMLII levels, ICP27 induced alternant splicing (140) and degradation of PML by ICP0 (115). In fact, PMLII expression decreases the replication of ICP0 null HSV (141). From these studies, it is clear that PMLII plays an important role in DNA virus replication that is still being elucidated. Further studies with AAV may clarify the role of PML in both DNA virus replication and other cellular processes.

Beyond rAAV transduction, we examined the effect of PML on the production of rAAV and on the production and infection of wild-type AAV2. We observed similar decreases in production of wild-type and recombinant AAV with PMLII overexpression and correlated this production defect with a small decrease in rAAV DNA replication and a large decrease in viral protein levels. With the complicated regulation of AAV expression (18, 142-145), it is unclear whether the decrease in protein levels results from the decrease in replication or an addition effect on the viral promoters. Given the known effects of PML on viral transcription (110, 113), PML repressing AAV's promoters would not be unprecedented. We are currently further investigating the roles of genome replication and viral promoter activity in PML's effect.

Additionally, we are investigating reversing this phenotype by knocking down PML and possibly increasing vector yields, which would significantly influence rAAV clinical applications.

In summary, we have demonstrated for the first time that PML inhibits rAAV transduction *in vivo* through inhibition of second-strand DNA synthesis. In addition, we demonstrated that human PML can also inhibit rAAV2 transduction and production and that PMLII is responsible for the majority of this effect. PMLII inhibited wild-type AAV2 production and infection, as well. Given the large in vivo effect of PML on rAAV transduction, rAAV's interaction with PML will be important to target with rational vector design as this pathway becomes better understood. Designing vectors that avoid PML interactions could lead to large increases in transduction, facilitating systemic gene therapy approaches. In conclusion, pursuing the interaction of AAV with PML may have important implications for understanding AAV biology, clinical vector production, enhancing rAAV transduction, and understanding of the biology of other parvoviruses.

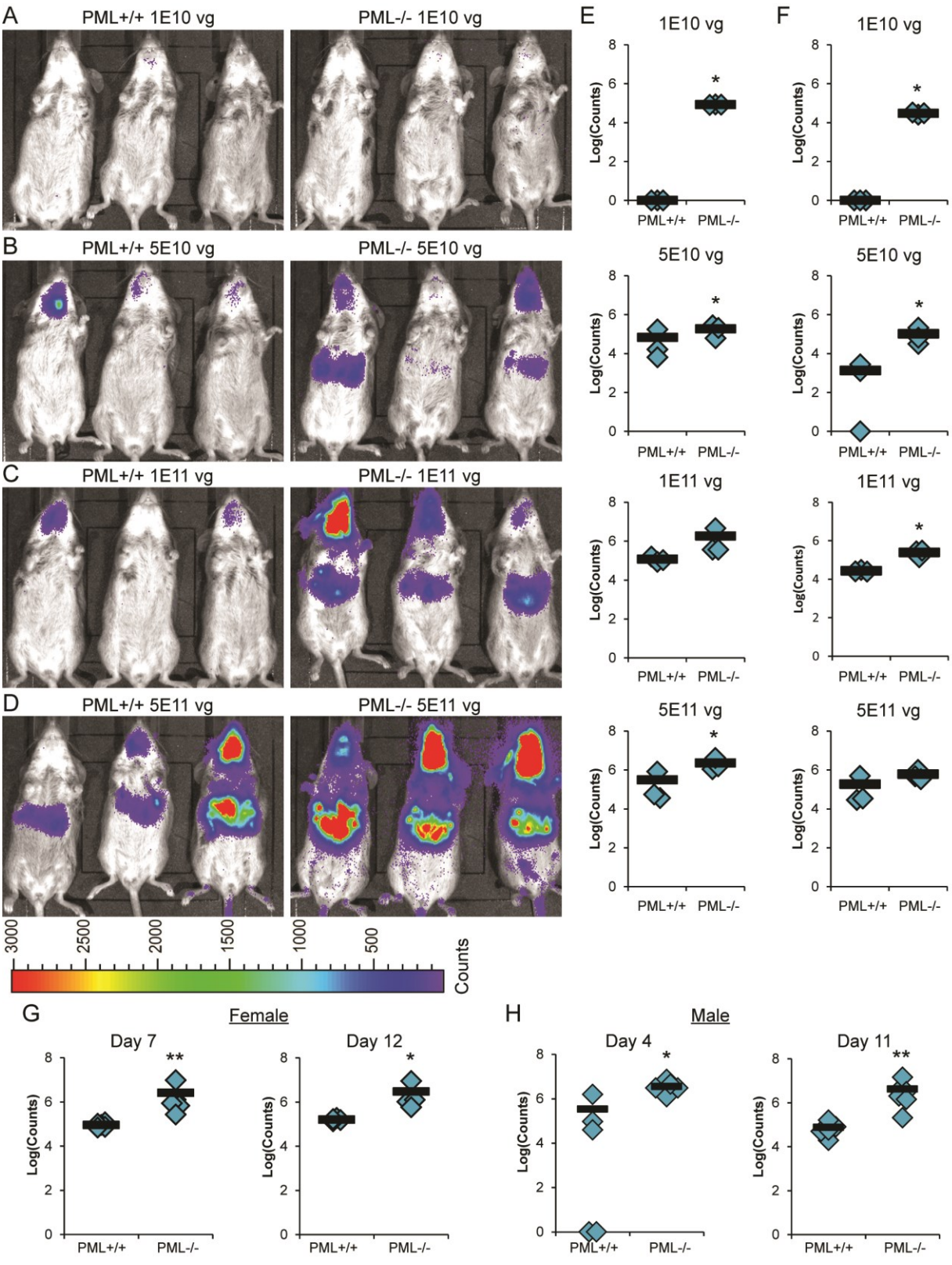
A
PML+/+ 1E10 vg
PML-/- 1E10 vg
B
PML+/+ 5E10 vg
PML-/- 5E10 vg
C
PML+/+ 1E11 vg
PML-/- 1E11 vg
D
PML+/+ 5E11 vg
PML-/- 5E11 vg
3000
2500
2000
1500
1000
500
Counts
E
1E10 vg
5E10 vg
1E11 vg
5E11 vg
F
1E10 vg
5E10 vg
1E11 vg
5E11 vg
Log(Counts)
PML+/+
PML-/-
G
Female
Day 7
Day 12
H
Male
Day 4
Day 11

Figure 2.1: PML knockout enhances rAAV2 transduction at several vector doses in both male and female mice. (A-D) Female $PML^{+/+}$ and $PML^{-/-}$ mice were transduced with (A) 1×10^{10} vg, (B) 5×10^{10} vg, (C) 1×10^{11} vg, or (D) 5×10^{11} vg rAAV2-CBA-luciferase and assayed by live luciferase imaging at 11 days post-transduction (5 minute exposure). **(E-F)** Light output from luciferase live imaging was quantified either from the whole mouse (E) or the area of the liver (F) (n=3). **(G-H)** Female (G) and male (H) $PML^{+/+}$ and $PML^{-/-}$ mice were transduced with 2×10^{11} vg rAAV2-CBA-luciferase, transduction was assayed by live luciferase imaging at two time points post-transduction, and light output from the whole mouse was quantified (all 5-minute exposures except males on day 11, which is a 1-minute exposure; n=5 for all groups except $PML^{-/-}$ males for which n=6). Individual mice are shown as diamonds while the bar indicates the mean. (*) $p<0.05$, (**) $p<0.01$ versus $PML^{+/+}$; Also see **Fig. 2.2**

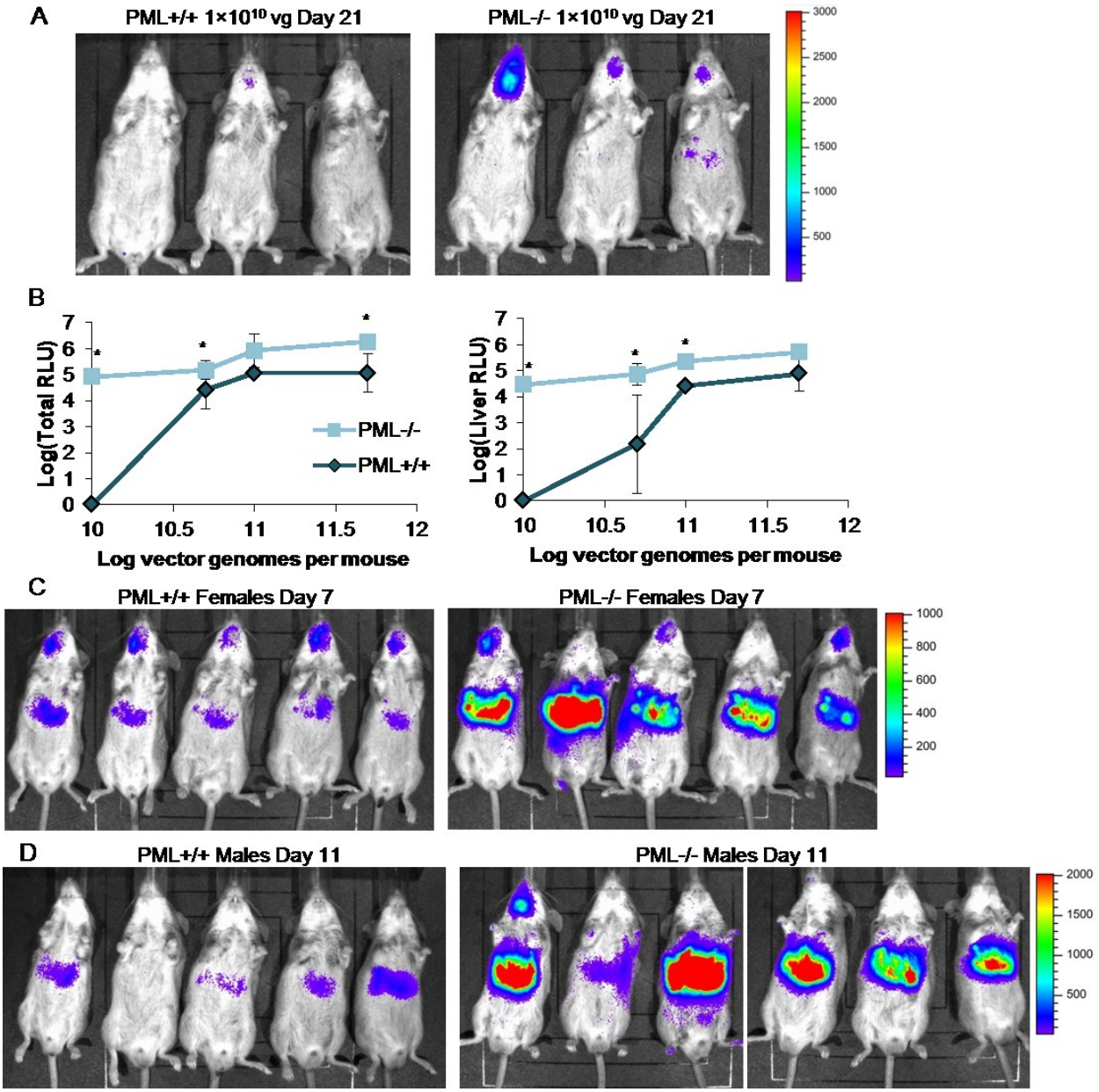

Figure 2.2, related to Figure 2.1: PML knockout enhances rAAV2 transduction at several vector doses and in both male and female mice.
(A) Luciferase live imaging data of $PML^{+/+}$ and $PML^{-/-}$ mice transduced with 1×10^{10} vg AAV2-CBA-luciferase from Figure 1A at a later time point (21 days post-transduction, 5 minute exposure), demonstrating visible transduction in the site of injection in both groups and the liver with $PML^{-/-}$ mice. **(B)** Dose curves for the rAAV2 doses shown in Figure 1 for total light output and light output from the area of the liver, demonstrating the changes in transduction between the doses. Values are indicated as the mean ± one SD. (*) $p<0.05$ versus corresponding $PML^{+/+}$ group. **(C)** Luciferase live imaging data of female $PML^{+/+}$ and $PML^{-/-}$ mice transduced with 2×10^{11} vg AAV2-CBA-luciferase corresponding to quantification in Figure 1G (5 minute

exposure), confirming the large effect of PML knockout on rAAV transduction at a commonly used rAAV2 dose. **(D)** Luciferase live imaging data of male $PML^{+/+}$ and $PML^{-/-}$ mice transduced with 2×10^{11} vg AAV2-CBA-luciferase corresponding to quantification in Figure 1H (1 minute exposure), demonstrating that the higher transduction observed in male mice from rAAV transduction does not mask the effect of PML on rAAV transduction.

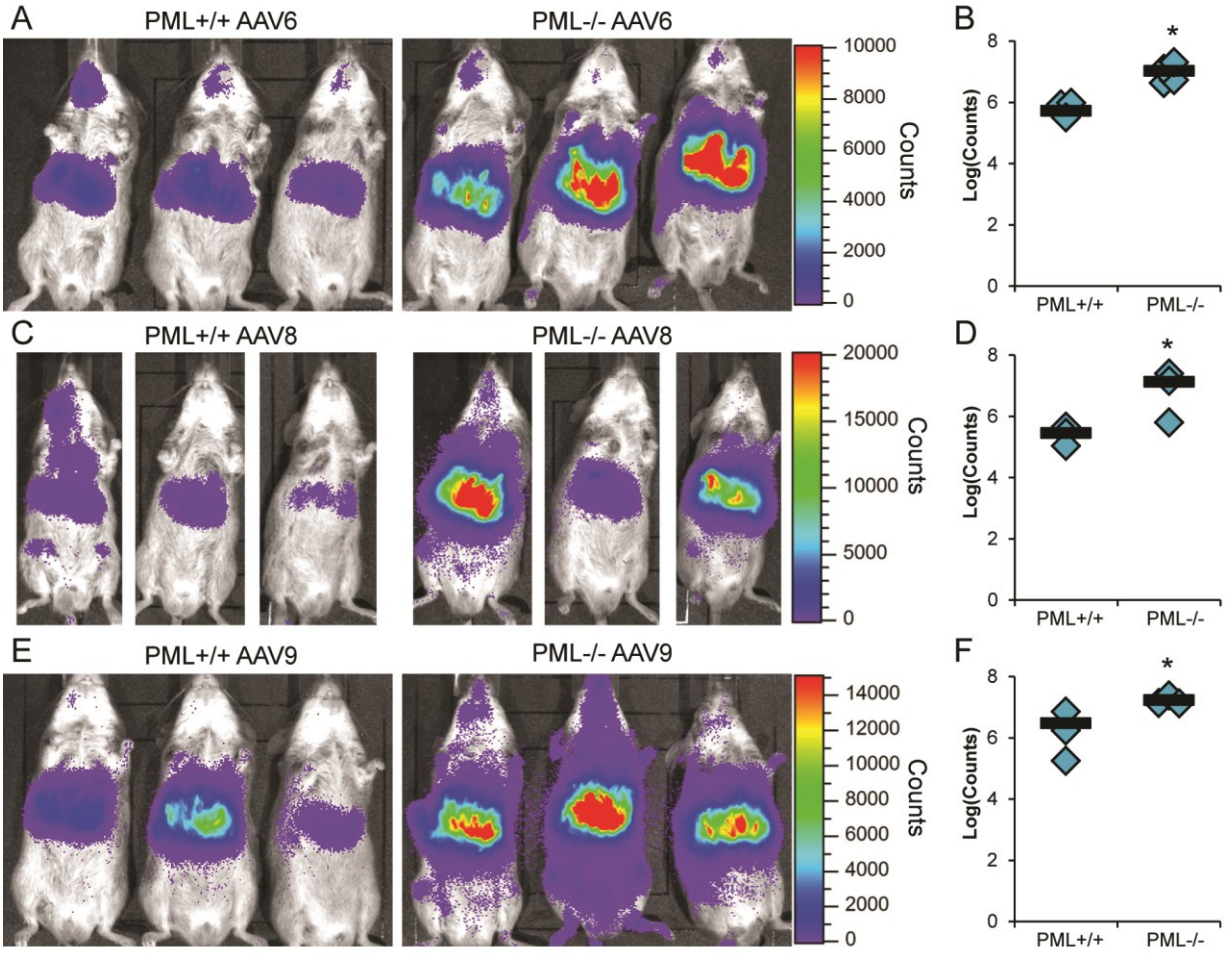

Figure 2.3. Enhancement of rAAV transduction by PML knockout is conserved among several serotypes. Male PML$^{+/+}$ and PML$^{-/-}$ mice were transduced with 1×10^{11} vg and assayed by live luciferase imaging. **(A)** Images of mice transduced with rAAV6-CBA-luciferase at 7 days post-transduction (30-second exposure). **(B)** Quantification of light output from mice in (A). **(C)** Images of mice transduced with rAAV8-CBA-luciferase at 3 days post-transduction (30-second exposure). **(D)** Quantification of light output from mice in (A). **(E)** Images of mice transduced with rAAV9-CBA-luciferase at 7 days post-transduction (30-second exposure). **(F)** Quantification of light output from mice in (A). Individual mice are shown as diamonds while the bar indicates the mean (n=3 for all groups except PML$^{-/-}$ rAAV6 for which n=4). (*) $p<0.05$ versus PML$^{+/+}$

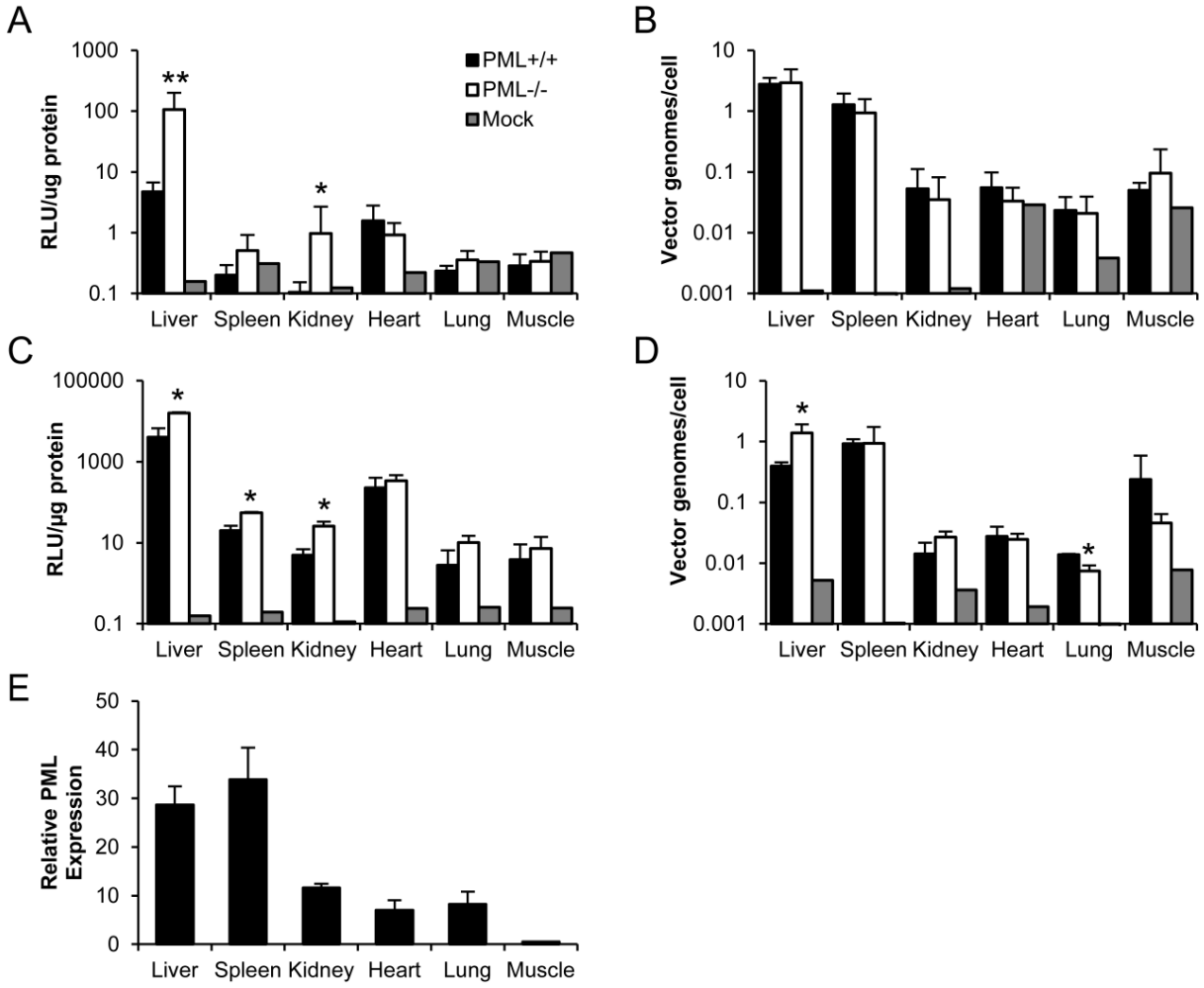

Figure 2.4: rAAV transduction enhancement is organ specific and correlates with PML expression. (A & B) $PML^{+/+}$ and $PML^{-/-}$ female mice were transduced with 2×10^{11} vg rAAV2-CBA-luciferase and indicated organs were harvested 14 days post-transduction. Tissue was assayed for (A) luciferase activity and (B) vector genome copy number (vg/cell) (n=5). **(C & D)** $PML^{+/+}$ and $PML^{-/-}$ male mice were transduced with 1×10^{11} vg rAAV9-CBA-luciferase and indicated organs were harvested 14 days post-transduction. Tissue was assayed for (C) luciferase activity and (D) vg/cell (n=3). Grey bars indicate values for an un-transduced mouse. **(E)** The indicated organs were harvested from un-transduced male $PML^{+/+}$ mice and RNA was purified. PML expression relative to GAPDH was determined by qRT-PCR (n=3). Values are indicated as mean ± one SD. (*) $p<0.05$, (**) $p<0.01$ versus $PML^{+/+}$; Also see **Fig. 2.5**

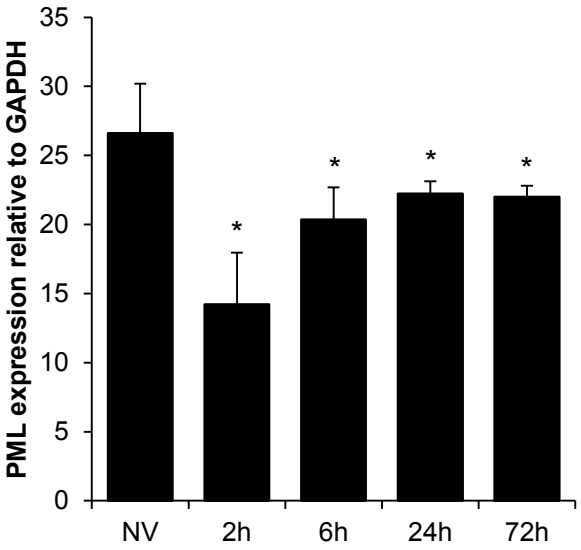

Figure 2.5, related to Figure 2.4. PML expression is not increased by rAAV2 transduction. PML+/+ mice were transduced with 1×1011 vg AAV2-CBA-Luciferase and livers were harvested for RNA at the indicated time points post-transduction. Relative expression of PML to GAPDH was determined by qRT-PCR (n=3), demonstrating that PML expression does not increase in response to rAAV2 transduction and, in fact, shows a small decrease common to many transcripts. Values are indicated as mean ± one SD. NV—no vector; 2h—2 hours post-transduction; 6h—6 hours post-transduction; 24h—24 hours post-transduction; 48h—48 hours post-transduction. (*) $p<0.05$

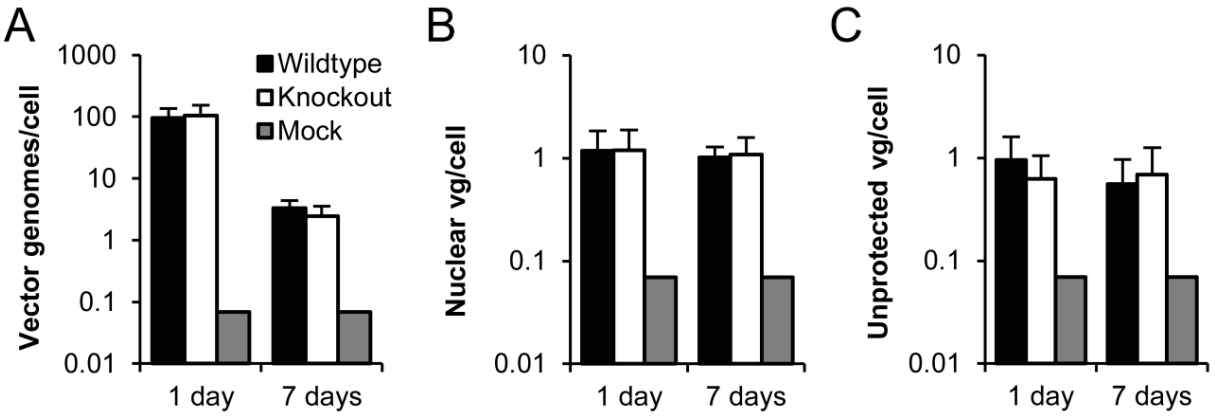

Figure 2.6: PML does not inhibit rAAV cell entry, nuclear localization, or uncoating. (A-C) $PML^{+/+}$ and $PML^{-/-}$ female mice were transduced with 1×10^{11} vg rAAV2-CBA-luciferase and livers were harvested at indicated time post-transduction. **(A)** Total vg/cell were measured by qPCR (n=5). **(B)** Nuclei were isolated by subcellular fractionation and nuclear vg/cell were measured by qPCR (n=5). **(C)** Nuclei were DNase digested to completion and number of remaining vg was determined. Unprotected vg/cell were calculated (n=5). Grey bars indicate values from un-transduced mice (n=2). Values are indicated as mean ± one SD.

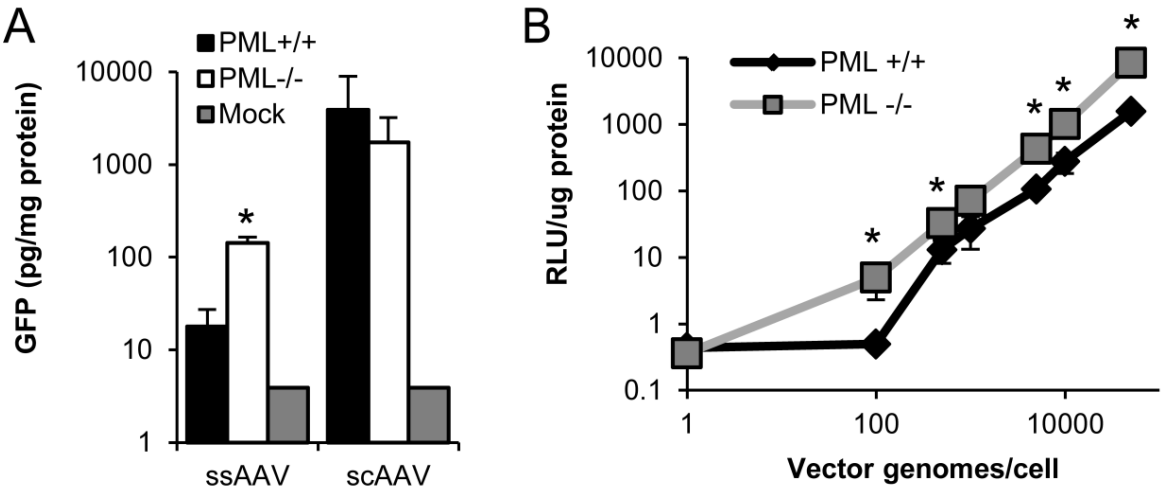

Figure 2.7: PML inhibits rAAV second-strand DNA synthesis. (A) $PML^{+/+}$ and $PML^{-/-}$ female mice were transduced with 1×10^{11} vg single stranded rAAV8-CMV-GFP (ssAAV) or self-complementary rAAV8-CMV-GFP (scAAV) and livers were harvested at 7 days post-transduction. Transduction was determined by GFP ELISA (n=3). Grey bars indicate value from an un-transduced mouse. **(B)** Adult mouse-tail fibroblasts from $PML^{+/+}$ and $PML^{-/-}$ mice were transduced with the indicated doses of rAAV2-CBA-luciferase and assayed at 48 hours by normalized luciferase assay. Fibroblast data represent three independent experiments. Values are indicated as mean ± one SD. (*) $p<0.05$ versus $PML^{+/+}$

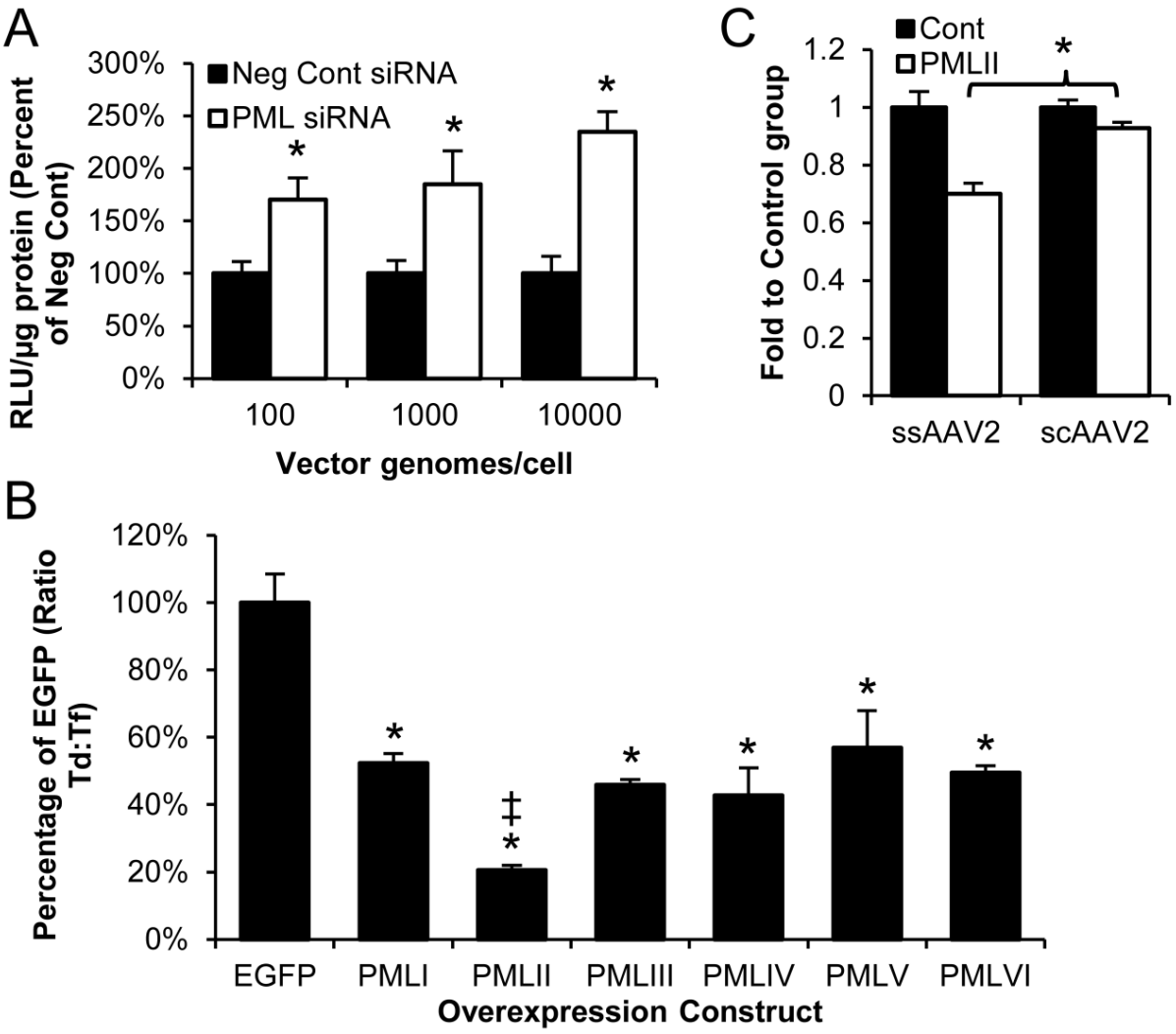

Fig 2.8: Human PML, especially isoform II, inhibits rAAV transduction and second-strand synthesis. (A) HuH7 cells were transfected with PML or negative control siRNA 48 and 24 hours prior to transduction with rAAV2-CBA-luciferase at indicated dose. Transduction was assayed by luciferase assay at 24 hours post-transduction. Values are indicated as percentage of the negative control (Neg Cont) for the vector dose. **(B)** HeLa cells were transfected with the indicated PML overexpression or control plasmid 24 hours prior to transduction with 500 vg/cell rAAV2-CBA-luciferase. Transduction was assayed by luciferase assay at 24 hours post-transduction and normalized to value from transfection. Values are indicated as a percentage of the control construct. **(C)** HeLa cells were transfected with PMLII or control plasmid 24 hours prior to transduction with either 1000 vg/cell single-stranded rAAV2-CMV-EGFP (ssAAV2) or 200 vg/cell self-complementary rAAV2-CMV-EGFP (scAAV2). At 24 hours post-transduction, cells were assayed by flow cytometry. Values indicated are percentage of cells transduced as fold of the control plasmid group. Data represent three independent experiments. Values are indicated as mean ± one SD. (*) $p<0.05$ versus control; (ǂ) $p<0.05$ versus other isoforms; Also see **Fig. 2.9**

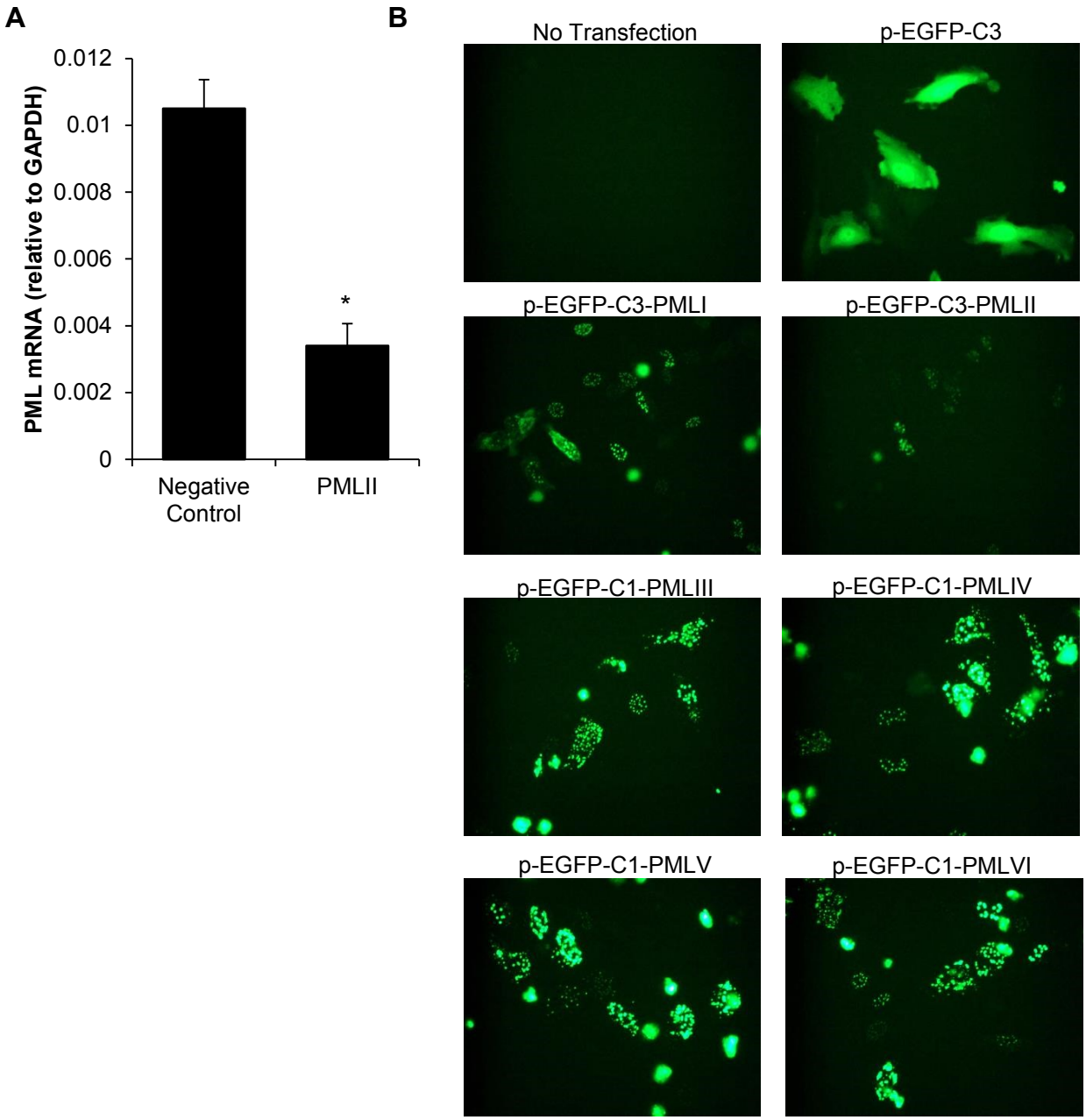

Figure 2.9, related to Figure 2.8. Human PML, especially isoform II, inhibits rAAV transduction and second-strand DNA synthesis. (A) After human PML knockdown by siRNA as described in **Fig. 2.8A**, cells were harvested for RNA and levels of PML mRNA relative to GAPDH were determined by qRT-PCR, demonstrating successful but not complete knockdown of PML. (*) $p<0.05$. **(B)** GFP fluorescence images showing expression and localization of GFP-tagged PML isoforms following transfection of overexpression constructs into HeLa cells as in **Fig. 2.8B**.

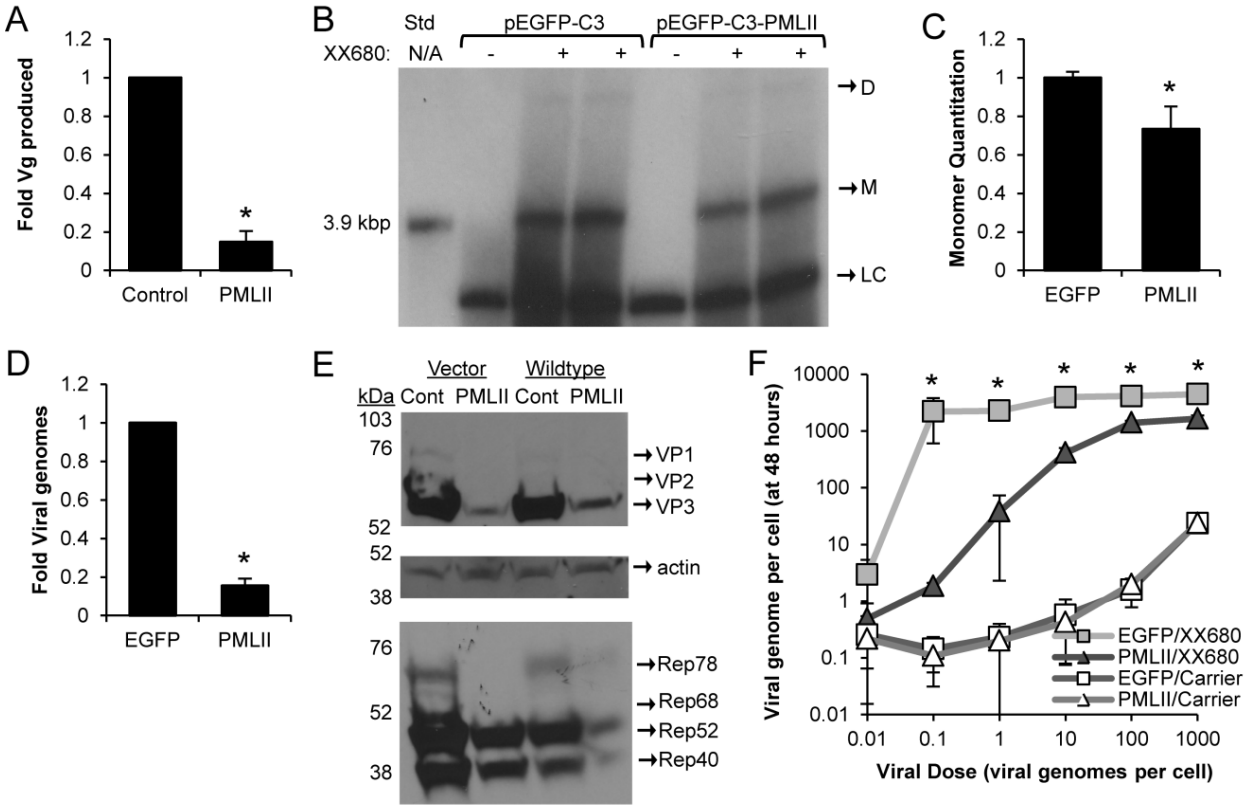

Fig 2.10 Production and replication of rAAV and AAV2 are inhibited by PMLII. (A) HEK293 cells were transfected for production of vector encoding either PMLII or a control gene (i.e. luciferase, EGFP). At 48 hours post-transfection, vector was harvested and purified. Vector produced was determined by qPCR. Values indicate mean fold to control transgene for three separate vector preparations ± SEM. **(B)** HEK293 cells were transfected with PMLII or control plasmid 24 prior to transfecting with viral production plasmids. At 72 hours post-transduction, small molecular weight DNA was harvested. Replicative forms of rAAV DNA were detected by Southern blot. No pXX680 lanes represent negative control for replication. M—monomer; D—dimer; LC—loading control (DPN1 digested plasmid). Image is representative of three trials on two blots. **(C)** Monomer bands from the three trials in (B) were quantified by densitometry. Values indicate mean ± one SD. **(D)** HEK293 cells were transfected with PMLII or control plasmid, pXX680, and an AAV2 infectious clone. At 48 hours post-transfection, virus was harvested and production was assayed by qPCR. Values indicate mean fold to control transgene for three separate vector preparations ± SEM. **(E)** HEK293 cells were treated as in (A) for vector groups and as in (D) for virus groups. Protein was harvested at 48 hours and AAV capsid proteins (VP1, VP2, and VP3) and non-structural proteins (Rep78, Rep68, Rep52, and Rep40) were assayed by immunoblotting. Actin serves as a loading control. Blot is representative of three independent experiments. **(F)** HEK293 cells were transfected with pXX680 or carrier DNA and the PMLII or control plasmid 24 hours prior to infection with the indicated dose of AAV2. AAV genome copy number was determined by qPCR at 48 hours post-infection. Data represent three independent experiments. Values indicate mean ± one SD. (*) $p<0.05$ versus control; Also see **Fig. 2.11**

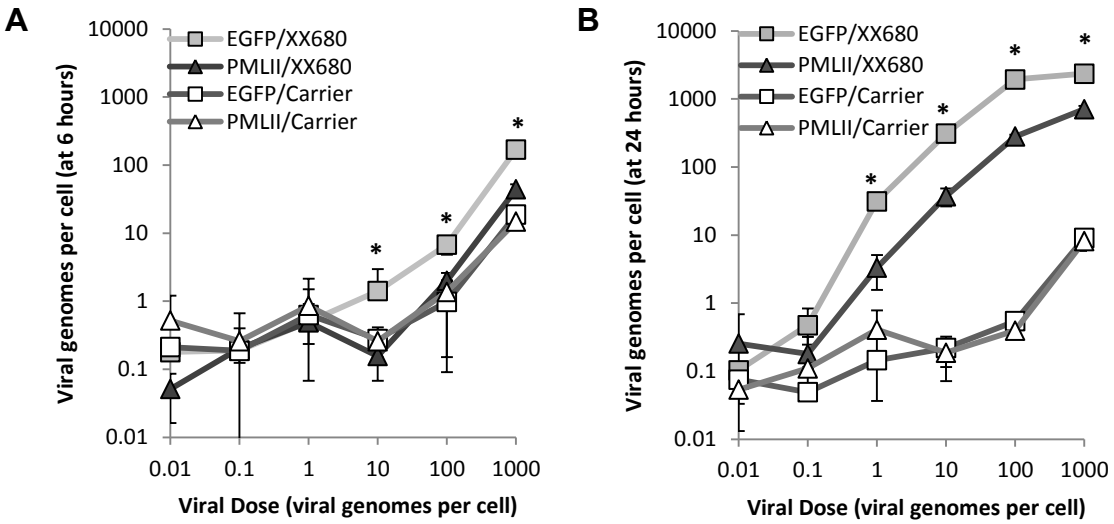

Figure 2.11, related to Figure 2.10. PMLII inhibits the infection of wildtype AAV2. (A-B) HEK293 cells were transfect, seeded and infected with wildtype AAV2 as in Figure 7F. Total DNA was harvested from the cells at either (A) 6 hours or (B) 24 hours post-infection and numbers of viral genomes per cell were determined by qPCR. (*) $p<0.05$

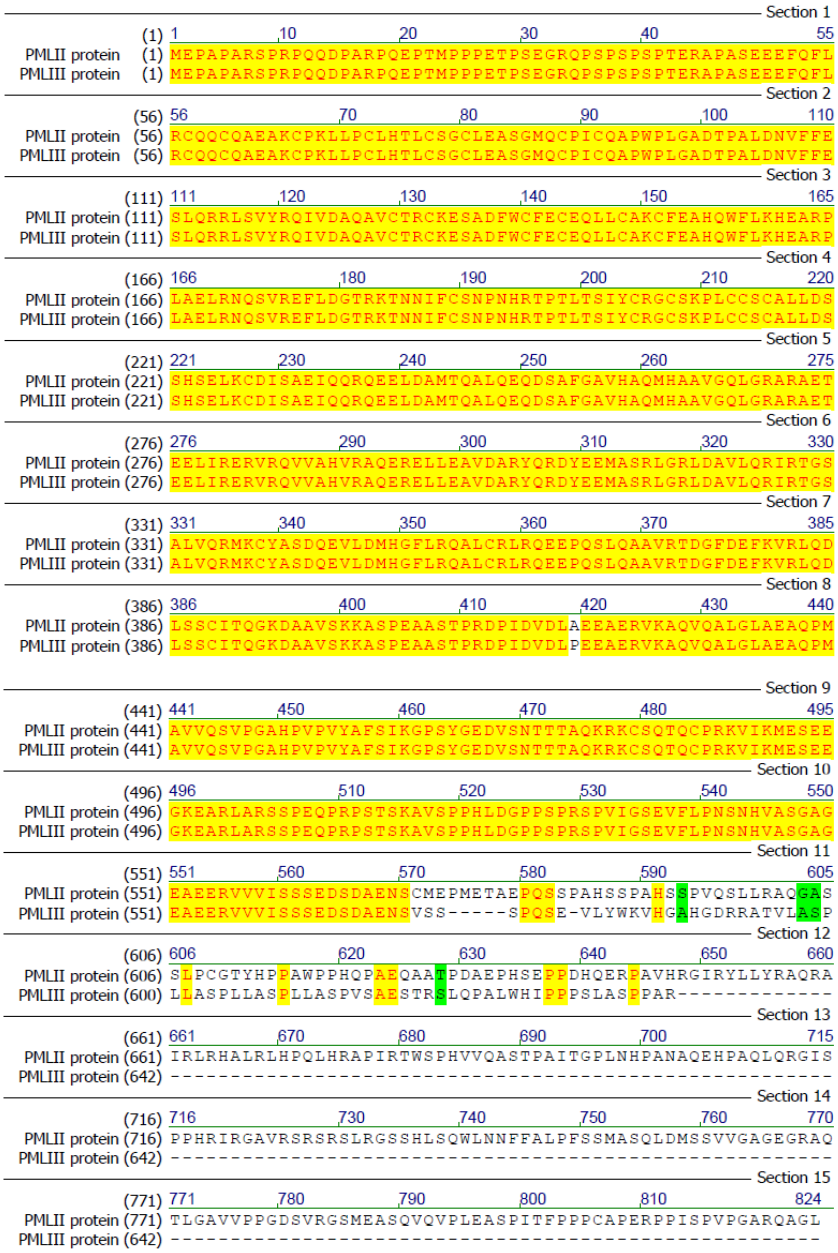

Figure 2.12. Alignment of PMLII and PMLIII protein sequences. Our data in **Fig. 2.8** demonstrated that PMLII has a greater effect on rAAV2 transduction than the other nuclear isoforms of PML. Therefore, the protein sequences of PMLII (accession number AF230403) and the most closely related PML isoform to PMLII, PMLIII (accession number S50913) were aligned to illustrate the similarity and differences between these isoforms. This alignment demonstrates that the extreme C-terminal region of PMLII (amino acids 571-824), unique among the PML isoforms, is responsible for its greater effect on AAV. Interestingly, this unique region is also known to bind adenovirus E4Orf3.

CHAPTER 3

Arsenic trioxide stabilizes accumulations of adeno-associated virus virions at the perinuclear region, increasing transduction *in vitro* and *in vivo*[2]

Summary

Interactions with cellular stress pathways are central to the lifecycle of many latent viruses. Here, we utilize adeno-associated virus (AAV) as a model to study these interactions as previous studies have demonstrated that cellular stressors frequently increase transduction of rAAV vectors and may even substitute for helper virus functions. Since several chemotherapeutic drugs are known to increase rAAV transduction, we investigated the effect of arsenic trioxide (As_2O_3), an FDA approved chemotherapeutic agent with known effects on several other virus lifecycles, on the transduction of rAAV. *In vitro*, As_2O_3 caused a dose-dependent increase in rAAV2 transduction over a broad range of cell lines from various cell types and species (e.g. HEK-293, HeLa, HFF hTERT, C-12, Cos-1). Mechanistically, As_2O_3 treatment acted to prevent loss of virions from the perinuclear region, which correlated with increased cellular vector genome retention, and was distinguishable from proteasome inhibition. To extend our investigation of the cellular mechanism, we inhibited reactive oxygen species formation and determined that the As_2O_3-mediated increase in rAAV2 transduction was dependent upon production of reactive oxygen species. To further validate our *in vitro* data, we tested the effect of As_2O_3 on rAAV transduction *in vivo* and determined that treatment initiated

[2]Adapted for this dissertation from: **Mitchell A.M., Li C., and R.J. Samulski**. 2013. Arsenic trioxide stabilizes accumulations of adeno-associated virus virions at the perinuclear region, increasing transduction *in vitro* and *in vivo*. J Virol **87**: 4571-83.

transgene expression as early as two days post-transduction and increased reporter expression by up to ten-fold. Moreover, the transduction of several other serotypes of rAAV was also enhanced *in vivo*, suggesting As_2O_3 affects a pathway used by several AAV serotypes. In summary, our data support a model wherein As_2O_3 increases rAAV transduction both *in vitro* and *in vivo* and maintains perinuclear accumulations of capsids, facilitating productive nuclear trafficking.

Introduction

Adeno-associated virus (AAV), a non-enveloped, single-stranded DNA virus, is a member of the family *Parvoviridae* and is classified as a dependovirus as it requires the presence of a helper virus, such as adenovirus or herpes simplex virus (HSV), in order to replicate. In the absence of a helper virus, AAV's genome can persist episomally for long time periods (146). The AAV genome consists of two genes, *rep* which encodes the non-structural proteins and *cap* which encodes the capsid assembly protein and capsid proteins, flanked by inverted terminal repeats. To make rAAV vectors, the two viral genes can be entirely removed from the genome with the terminal repeats being the only *cis* elements required for vector production (5), allowing for the examination of the viral transduction pathway leading up to gene expression. Although no pathogenesis has been linked to AAV, rAAV plays an important role as a gene delivery vector and is increasingly used for clinical gene therapy applications (reviewed in (4)).

While there are several naturally occurring serotypes of AAV, the majority of AAV biology has been elucidated using rAAV serotype 2 (AAV2) vectors. rAAV2 is brought into cells through receptor-mediated endocytosis (13) and is trafficked through endosomal pathways, along microtubules, to the microtubule organizing center (MTOC) (14). rAAV2 then escapes from the endosome and is trafficked to the nucleus where it uncoats (15), exposing the genome

for second-strand synthesis and transcription. Several steps in the rAAV transduction pathway are inefficient, including nuclear entry (125) and second strand synthesis (16, 53), and modifying the environment of the cell can lead to increased efficiency in these steps (15, 16). Specifically, several forms of cellular stress, including endoplasmic reticulum stress associated with unfolded protein responses (147), treatment with chemotherapeutic agents (15, 16), and heat shock (16, 148), have been shown to positively influence AAV transduction. In fact, our group was the first to demonstrate that heat shock, hydroxyurea, UV light, and X-rays are capable of increasing rAAV transduction through a mechanism involving the enhancement of second-strand DNA synthesis (16). Two of these treatments, hydroxyurea treatment and UV light in the presence of SV40 T antigen, were later shown to be able to substitute for helper virus functions and allow AAV replication in the absence of adenovirus (149). Moreover, dependence on stress responses in viral lifecycles in not unique to AAV and has in fact been demonstrated to be important to the reactivation of many latent viruses from lambda phage (150) to herpesviruses (151, 152). Although some stress response dependent reactivation is due to disregulation of the immune system (152), some may result from specific changes in the intracellular environment. In addition, the role of stress in the initial transduction of viruses other than AAV is less well understood than its role in latency.

The dependence of the AAV lifecycle on cellular stress has been exploited to attempt to increase the efficiency of rAAV-mediated gene delivery and improve efficacy in clinical gene therapy applications. A number of chemotherapeutic agents have been used to induce cell stress and enhance rAAV transduction including proteasome inhibitors such as MG-132, calpain inhibitor I, and bortezomib, DNA synthesis inhibitors such as hydroxyurea and aphidicolin, and topoisomerase inhibitors such as etoposide and camptothecin (15, 104-106, 109, 153, 154). Thus

far, the leading candidate for enhancing rAAV transduction *in vivo* is bortezomib, a proteasome inhibitor, which has been demonstrated to increase expression of a clinically relevant transgene 3- to 6-fold in a large animal model (109). Although bortezomib is approved for use in humans, it has serious toxic side effects and, in rare cases, its use can lead to liver failure and death (109, 155). Therefore, exploring the possibility of other less toxic agents to enhance rAAV transduction *in vivo* remains an advantageous approach.

One specific cellular stressor that has not been examined for its effect on AAV biology is arsenic trioxide (As_2O_3). As_2O_3 was approved for the treatment of acute promyelocytic leukemia in 2000 (119) and is currently being evaluated treatment of other forms leukemia (120, 121). As_2O_3 is often considered to be a less toxic alternative to traditional chemotherapeutic agents. In fact, clinical studies have been published on the treatment of more than 1100 promyelocytic leukemia patients with As_2O_3 (156) and the side effects of the current course of treatment (five weeks of daily doses) are relatively mild, including dermatological issues, fatigue, and nausea. A comparatively severe cardiac side effect is prolonged QT interval; however, this effect is reversible after treatment ceases and has not led to any As_2O_3 associated deaths (120). Furthermore, oral preparations of As_2O_3 are being investigated and appear to avoid this complication (119). These clinical features make As_2O_3 a promising stressor to consider for use in enhancing rAAV transduction.

Numerous studies have worked to define the mechanisms by which As_2O_3 acts to treat promyelocytic leukemia. When cells are treated with As_2O_3, it is taken up through aqua-glyceroporins and then acts on a molecular level by binding thiol ligands from cysteine residues (157). On a cellular level, As_2O_3 has many effects including inducing reactive oxygen species (ROS) formation (158), inhibiting NFκB activation (159), degrading the promyelocytic leukemia

protein (PML) (160), changing mitochondrial membrane potentials (161), inducing global changes in transcriptional patterns (162), and, at high doses, inducing apoptosis (121, 163). Therefore, As_2O_3 can lead to widespread changes in the cellular environment. In addition, As_2O_3 has previously been demonstrated to have effects on several different viruses. Specifically, As_2O_3 increases human immunodeficiency virus (HIV) infection in non-permissive cell types but has no effect in permissive cell types (164-166). Moreover, treatment of patients with As_2O_3 often leads to the reactivation of varicella zoster virus (VZV) and HSV (167, 168); in fact, the risk of patients developing herpes zoster after As_2O_3 treatment is 26%, which is higher than the 20% risk found with severe immunosuppression after hematopoietic stem cell transplant (167). Indeed, the high rate of herpes reactivation has led some groups to proscribe prophylactic acyclovir during As_2O_3 treatment (119).

As As_2O_3 affects these other viruses and chemotherapeutic agents such as proteasome inhibitors (15, 169) and topoisomerase inhibitors (104) have been demonstrated to enhance rAAV transduction, we determined whether As_2O_3 has an effect on initial rAAV transduction. We utilized rAAV2 vectors and examined transduction both in As_2O_3 treated cells and *in vivo*. We determined that transduction of rAAV2 was enhanced *in vitro* and *in vivo* and that the transduction of several different rAAV serotypes was also enhanced *in vivo*. In addition, we determined that As_2O_3 treatment of cells maintained the accumulation of rAAV2 virions at the MTOC and that this effect was dependent on induction of ROS formation. The enhancement of rAAV transduction by As_2O_3, as well as mechanisms behind this enhancement, has implications for the enhancement of rAAV-mediated gene delivery and possibly for the initial infection pathways of other viruses impacted by As_2O_3.

Materials and Methods

Cell culture and chemicals. HEK-293 cells, HeLa cells, human foreskin fibroblasts immortalized with telomerase (HFF hTERT), and Cos-1 cells were maintained in Dulbecco's modified eagles media. C-12 cells were maintained in minimal essential media (MEM) alpha without ribonucleosides and deoxyribonucleosides and Cho-K1 cells were maintained in Ham's F-12 media. Cell utilized in confocal microscopy experiments were maintained in MEM without phenol red supplemented with 2 mM L-glutamine and 1x MEM non-essential amino acids for at least two passages before imaging. All cells were maintained at 37°C and 5% CO_2 and media was supplemented with 10% fetal bovine serum, 100 U/ml penicillin, and 100 g/ml streptomycin.

As_2O_3 (Sigma-Aldrich) was prepared for *in vitro* use as a 1 mM solution in 200 mM NaOH and compared to a vehicle control of the same pH. For *in vivo* use, a 50 mg/ml solution of As_2O_3 in 1 M NaOH was prepared, diluted to 0.5 mg/ml in PBS, and brought to a neutral pH with HCl. A proteasome inhibitor, MG-132 (Calbiochem), was prepared at 10 mM in DMSO. N-acetyl-L-cysteine (NAC; Sigma-Aldrich) was prepared at 500 mM in PBS. Dihydroethidium (DHE; Sigma-Aldrich) was prepared at 10 mM in DMSO.

Virus production. rAAV vector was produced in HEK-293 cells as has been previously described (52). Briefly, rAAV was prepared by transfection of HEK-293 cells with pXX680, a pXR plasmid (pXR2, pXR6, pXR8, or pXR9 for the different serotypes of rAAV produced), and either pTR-CBA-EGFP or pTR-CBA-Luc. After 48 hours, cells were harvested, lysed and DNase treated. For general use, vector was purified on a cesium chloride gradient and then dialyzed to remove the cesium. To produce pure vector for fluorescent labeling, the vector was purified on a discontinuous iodixanol gradient followed by ion exchange chromatography and dialysis. Vectors were titered by quantitative PCR (qPCR) as has been previously described (52).

Transduction assays. For transduction experiments, 8×10^4 cells were seeded per well of a 24-well plate 16-18 prior to transduction and, where indicated, treated with the stated doses As_2O_3 or vehicle control at the time of seeding. Vector was added in fresh media at the indicated vector dose. For proteasome inhibition experiments, 1 μM MG132 or a DMSO control were added concurrent with transduction. Cells were harvested by trypsinization at 48 hours post-transduction unless otherwise noted. For flow cytometry, trypsinized cells were resuspended in 2% para-formaldehyde and analyzed using a Beckman-Coulter CyAn ADP instrument. EGFP fluorescence was measured using a 488 nm excitation laser and 530/40 nm emission filter.

DNA purification and qPCR of viral genome copy number. For quantification of intracellular vector genome copies (vg), transduced cells were harvested by trypsinization, washed with PBS, and total DNA was harvested using the Qiagen DNeasy Blood and Tissue Kit as per the manufacturer's instructions. Viral genomes and cellular endogenous control genes were quantified as has previously been described (15). Briefly, the following primers were utilized to quantitate EGFP (forward: 5'-AGC AGC ACG ACT TCT TCA AGT CC-3', reverse: 5'-TGT AGT TGT ACT CCA GCT TGT GCC-3'), luciferase (forward: 5'-AAA AGC ACT CTG ATT GAC AAA TAC3', reverse: 5'-CCT TCG CTT CAA AAA ATG GAA C-3'), human LB2C1 (forward: 5'-GTT AAC AGT CAG GCG CAT GGG CC-3', reverse: 5'-CCA TCA GGG TCA CCT CTG GTT CC-3'), mouse β-actin (forward: 5'-TGG CAC CAC ACC TTC TAC AAT-3', reverse: 5'-AGG CAT ACA GGG ACA GCA CA-3'), and hamster GAPHD (forward: 5'-CGT ATT GGA CGC CTG GTT AC-3', reverse: 5'-GGC AAC AAC TTC CAC TTT GC-3'). The human LB2C1 primer set was also used to quantitate Cos-1 cellular genomes. All reactions were run with SyBR Green master mix (Roche Applied Science) on the Roche Lightcycler 480. The following run protocol was used: 95°C 10 minutes; 45 cycles 95°C 10 s,

60°C 10 s, 72°C 10 s. Absolute quantification was performed based 2nd derivative max comparisons to standard curves of plasmid DNA (EGFP and luciferase) or un-transduced cellular DNA.

Cell cycle analysis. For analysis of the proportion of cells in each stage of the cell cycle, cells were treated overnight with As_2O_3 as for transduction assays and then harvested at the conclusion of As_2O_3 treatment. Propidium iodide staining was performed as has been previously described (170), with slight modifications. Briefly, cells were washed twice with PBS + 0.1% fetal bovine serum then fixed in ethanol overnight. After fixation, cells were washed and then resuspended in the propidium iodide staining solution (40 μg/ml propidium iodide [Sigma-Aldrich] in PBS with 3.8 mM sodium citrate) and 0.5 μg RNase A (Sigma-Aldrich) and allowed to stain for at least 3 hours at 4°C. DNA content was analyzed by flow cytometery at a low rate of flow. Flow cytometry was performed on the Beckman-Coulter CyAn ADP instrument using a 488 nm excitation laser and a 613/20 nm emission filter.

Capsid labeling and confocal microscopy. rAAV2 virions were fluorescently labeled with Cy5 and used for confocal imaging as has been previously described (171), with slight modifications. Briefly, pure rAAV2 virions were incubated with 5000 molecules of mono-NHS-Cy5 (GE Healthcare) per vector genome for 45 minutes at room temperature and then extensively dialyzed to remove excess dye. Labeled vector was titered by qPCR. For confocal imaging experiments, Cho-K1 cells were seeded and treated with As_2O_3 as in transduction experiments on poly-L-lysine coated coverslips. Cy5 labeled rAAV2 was added to the cells at 10 000 vg/cell 16-18 hours after seeding. At the time of harvest, cells were washed three times with PBS, fixed with 2% paraformaldehyde for 15 minutes at room temperature, washed 2 times with

PBS and 1 time with ddH_2O, and mounted on slides with ProLong Gold Antifade Reagent with DAPI (Molecular Probes).

For confocal microscopy, rAAV2 virion localization was analyzed with a Zeiss LSM 710 Spectral Confocal Laser Scanning microscope using a Plan-Apochromat 63x/1.40 oil objective. Z stacks of 12-14 focal planes were acquired at 0.63 μm Z intervals and these images were used to create 3D reconstructions. Images were deconvoluted using the AutoQuant X3 program (MediaCybernetics) to perform 3D blind adaptive point spread function deconvolution. The IMARIS software package (Bitplane AG) was used to create 3D projections of the stacks.

Reactive oxygen species quantification and scavenging. Cells were seeded and treated as for transduction experiments. For ROS scavenging experiments, NAC was added to cells at the indicated doses at the time of As_2O_3 treatment. The NAC and As_2O_3 were removed at the time of transduction and transduction was assayed as above. Quantification of ROS levels by DHE staining has been previously described (172). Briefly, cells were harvested by trypsinization 16-18 hours after treatment, washed twice with PBS, and then incubated for 30 min at 37°C in 10 μM DHE in PBS. After incubation, the cells were washed once with PBS. Flow cytometry was performed on the Beckman-Coulter CyAn ADP instrument using a 488 nm excitation laser and a 575/25 nm emission filter.

***In vivo* transduction assays.** All mouse experiments were conducted in accordance with the policies of the University of North Carolina at Chapel Hill's Institutional Animal Care and Use Committee. For *in vivo* transduction experiments, age and strain matched female mice (Jackson Laboratories) were treated with 5 μg/g/day As_2O_3 or a PBS vehicle control by intraperitoneal (i.p.) injection for five days. On the third day of treatment, mice were transduced with the indicated dose of AAV vector in PBS by retro-orbital injection. Live imaging of

luciferase expression from AAV vectors has been previously described (173). Briefly, mice were given 150 mg/kg D-luciferin (Caliper LifeSciences) by i.p. injection, and, after 5 minutes, luminescence was measured using the IVIS-Lumina imaging system (Caliper LifeSciences). The Igor Pro 3.0 software was used to quantitate luminescence signals.

Results

Arsenic trioxide treatment increases the percentage of cells transduced with rAAV2.

To expand our knowledge of AAV's responses to cellular stressors, we set out to determine whether As_2O_3 treatment had an effect on rAAV2's initial transduction. We first treated HEK-293 cells overnight with varying doses of As_2O_3, then transduced with rAAV2-EGFP and assayed the percentage of cells transduced after 48 hours. After As_2O_3 treatment, we observed a dose-dependent increase in the percentage of cells transduced by rAAV2 (**Fig. 3.1A**), with a maximum increase of 19.4-fold in the eight μM As_2O_3 group. Due to toxicity from higher As_2O_3 concentrations (data not shown), further experiments were conducted in HEK-293 cells with the 4 μM As_2O_3 dose to verify that the increase in the percentage of cells transduced observed with As_2O_3 treatment was due to an increase in transduction and not an increase in transgene expression. We assayed the numbers of vector genomes present in the cells 48 hours post-transduction and determined that the increase in the intracellular vector genome copy number correlated very well with the percentage of cells transduced (**Fig. 3.1B**). In addition, we observed no increase in transgene expression from a plasmid carrying the transgene cassette following As_2O_3 treatment (data not shown). To determine whether As_2O_3's transduction effect is stable over time, we treated the cells as before, assayed transduction from 24 to 96 hours post-transduction, and determined that As_2O_3 increased transduction to a similar extent at all of the

time points assayed (**Fig. 3.1C**). Furthermore, we also investigated whether the effect of As_2O_3 would be maintained at a range of vector doses. In fact, we observed significant increases in transduction with As_2O_3 treatment with rAAV2 doses from 250 to 4000 vg/cell (**Fig. 3.1D**). The increase in the numbers of vector genomes per cell in both the vehicle treated and As_2O_3 treated cells was linear (R^2 values 0.996 and 0.999 respectively).

The effects of As_2O_3 treatment on HIV infection can only be observed in non-permissive cell types (164-166); therefore, given the increase in rAAV2 transduction observed with As_2O_3 treatment in HEK-293 cells, we tested the effect of As_2O_3 in other human and non-human cell lines. We optimized rAAV2 doses to result in 5-10% of cells transduced without treatment and performed dose curves to identify doses of As_2O_3 capable of increasing rAAV2 transduction without overt toxicity (data not shown), as sensitivity of cells to As_2O_3 varies based on cellular glutathione levels (158). In HeLa cells, which have been commonly utilized as a model cell line for exploring AAV biology, we observed a 2.4-fold increase in AAV2 transduction following As_2O_3 treatment that correlated well with an increase in the vector genome copy number (**Fig. 3.2A**). We then investigated a human diploid cell line, HFF hTERT. In these cells, we observed a 4.2-fold increase in the percentage of cells transduced with rAAV2; however, the increase in the vector genome copy number was smaller, although still significant (**Fig. 3.2B**).

To determine whether the effect of As_2O_3 on rAAV2 transduction is restricted to human cells, we investigated the effect of As_2O_3 in several non-human cell lines. In Cos-1 cells, which are of non-human primate origin, we observed a 2.7-fold increase in the percentage of cells transduced that correlated well with an increase in the vector genome copy number (**Fig. 3.2C**). As rAAV2 is liver-tropic, we next investigated the effect of As_2O_3 on transduction of a mouse hepatoma derived cell line, C-12 cells. As_2O_3 treatment increased the percentage of cells

transduced with rAAV2 by 4.2-fold in this cell line and this increase correlated well with the increase in the vector genome copy number (**Fig. 3.2D**). Finally, we tested the effect of As_2O_3 in Cho-K1 cells, which are hamster cells with normal protein modification pathways, and observed a 5.0-fold increase in the percentage of cells transduced with As_2O_3 treatment, although the increase in the vector genome copy number was smaller (**Fig. 3.2E**). Therefore, the increase in transduction observed after As_2O_3 treatment is not restricted to a specific cell type or to a specific species origin.

Arsenic trioxide acts in the first 24 hours of transduction through a post-entry mechanism. To gain mechanistic insights into the actions of As_2O_3 on rAAV2 transduction, we first examined the effect of As_2O_3 on self-complementary rAAV2 transduction, which does not require second-strand DNA synthesis. We determined that As_2O_3 caused a similar increase in rAAV transduction with both single-stranded (ssAAV) and self-complementary (scAAV) rAAV, suggesting that As_2O_3 affects a step in rAAV transduction prior to second-strand synthesis (**Fig. 3.3A**). To determine when after transduction this effect occurs, we investigated the effect of the timing of As_2O_3 addition on the transduction of rAAV2. We treated cells with As_2O_3 from -18 hours, 0 hours, 3 hours, 7 hours, or 24 hours post-transduction to the time of harvest and assayed the percentage of cells transduced with rAAV2. We observed that the majority of the As_2O_3 effect was confined to pre-treatment and treatment within the first 24 hours of transduction (**Fig. 3.3B**). Since As_2O_3 acts in the first 24 hours of transduction (**Fig. 3.3B**) and the vector genome copy number is increased similarly to the percentage of cells transduced at 48 hours post-transduction (**Fig. 3.1B**), we then investigated the change in numbers of intracellular vector genomes over time. The vector genome copy number was similar between As_2O_3 and vehicle treated cells until 15 to 18 hours post-transduction; however, vector genome copy number in the

vehicle treated cells then decreased at a faster rate than that of As_2O_3 treated cells (**Fig. 3.3C**). The difference in the percentage of cells transduced at each time point correlated well with the difference in the vector genome copy numbers (data not shown). These data suggest that the effect of As_2O_3 occurs after rAAV2 has entered the cell and prior to second-strand DNA synthesis. To determine whether the increase in rAAV vector genome copy number or transduction might be due to inhibition of the cell cycle following As_2O_3 treatment, we treated cells overnight with As_2O_3 or a vehicle control and then measured the proportion of cells in each stage of the cell cycle. We determined that there was very little or no change in the percentage of cells in each cell cycle stage following As_2O_3 treatment (**Fig. 3.3D**) and that any changes were within the range of variability between experiments. These data are substantiated by our toxicity assays in which equal numbers of total and viable cells were observed following As_2O_3 treatment (data not shown). Given these data, it is unlikely that the 3 to 4-fold changes in rAAV transduction and vector genome copy number could result from a decrease in cell division rates. Therefore, these data suggest that the increase in vector genome copy number and in rAAV transduction is not due to cell cycle arrest but instead due to another change in the intracellular environment.

Increased vector copy number is also observed with proteasome inhibition of AAV transduced cells, which induces the nucleolar localization of rAAV2 (15); therefore, we investigated whether the effects of proteasome inhibition and As_2O_3 treatment on AAV2 transduction overlap. When cells were pretreated with As_2O_3 then co-treated with a proteasome inhibitor, MG132, and rAAV2, there was no additional increase in the percentage of cells transduced between MG132 alone and the MG132/As_2O_3 treatment. However, the median fluorescence intensity (MFI) of the positive cells was greater for the combined MG132/As_2O_3

treatment than for MG132 alone (**Fig. 3.3E**). As both of these drugs appear to act through post-entry mechanisms, this may suggest that the combination of the drugs leads to more successful intracellular trafficking, despite the lack of increase in the numbers of cells transduced when the drugs were combined; nevertheless, the additional increase in the MFI with MG132 and As_2O_3 treatment suggests at least partially independent mechanisms for these two drugs.

Arsenic trioxide treatment stabilizes accumulations of rAAV2 virions over time and acts through reactive oxygen species formation. To determine whether the slower rate of vector genome loss we observed occurred on the level of the virion or on the level of the genome, we transduced Cho-K1 cells, which are amenable with imaging techniques, with fluorescently labeled rAAV2 virions and tracked their intracellular trafficking through confocal microscopy after either vehicle or As_2O_3 pre- and co-treatment. Previous observations have suggested that rAAV traffics to the perinuclear region on microtubules where it accumulates and then some portion of virions proceeds to the nucleus where uncoating occurs (14, 15, 174). At 8 hours post-transduction, a time at which the vector genome copy number was similar between vehicle and arsenic treated HEK-293 cells (**Fig. 3.3A**), we observed very little difference in the localization of virions between the vehicle (**Fig. 3.4A**) and As_2O_3 (**Fig. 3.4B**) treated cells. However, at 24 hours post-transduction, although we observed some perinuclear accumulation of virions with vehicle treatment (**Fig. 3.4C**), much larger perinuclear accumulations of virions were present in As_2O_3 treated cells (**Fig. 3.4D**). This effect was even more pronounced at 32 hours post-transduction when many vehicle treated cells had few or no AAV virions remaining (**Fig. 3.4E**), but As_2O_3 treated cells still had large, condensed perinuclear accumulations of virions (**Fig. 3.4F**). We observed no clear differences in the amount or localization of intact

virions in the nucleus at any of these time points. Together, these data suggest that As_2O_3 prevents the loss of intracellular rAAV2 virions during transduction.

Many cellular effects of As_2O_3 are mediated through the formation of ROS (reviewed in (175)). Consequently, we investigated whether the effect of As_2O_3 on rAAV2 transduction was mediated by ROS formation. When cells were treated with increasing doses of As_2O_3, we observed a dose-dependent increase in the levels of intracellular ROS as evidenced by increased red fluorescence following DHE staining of treated cells (**Fig. 3.5A**). Specifically, significant increases in the MFI were observed with the 2 μM, 4 μM, and 8 μM As_2O_3 treatments (**Fig. 3.5C**). As the dose-dependent increase in ROS mirrors the dose-dependent increase in AAV2 transduction following As_2O_3 treatment, we then investigated whether inhibiting ROS formation, by treating cells with N-acetyl-L-cysteine (NAC), would inhibit the transduction effects of As_2O_3. We treated cells overnight with As_2O_3 and NAC, transduced with rAAV2, and measured the levels of ROS species present at the time of transduction and the percentage of cells transduced 48 hours post-transduction. Although treatment with As_2O_3 induced ROS formation, treatment with NAC caused a dose-dependent decrease in ROS formation, where 10 mM NAC treatment of As_2O_3 treated cells resulted in a population that overlaid that of the vehicle control (**Fig. 3.5B**). When we assayed for transduction, we observed a dose-dependent decrease in transduction following NAC and As_2O_3 co-treatment compared to treatment with As_2O_3 alone (**Fig. 3.5D**). NAC had no effect on the transduction of vehicle treated cells. These data suggest that As_2O_3 acts through the formation of ROS, leading to a decrease in the loss of rAAV2 virions over time and so to increased AAV transduction.

Arsenic trioxide increases rAAV2 transduction *in vivo*, but does not change tropism. To determine whether the increase in rAAV2 transduction we observed with As_2O_3 *in vitro* could

be replicated *in vivo*, we treated mice for five days with a dose of 5 μg/g/day As_2O_3, which replicates the levels of serum As_2O_3 observed in promyelocytic leukemia patients treated with this drug (176, 177). With this dose of As_2O_3, we observed no weight loss or overt toxicity and no increase in serum liver enzyme levels (alanine aminotransferase [ALT] and aspartate aminotransferase [AST]) over those of the vehicle control, suggesting a lack of acute liver toxicity (data not shown). We transduced mice systemically with 2×10^{11} vg rAAV2-luciferase on the third day of As_2O_3 treatment and measured transduction through luciferase live imaging. We observed measurable luciferase activity in As_2O_3 treated mice at as early as 2 days post-transduction, at which time the activity of vehicle treated mice was close to background (**Fig. 3.6A**). By day 7 post-transduction, all As_2O_3 treated mice were expressing strongly, while the vehicle treated mice were showing early, low levels of expression (**Fig. 3.6B**). Furthermore, when we quantified expression in the whole mouse (**Fig. 3.6C**) or the area of the liver alone (**Fig. 3.6D**) we observed significant increases in transduction at 5 days to 12 days post-transduction. In fact, at day five post-transduction, the As_2O_3 treated mice had liver expression 19.3-fold greater than that of the vehicle treated mice (**Fig. 3.6D**). These data suggest that As_2O_3 can increase rAAV2 transduction *in vivo*. To confirm the increased expression observed in our live imaging data, we harvested the organs from mice at 14 days post-transduction and performed biodistribution experiments. In the liver, we observed a 3.8-fold increase in normalized luciferase activity with As_2O_3 treatment and minimal expression in the other organs tested (data not shown). Furthermore, analysis of vector genome copy number suggested no changes in vector tropism due to As_2O_3 treatment (data not shown). These data suggest that As_2O_3 can increase rAAV2 transduction *in vivo* without altering vector tropism.

Arsenic trioxide increases the transduction of several serotypes of AAV *in vivo*. To determine whether As_2O_3's effect is specific to rAAV2 or can be applied to other rAAV serotypes, we treated mice with As_2O_3 as before, transduced with 1×10^{11} vg rAAV6, rAAV8, or rAAV9, and assayed transduction by luciferase live imaging. With rAAV6, we observed a clear increase in transduction at day 7 post-transduction (**Fig. 3.7A**), which could also be observed at 14 days post-transduction (data not shown). Quantification of this increase demonstrated a 5.5-fold enhancement at day 7 (**Fig. 3.7B**). With rAAV8, we observed an enhancement of transduction from As_2O_3 treatment at day 2 post-transduction (**Fig. 3.7C**), which was quantified at 3.0-fold (**Fig. 3.7C**); however, this enhancement was not observed at later time points (data not shown). Finally, with rAAV9, we observed an enhancement of transduction at day five post-transduction (**Fig. 3.7E**), which was quantified at 4.2-fold (**Fig. 3.7F**). In fact, As_2O_3 enhanced in rAAV9 transduction from 2 days post-transduction through 3 weeks post transduction (**Fig. 3.7G, 3.7H,** and data not shown). Therefore, the enhancement of transduction caused by As_2O_3 treatment is not unique to rAAV2 but can also be observed with several other serotypes of rAAV.

Discussion

In this study, we investigated the effect of As_2O_3 on the initial transduction of rAAV vectors. We determined that As_2O_3 increased rAAV2 transduction both *in vitro* and *in vivo* and that, with As_2O_3 treatment, perinuclear accumulations of rAAV virions were maintained over time, leading to the increase in the intracellular vector genome copy number observed during transduction. We observed increased rAAV2 transduction with As_2O_3 at several vector doses, time points, and in several cell lines with different tissue and species origins, suggesting that the

effect of As_2O_3 on rAAV transduction is wide spread. As the increased numbers of cells transduced correlated with an increase in vector genome copy number (**Fig. 3.1B**) and As_2O_3 had no effect on transgene expression independent of rAAV (data not shown), we determined that the effect of As_2O_3 on rAAV transduction occurs at a step in transduction prior to gene expression. In addition, the fold increase in rAAV transduction caused by As_2O_3 treatment was stable from 24 to 96 hours post-transduction (**Fig. 3.1C**) and was observed *in vivo* in cell types which divide very slowly (**Fig. 3.6** and **Fig. 3.7**); this suggests that the increase in transduction observed was not due to any possible difference in cell division rates as, in this case, we would expect the difference in transduction to be minimal *in vivo* and, *in vitro*, to increase over time as vector copies were diluted in untreated cells. Furthermore, we analyzed the portion of cells in each stage of the cell cycle following As_2O_3 treatment and observed no indications of cell cycle arrest (**Fig. 3.3D**). Instead, this suggests that the difference in transduction and in intracellular genome copy number is due to a difference in the intracellular transduction pathway of rAAV. Consequently, we investigated the intracellular fate of the rAAV through both molecular and imaging techniques.

Our data demonstrate that the intracellular vector genome copy number was similar between vehicle and As_2O_3 treated cells out to 15 to 18 hours post-transduction and then the vector genome copy number decreased more quickly in vehicle treated cells than in As_2O_3 treated cells (**Fig. 3.3C**). This correlates well with our confocal imaging data which demonstrate an increased persistence of the perinuclear accumulation of rAAV virions in As_2O_3 treated cells (**Fig. 3.4**). These data suggest a model in which, both in As_2O_3 treated and untreated cells, rAAV virions enter the cell and are trafficked along microtubules to the MTOC where they accumulate (14, 174). At the MTOC, the virions can continue their trafficking either productively by

trafficking to the nucleus or non-productively by eventually being targeted for degradation by proteasomal or lysosomal means. Without treatment, many rAAV virions are targeted for degradation, leading to relatively few virions continuing on their productive pathway (**Fig. 3.8A**). With As_2O_3 treatment, fewer virions are degraded leading to viral stability in the perinuclear region and an increase in the productive trafficking of virions (**Fig. 3.8B**). This difference in the trafficking pathways then causes the difference in vector genome copy number and transgene expression observed.

The assertion that virions maintained at the perinuclear region are capable of continuing their trafficking productively is supported by recent work demonstrating that the perinuclear region acts as a sink for rAAV particles and, thus, that disruption of the MTOC shortly after rAAV has accumulated can lead to increased rAAV transduction (P.J. Xaio and R.J. Samulski, unpublished data). In this study however, we are examining later time points during which perinuclear accumulations are generally being cleared and are preventing virion degradation at the perinuclear region. Taken together, the previous work and our data suggest that maintaining the perinuclear accumulation of rAAV, rather than allowing it to be degraded over time, may allow more virions to escape from this region and continue down a productive transduction pathway. In addition, previous work has suggested that rAAV virions are carried on microtubules in endosomal compartments to the MTOC where endosomal escape presumably occurs (14). This suggests that perhaps, if virions remain in the perinuclear region for longer periods of time, more virions can be released from endosomes and escape perinuclear retention to continue on a productive trafficking pathway to the nucleus.

Proteasome inhibitors, such as MG132, have previously been demonstrated to lead to increased nucleolar accumulation of rAAV virions and to increased intracellular vector genome

copy number, leading to higher transduction (15). Given the probable role of degradation in the effect of As_2O_3 on rAAV transduction, we find it interesting that As_2O_3 and MG132 have at least partially independent effects on rAAV transduction (**Fig. 3.3E**) and appear to act at different levels on the intracellular trafficking of rAAV (**Fig. 3.4**, (15)). This suggests one of the following possibilities: 1. rAAV virions are being degraded in significant numbers by a non-proteasomal mechanism that As_2O_3 affects, leading to the separate roles of MG132 and As_2O_3; 2. MG132 increases rAAV transduction through a mechanism that is separate from inhibition of the proteasome and so the decrease in degradation observed with As_2O_3 is separated from that of MG132; or, 3. MG132 and As_2O_3 each have partial effects on the proteasomal degradation of rAAV in separate steps in intracellular trafficking, perhaps in perinuclear degradation for As_2O_3 and in nuclear degradation for MG132, leading to their separate effects. We are currently investigating the specific mechanisms of rAAV degradation modified with As_2O_3 treatment, which should lend clarity to these issues.

In addition to rAAV2, we investigated the ability of As_2O_3 to enhance the transduction of several other rAAV serotypes *in vivo*. As_2O_3 enhanced the transduction of rAAV6, rAAV8, and rAAV9 *in vivo* early after transduction (**Fig. 3.7**); however, the kinetics of the enhancement varied based on the serotype. Specifically, As_2O_3 enhanced the transduction of rAAV2 and rAAV9 at time points ranging from 2 days post-transduction to 14 days or more post-transduction, while rAAV8's transduction is enhanced at 2 days post-transduction but not at later time points (**Fig. 3.6**, **Fig. 3.7,** and data not shown). This is of interest as it suggests that there is capsid specificity in the response to As_2O_3, perhaps derived from differences in intracellular trafficking patterns or efficiencies with different serotypes. Although the intracellular trafficking of rAAV2 has been most thoroughly studied, several reports have begun to compare the

trafficking pathways of different rAAV serotypes. For instance, rAAV1 and rAAV5 can traffic to the nucleus of HeLa cells more quickly than rAAV2, but have lower transduction due to either poor uncoating or rapid degradation, respectively (178). In addition, a recent report suggested that, perhaps due to differences in receptor usage, rAAV2 and rAAV8 differentially traffic through endosomal compartments and have different requirements for endosomal escape (179). Specifically, rAAV2 is reported to traffic through early, recycling, and late endosomes and to require low pH for endosomal escape, while rAAV8 does not traffic through late endosomes, only early and recycling endosomes, and low pH is not sufficient for its endosomal escape. Given the difference in the kinetics of As_2O_3's effect on rAAV2's and rAAV8's transduction, this may suggest a role for endosomal trafficking in the As_2O_3 effect. Determining the role of endosomes in As_2O_3's transduction effect and determining the specific regions of the capsid responsible for the differences in the As_2O_3 effect will be interesting avenues to pursue in the future.

As_2O_3 has well known effects on cellular concentrations of ROS and ROS are thought to act as intermediates in some of As_2O_3's other cellular effects; therefore, we investigated whether the effects of As_2O_3 on rAAV2 transduction were mediated through ROS formation. We determined that As_2O_3 causes a dose-dependent increase in ROS that corresponds well to the dose-dependent increase in rAAV2 transduction and that inhibiting the formation of ROS inhibits As_2O_3's enhancement of rAAV2 transduction (**Fig. 3.5**). Interestingly, ROS formation has previously been demonstrated to be important for enhancement of rAAV transduction by hydroxyurea and UV light and a role for second-strand DNA synthesis was suggested (16, 180), although later reports questioned this assertion (15, 181). As we determined that As_2O_3 can enhance the transduction of self-complementary rAAV2 (**Fig. 3.3A**), which does not require

second-strand synthesis, and also observed changes in earlier steps in transduction (**Fig. 3.4**), it is unlikely that As_2O_3 is acting through enhancement of second-strand synthesis. Furthermore, although hydroxyurea acts through ROS, similar to As_2O_3, it increases the nuclear localization of rAAV2 without increasing the intracellular vector genome copy number (15), whereas As_2O_3 increases vector genome copy number (**Fig. 3.1B**) and acts at an earlier step in transduction (**Fig. 3.4**). This suggests that, depending on the initiator, ROS can act on several different steps in rAAV's transduction pathway. In this case, ROS may have a broad role on a number of steps AAV's lifecycle.

As_2O_3 has many effects on the cellular level, involving ROS formation, which may play a role in its enhancement of rAAV transduction. For instance, As_2O_3 has been shown to inhibit NFκB activation by directly binding a cysteine residue on the activation loop of the protein (159); however, as the concentration of As_2O_3 necessary to inhibit NFκB activation was higher than those used in our studies and the timing of As_2O_3 addition was different, the status of NFκB activation in our experiments is unclear. Several studies have suggested a positive role for NFκB activation in rAAV transduction (181, 182) and, in fact, several other ROS generators such UV light and H_2O_2 have been shown to increase NFκB activation, although this activation was not necessary for their effects on AAV transduction (180, 181). Nevertheless, it will be enlightening to explore the role of NFκB in As_2O_3 mediated enhancement of rAAV transduction further. Another effect of As_2O_3 and ROS is to degrade the promyelocytic leukemia protein (160), which has well known cell-intrinsic antiviral activities against many different viruses (reviewed in (126)). However, we observed an increase in rAAV2 transduction with no apparent change in PML levels or localization and, in addition, could observe an increase in transduction in the absence of PML (data not shown). These data suggest that PML is not a key factor in the effect

of As_2O_3 on rAAV transduction. Therefore, identification of the specific cellular mechanisms responsible for the enhancement of rAAV transduction upon As_2O_3 treatment will continue to be an interesting avenue of research.

As_2O_3 has several known effects on other viruses, either inhibiting or enhancing their replication. As_2O_3 strongly inhibits hepatitis C virus replication through a mechanism involving ROS and independent of PML (183, 184); although the specific mechanism has not been elucidated, this is interesting as As_2O_3's enhancement of rAAV transduction is also mediated by ROS and independent of PML. Moreover, the replication of several other viruses is enhanced by As_2O_3 treatment. As_2O_3 causes an enhancement of HIV replication only in non-permissive cell types in a manner that depends on the expression of TRIM5α and APOBEC3G (165, 166). It is noteworthy that the effects of As_2O_3 on HIV are cell line specific, while the effects on AAV are more general, and that As_2O_3 acts on HIV through two cellular proteins which are unlikely to, or known not to, interact with AAV (185). This suggests that, although As_2O_3 has effects on several viruses, the effects may be caused by widespread, diverse mechanisms.

Interestingly, several lines of evidence have suggested that trivalent arsenic can induce lytic replication in alpha- (HSV, VZV), beta- (human cytomegalovirus [HCMV]), and gamma- (Epstein-Barr virus [EBV]) herpesviruses (167, 168, 186, 187). Specifically, reactivation of HSV and VZV has been observed in acute promyelocytic leukemia patients treated with As_2O_3 at a rate higher than that found with general immunosuppression and in a manner which is not consistent with reactivation from immunosuppression (167, 168). To our knowledge, no studies have been published investigating the mechanism for the reactivation of HSV or VZV in response to As_2O_3. However, activation of EBV replication in response to As_2O_3 was correlated with the degradation of PML, although no direct evidence of a link was presented (187), while

the induction of HCMV immediate early gene synthesis by sodium arsenite, another trivalent arsenic compound, was suggested to be the result of heat shock protein activation (186). Overall, the mechanisms for herpesvirus reactivation following As_2O_3 treatment remain incompletely understood and delving into the mechanisms by which As_2O enhances the replication of other viruses may led to useful insights into herpesvirus reactivation. For instance, as cellular degradation pathways may play a role in the enhancement of rAAV2 transduction by As_2O_3, it would be interesting to determine whether there is a role for these pathways in As_2O_3 mediated reactivation of HSV or VZV.

In addition to elucidating possible mechanisms to explore in the effect of As_2O_3 on the replication of other viruses, the enhancement of rAAV transduction observed with As_2O_3 treatment may become important for gene therapy applications. We observed an increase in rAAV2 transduction both *in vitro* (**Fig. 3.1**, **Fig. 3.2**) and *in vivo* in several serotypes of rAAV with no apparent toxicity (**Fig. 3.6**, **Fig. 3.7**, data not shown). For some gene therapy applications, especially those involving systemic gene delivery, low levels of transgene expression or loss of transgene expression over time have limited the efficacy observed in clinical settings (86, 88). Pharmacological treatments are a promising approach to increasing rAAV transduction in order to address these issues, particularly when pharmacological agents currently approved for use in humans are utilized. In fact, bortezomib, a proteasome inhibitor, has been used in large animal models to enhance rAAV transduction (109); however, the serious and even fatal side effects associated with this drug makes its clinical use for enhancement of rAAV transduction problematic (109, 155). For this reason, identifying other agents, such as As_2O_3, capable of enhancing rAAV transduction is important to the clinical applications of rAAV. In addition, investigating the mechanism behind the increase in transduction observed

with pharmacological treatments may allow us to identify steps in transduction or cellular factors which limit rAAV transduction and to design other strategies to circumvent these difficulties. Therefore, our data demonstrating that As_2O_3 increases the transduction of rAAV vectors both *in vitro* and *in vivo* and suggesting that it acts to stabilize perinuclear accumulations of rAAV in a way dependent on ROS may broaden our toolkit for understanding AAV biology and improving its gene therapy applications. In conclusion, pursuing the biology behind the effects of As_2O_3 on rAAV transduction may have important implications both for AAV mediated gene therapy and for elucidating the mechanism by which As_2O_3 affects the replication of other clinically relevant viruses.

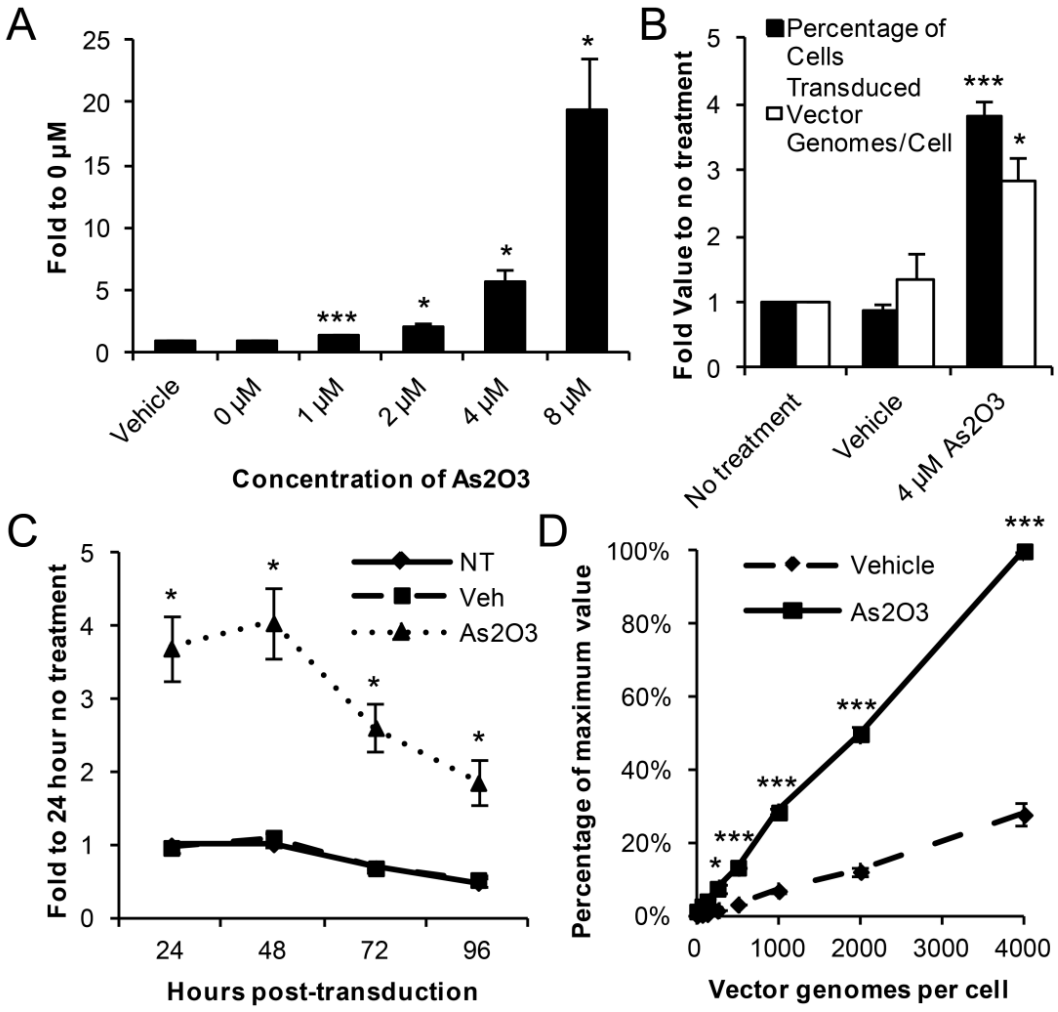

Figure 3.1: HEK-293 cells transduced by rAAV2 after As_2O_3 treatment. HEK-293 cells were treated overnight with As_2O_3 or a vehicle control and then transduced with rAAV2-CBA-EGFP. **(A)** Cells were treated with the indicated dose of As_2O_3 and transduced with 500 vg/cell rAAV2. The percentage of cells transduced at 48 hours post-transduction is shown as a fold value to the 0 µM treatment group. **(B)** The numbers of vector genome copies per cell present and percentages of cells transduced were assayed at 48 hours post-transduction following the indicated treatment and transduction with 500 vg/cell. Values are indicted as fold to the no treatment group. **(C)** Cells were treated and transduced as in (B), harvested at the indicated time points, and assayed for the percentage of cells transduced. Values are indicated as fold to 24 hour no treatment group. (NT) no treatment, (Veh) vehicle. **(D)** After treatment as in (B), cells were transduced with the indicated doses of rAAV2 and the percentage of cells transduced was assayed at 48 hours post-transduction. Values represent the percentage of the maximum value reached in each experiment. Data shown are the mean of at least 3 independent experiments; error bars represent the SEM. (*) $p < 0.05$, (***) $p < 0.005$ based on comparisons of sample means by the Student's t-test.

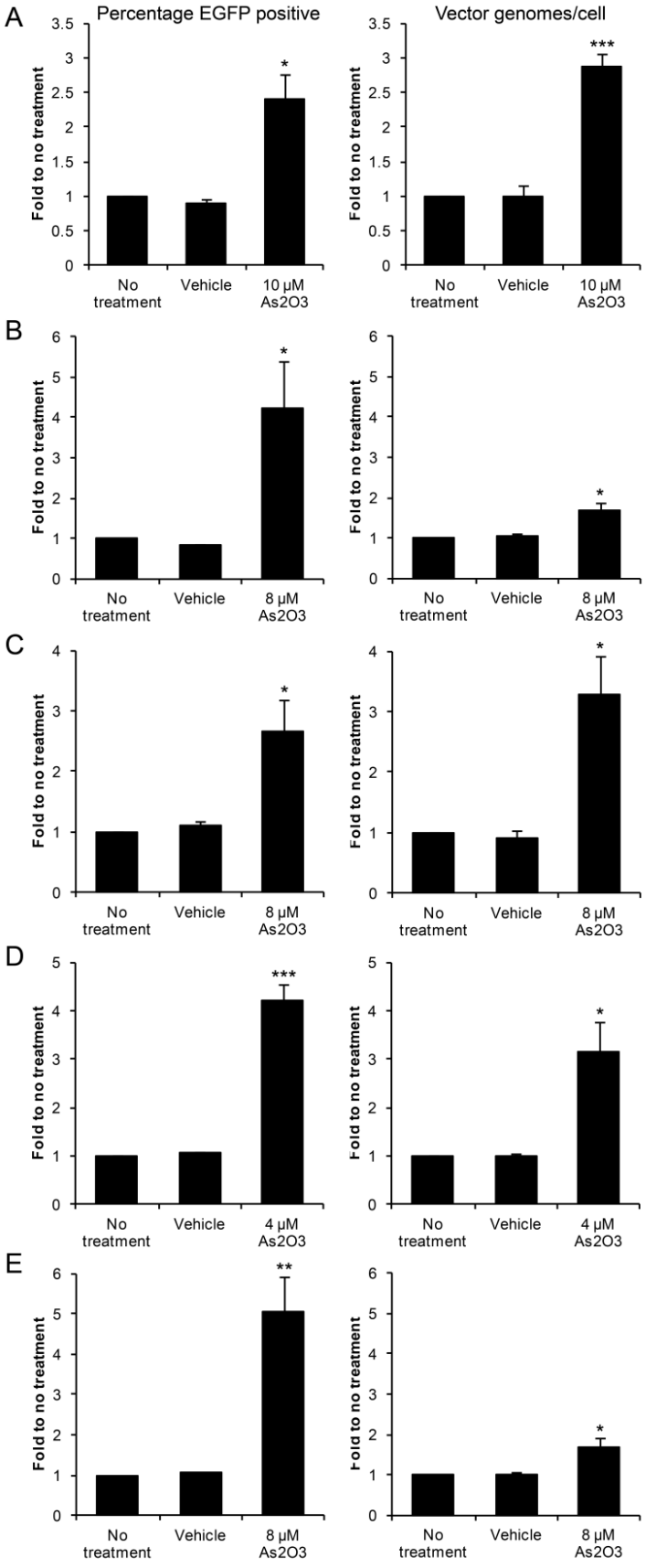
A
Percentage EGFP positive
Vector genomes/cell
Fold to no treatment
No treatment
Vehicle
10 μM As2O3
B
8 μM As2O3
C
8 μM As2O3
D
4 μM As2O3
E
8 μM As2O3

Figure 3.2: rAAV2 transduction after As_2O_3 treatment of several human and non-human cell lines. Cells were treated overnight with the indicated doses of As_2O_3 and a cell line specific dose of rAAV2. The percentage of cells transduced (left panel) and numbers of vector genomes per cell (right panel) were assayed at 48 hours post-transduction in HeLa cells transduced with 250 vg/cell **(A)**, HFF hTERT transduced with 5000 vg/cell **(B)**, Cos-1 cells transduced with 1000 vg/cell **(C)**, C-12 cells transduced with 3000 vg/cell **(D)**, and Cho-K1 cells transduced with 5000 vg/cell **(E)**. Values represent fold to no treatment and are the mean of at least 3 independent experiments. Error bars represent the SEM. (*) $p<0.05$, (**) $p<0.01$, (***) $p<0.005$ based on comparisons of sample means by the Student's t-test.

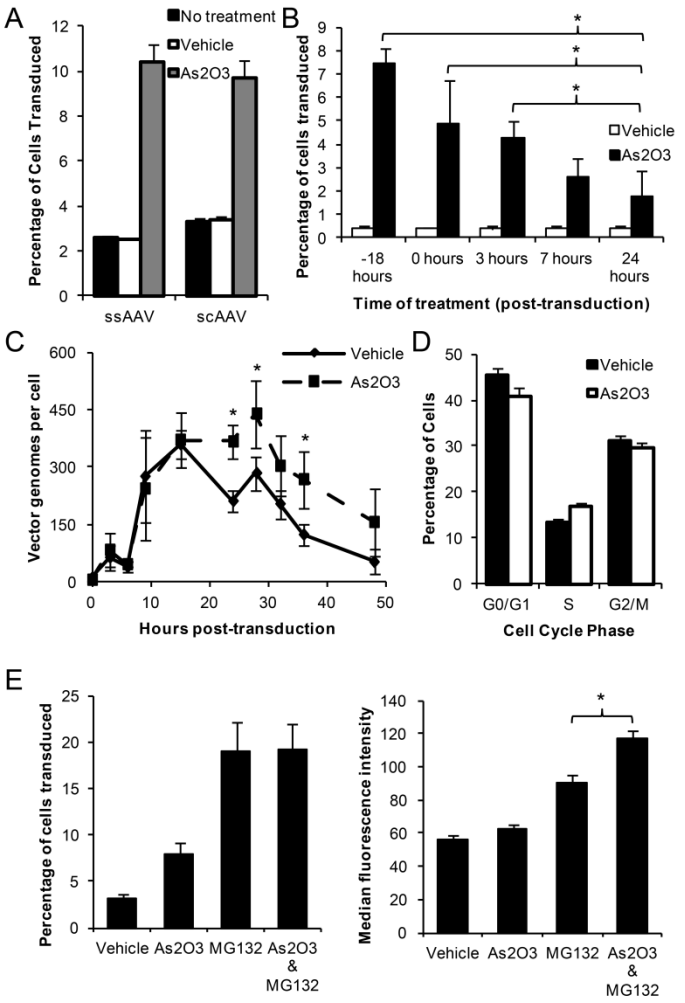

Figure 3.3: Mechanistic insights regarding rAAV2 transduction after As_2O_3 treatment. (A) HEK-293 cells were treated overnight with 4 μM As_2O_3 or a vehicle control, then transduced with 500 vg/cell single stranded rAAV2 (ssAAV) or 100 vg/cell self-complementary rAAV2 (scAAV), and the percentage of cells transduced was assayed at 48 hours post-transduction. **(B)** HEK-293 cells were treated with 4 μM As_2O_3 or a vehicle control starting at the indicated times and continuing to the time of harvest, 48 hours post-transduction with 500 vg/cell rAAV2, and the percentage of cells transduced was assayed. **(C)** HEK-293 cells were treated overnight with 4 μM As_2O_3 or vehicle and then transduced with 1000 vg/cell rAAV2 and numbers of intracellular vector genomes were assayed at the indicated times post-transduction. **(D)** HEK-293 cells were treated overnight with 4 μM As_2O_3 or a vehicle control, and then stained with propidium iodide to determine the percentage of cells in each cell cycle stage. **(E)** HEK-293 cells were treated as in (C) and 1 μM MG132, a proteasome inhibitor, or a vehicle control was added at the time of transduction. Cells were harvested at 24 hours post-transduction and the percentage of GFP positive cells and the median fluorescence intensity of the positive cells were assayed. Data representative of three independent experiments is shown. Error bars represent one SD. (*) $p<0.05$ based on the non-parametric Kruskal-Wallis test.

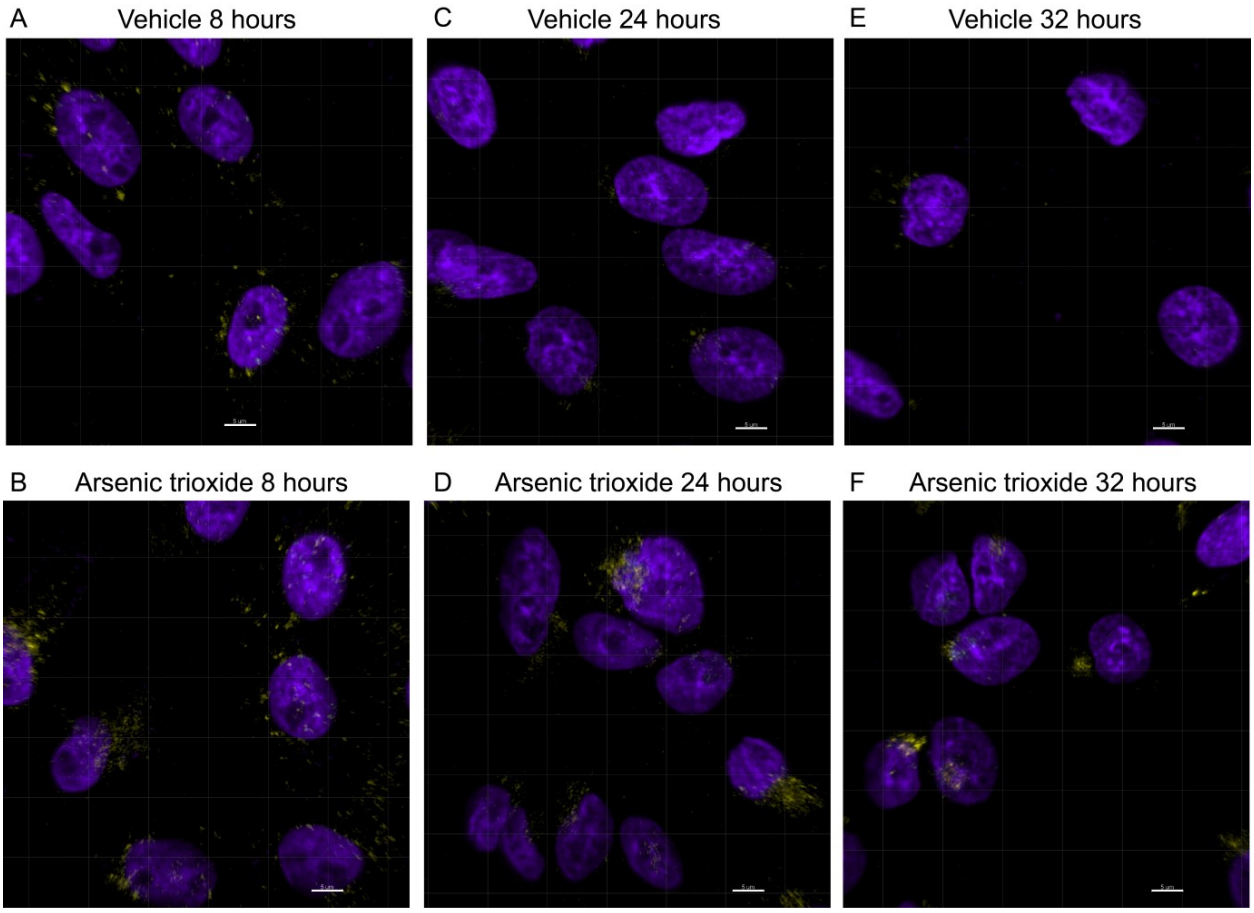

Figure 3.4: Subcellular localization of rAAV2-Cy5 virions after As_2O_3 treatment. Cho-K1 cells were treated with a vehicle control **(A, C, & E)** or 8 μM As_2O_3 **(B, D, & F)** from 18 hours pre-transduction to the time of harvest and transduced with 10 000 vg/cell rAAV2-Cy5. Cells were fixed at 8 hour post-transduction **(A & B)**, 24 hours post-transduction **(C & D)**, or 32 hours post-transduction for **(E & F)**. The localization of rAAV virions was determined by confocal microscopy and representative deconvoluted 3D projections are shown. Cy5 signal is shown in yellow; DAPI signal is shown in purple. Scale bars represent five μm.

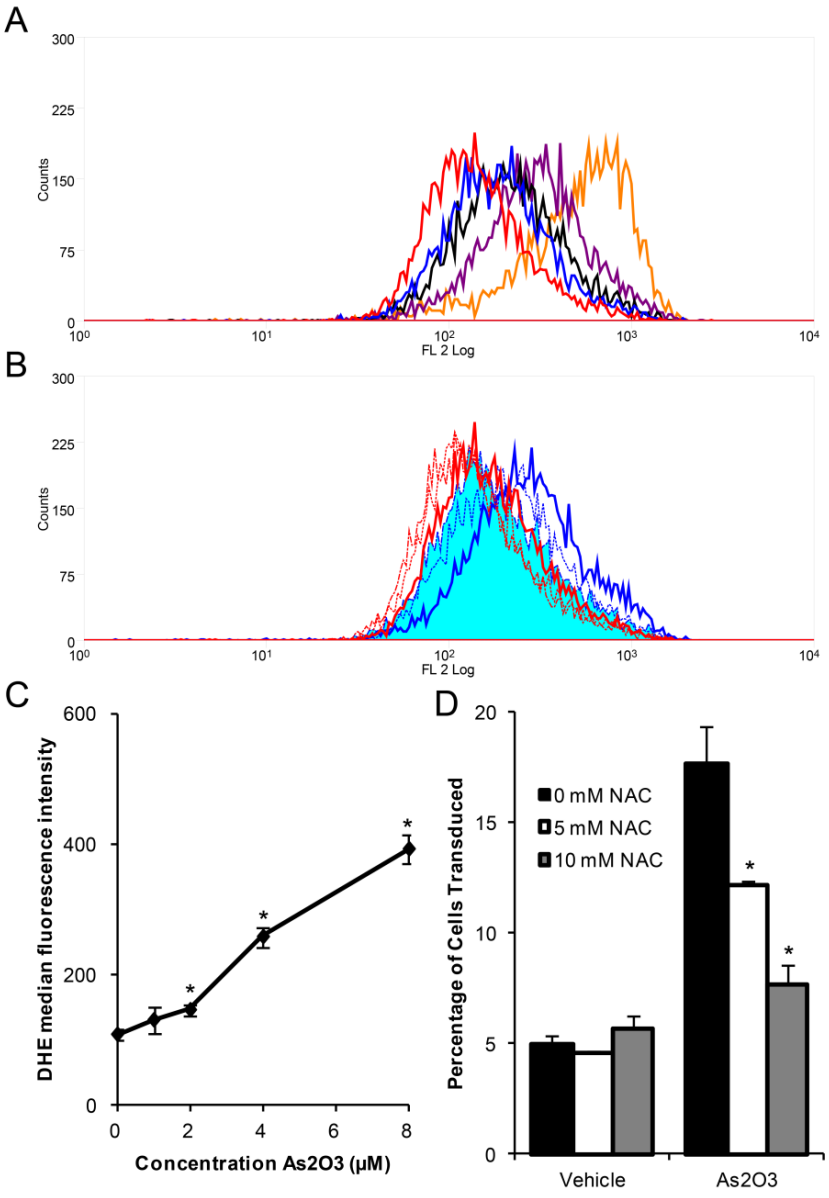

Figure 3.5: The role of ROS in the rAAV2 transduction effects of As_2O_3. (A) HEK-293 cells were treated overnight with no treatment (red), 1 μM As_2O_3 (blue), 2 μM As_2O_3 (black), 4 μM As_2O_3 (purple), or 8 μM As_2O_3 (orange) and ROS were measured with DHE. A histogram of fluorescence intensity is shown. **(B)** HEK-293 cells were treated overnight with a vehicle control (red) or 4 μM As_2O_3 (blue) and with PBS (solid line), 5 mM NAC (small dashed line), or 10 mM NAC (intermediate dashed line) to scavenge ROS. ROS were measured with DHE and a histogram of fluorescence intensity is shown. As_2O_3 10 mM NAC treated curve is solid in histogram. **(C)** Cells were treated as in (A) and the median fluorescence intensity was plotted versus As_2O_3 concentration. **(D)** Cells were treated as in (B) and then transduced with 500 vg/cell rAAV2 and the percentage of cells transduced was assayed at 48 hours post-transduction. Data is representative of three independent experiments. Error bars represent one SD. (*) $p<0.05$ based on the Kruskal-Wallis test.

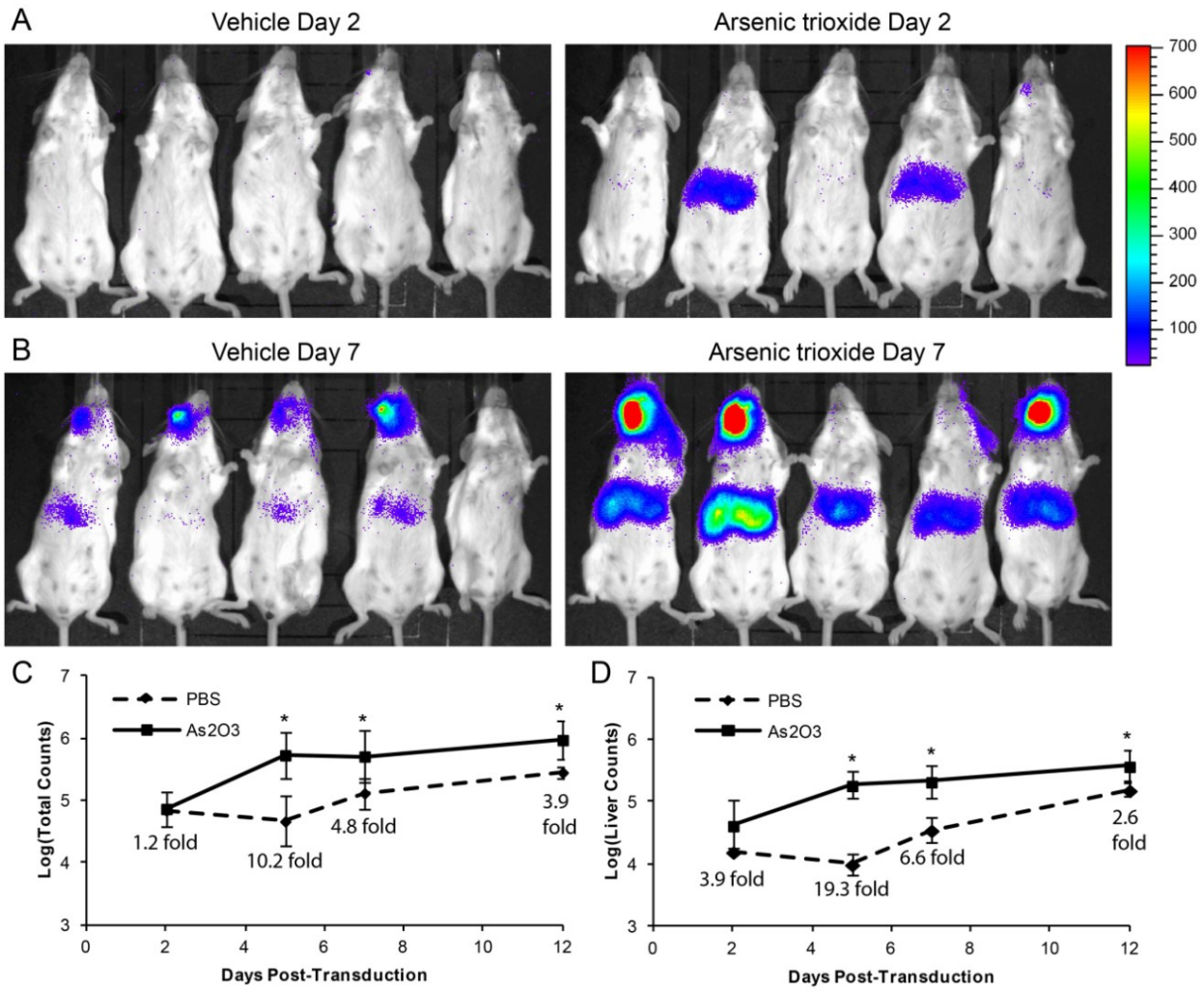

Figure 3.6: rAAV2 transduction effects of As_2O_3 *in vivo*. Five to six week old BALB/c mice were treated for 5 days with 5 µg/g/day As_2O_3 or a PBS vehicle control by intraperitoneal injection and transduced with 2×10^{11} vg rAAV2-CBA-luciferase on the third day of treatment. Images from luciferase live imaging at 2 days **(A)** and 7 days **(B)** post-transduction are shown (5 minute exposure). Quantification of luciferase activity from live imaging from 2 days to 12 days post-transduction from the whole mouse **(C)** and from the area of the liver **(D)** is shown with fold values of As_2O_3 over vehicle (n=5). Error bars represent one SD. (*) $p<0.05$ based on the Kruskal-Wallis test.

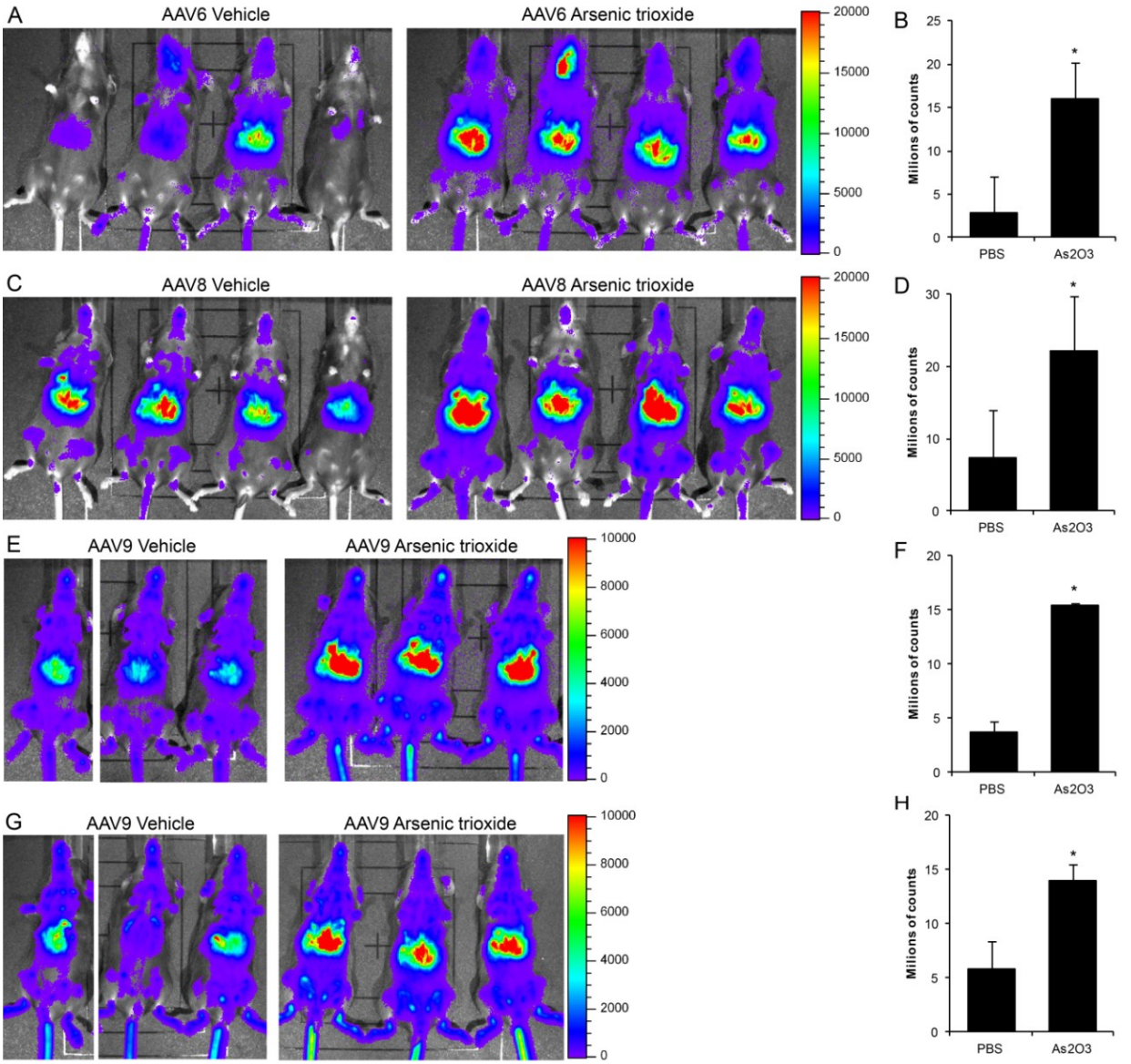

Figure 3.7: Transduction from several serotypes of rAAV after As_2O_3 treatment. Five to six week old C57BL/6 mice were treated for 5 days with 5 µg/g/day As_2O_3 or a PBS vehicle control by intraperitoneal injection and transduced with 1×10^{11} vg rAAV6-CBA-luciferase **(A** & **B)**, rAAV8-CBA-luciferase **(C** & **D)**, or rAAV9-CBA-luciferase **(E**, **F, G, & H)** on the third day of treatment. Images from live luciferase imaging are shown on day 7 for rAAV6 **(A)** (5 minute exposure), day 2 for rAAV8 **(C)** (5 minute exposure), day 5 for rAAV9 **(E)** (1 minute exposure), and day 21 for rAAV9 **(G)** (1 minute exposure). Quantification of luciferase activity from live imaging is shown at the same time points for rAAV6 **(B)** (n=4), rAAV8 **(D)** (n=4), and rAAV9 **(F** & **H)** (n=3). Error bars represent one SD. (*) $p<0.05$ based on the Kruskal-Wallis test.

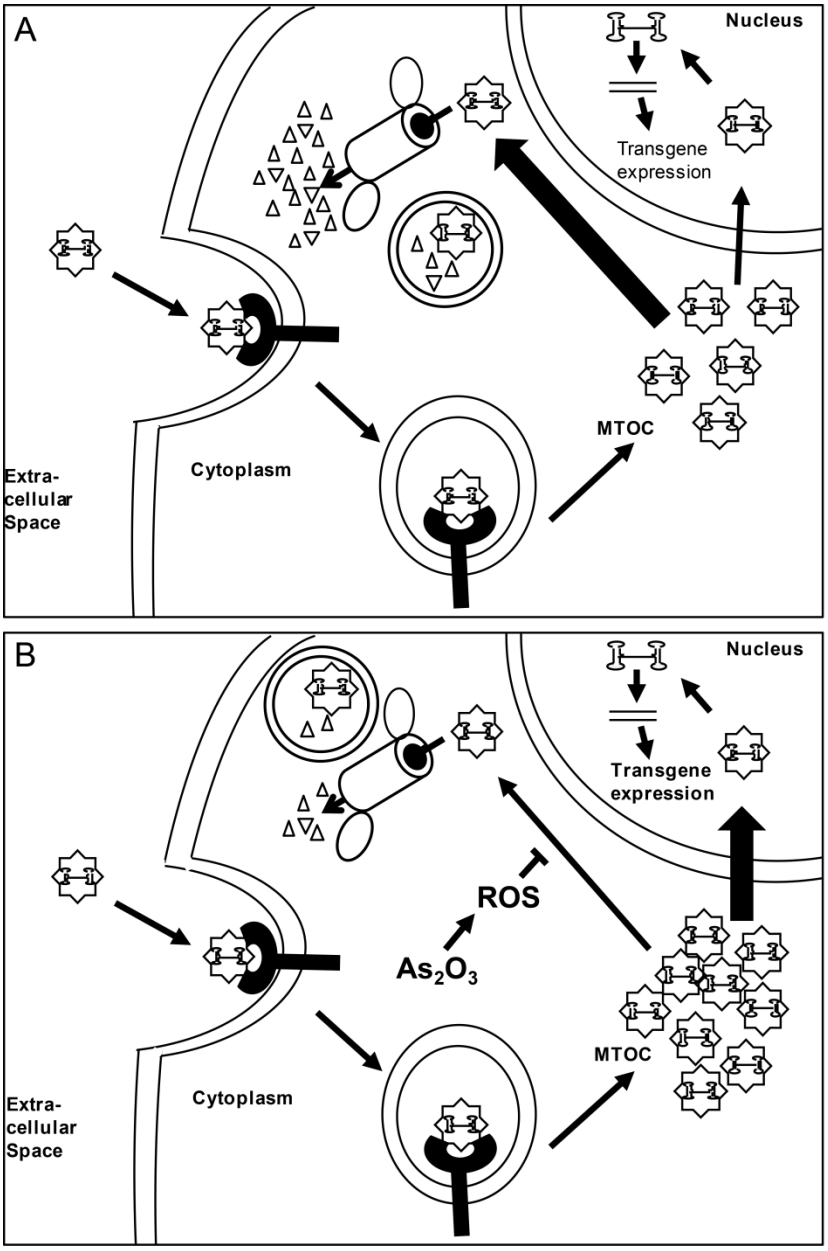

Figure 3.8: Model for effect of arsenic trioxide on AAV transduction. (A) In untreated cells, rAAV enters the cell through receptor-mediated endocytosis and is trafficked to the MTOC. At the MTOC, virions can be retained for a time or proceed to the nucleus; however, the majority of the virions are degraded through mechanisms possibly involving the proteasome or lysosomes and the perinuclear accumulation clears by 32 hours post-transduction. **(B)** In As_2O_3 treated cells, cell entry and trafficking to the MTOC occurs as in (A); however, As_2O_3, through ROS formation, acts to block the degradation of the virion. Consequently, more virions continue on in the transduction pathway, ultimately leading to greater transgene expression.

CHAPTER 4

Mechanistic insights into the enhancement of adeno-associated virus transduction by proteasome inhibitors[3]

Summary

Proteasome inhibitors (e.g. bortezomib, MG132) are known to enhance adeno-associated virus (AAV) transduction; however, whether this results from pleotropic proteasome inhibition or off-target serine and/or cysteine protease inhibition remains unresolved. Here, we examined rAAV effects of a new proteasome inhibitor, carfilzomib, which specifically inhibits chymotrypsin-like proteasome activity and no other proteases. We determined proteasome inhibitors act on rAAV through proteasome inhibition and not serine or cysteine protease inhibition, likely through positive changes late in transduction.

Introduction

Adeno-associated virus (AAV) is frequently utilized as a gene delivery vector for clinical application; thus, several approaches have been undertaken to increase efficacy, including transgene optimization (188-190), capsid alteration (reviewed in (4)), and drug treatments to enhance transduction (16, 104-107, 109, 132, 153, 154). Proteasome inhibitors (PIs) were first described to enhance rAAV polarized airway cell transduction (105) and since then PIs including, N-acetyl-L-leucinyl-L-leucinyl-norleucinal (LLnL) (105, 191-196), MG132

[3]Adapted for this dissertation from: **Mitchell A.M. and R.J. Samulski**. Posted September 11th, 2013. Mechanistic insights into the enhancement of adeno-associated virus transduction by proteasome inhibitors. J Virol**.** doi:10.1128/JVI.01826-13.

(105-107, 109, 169, 179, 191, 194, 197-199) bortezomib (108, 109), and celastrol (200), have been observed to enhance transduction in many cell types both *in vitro* and *in vivo*. Nevertheless, questions remain regarding the mechanism of this enhancement. Although ubiquitinated rAAV2 capsids proteins accumulate after PI treatment, suggesting PIs prevent the degradation of ubiquitinated AAV capsids and lead to increased transgene expression, some level of capsid dissociation (105) or phosphorylation (201, 202) appears to be necessary for ubiquitination and the role of the proteasome in these effects has not been directly examined. In addition to proteasome inhibition, PIs are commonly observed to inhibit other proteases such as cysteine (MG-132) and serine (MG-132 and bortezomib) proteases (123). These proteases have very different cellular roles from the proteasome, which degrades ubiquitinated cytoplasmic and nuclear proteins, including lysosomal degradation and calcium dependent intracellular signaling. In fact, the *in vivo* peripheral neuropathy caused by bortezomib is the result of serine protease inhibition leading to neurotoxicity (203), demonstrating the importance of off-target effects with clinically relevant dosing of PIs. The broad range of inhibition caused by PIs has caused many in the field of rAAV research to hypothesize that the effects of PIs on rAAV transduction are due to off-target effects of PIs and not inhibition of the proteasome. In addition, whether the enhancement of rAAV transduction occurs through proteasome inhibition or protease inhibition, it is also unclear whether the effects of PIs prevent the degradation of rAAV virions or whether the cause a positive change in transduction.

The promiscuity of so called "first-generation" PIs led to the development of new PIs with restricted specificity. Proteases, including the proteasome, act through a nucleophilic attack by their active site residue, which can be serine, cysteine, threonine, or by water in the case of aspartic and metalloproteases. The protease's active site residue is used to classify the protease

(e.g. serine protease). Unlike other classes of proteases, active site threonine of the proteasome is the N-terminal residue of each catalytic subunit, exposing the amino group to possible reactivity (204). Carfilzomib, a second-generation PI, relies on this amino group to form a morpholino, covalently inhibiting cleavage (205), and so cannot inhibit other proteases (206, 207). In fact, carfilzomib highly inhibits only the chymotrypsin-like activity of the proteasome (207), making it a useful tool for examining the importance of proteasome inhibition on enhancement of rAAV transduction and addressing the hypothesis above that PIs act on rAAV transduction through off-target effects on other proteases. To determine whether the enhancement of rAAV transduction observed with PI, treatment occurs from proteasome inhibition or from inhibition of other proteases, we utilized several PIs as well as cysteine and serine protease inhibitors and assessed their effect on rAAV transduction.

Results and Discussion

Carfilzomib enhances rAAV2 transduction *in vitro*. To address the question of whether a specific PI is sufficient to enhance rAAV transduction, we utilized three PIs, MG132, bortezomib, and carfilzomib (Selleck Chemicals), and a rAAV serotype 2 (rAAV2) vector expressing luciferase or EGFP transgenes (52). We co-administered the drugs with 1000 vector genomes per cell (vg/cell) rAAV2 to HeLa cells and compared their effects on transduction at 24 hours (107). Using luciferase vector, we determined that all of these PIs enhanced rAAV2 transduction at a range of doses, although we observed shifts in the curves that correlate with differing IC50 values (bortezomib—0.6 nM, carfilzomib—5 nM, and MG132—100 nM (208-210)) (**Fig. 4.1A**). To differentiate between the numbers of cells transduced and the level of their transduction, we treated with 1 μM PI, transduced with 500 vg/cell rAAV2-EGFP, and assayed

EGFP expression by flow cytometry (132). The PIs enhanced both the percentage of cells transduced (**Fig. 4.1B**) and their fluorescence intensity (**Fig. 4.1C**). This enhancement can also be observed visually (**Fig. 4.1D**). Carfilzomib's transduction enhancement suggests that proteasome inhibition is sufficient for PI effects on rAAV transduction, as this is carfilzomib's only activity. Furthermore, the similar enhancement observed between bortezomib and carfilzomib suggests that the enhancement from bortezomib may be primarily due to proteasome inhibition.

Serine and cysteine protease inhibition do not enhance rAAV2 transduction. As we found proteasome inhibition sufficient for the enhancement of rAAV transduction, we asked whether serine protease inhibition, observed with MG132 and bortezomib, or cysteine protease inhibition, observed with MG132, have effects on rAAV2 transduction. We treated HeLa cells twice with phenylmethane sulfonylfluoride (PMSF) to inhibit serine proteases as has been described (211), co-administer 1000 vg/cell rAAV2 with the second dose, and analyzed transduction by luciferase assay at 24 hours. We observed no increases in rAAV2 transduction from treatment with a 1000-fold range of PMSF doses with a maximum dose 10-fold over PMSF's working concentration (**Fig. 4.2A**), suggesting serine protease inhibition does not enhance rAAV2 transduction. We confirmed the ability of PMSF to inhibit serine proteases at these concentrations with a colorimetric trypsin activity assay (BioVision Inc), which measured cleavage of a trypsin substrate over time (**Fig. 4.2B**). To investigate whether cysteine proteases affect rAAV transduction, we treated cells with E-64 and assayed transduction as above. rAAV2 transduction did not change over a 10 000-fold range of E-64 doses with a maximum dose 10- to 100-fold over E-64's working concentration (**Fig. 4.2C**), suggesting that cysteine protease inhibition also does not enhance rAAV2 transduction. We confirmed the ability of E-64 to

inhibit cysteine proteases at these concentrations with a luminescent calpain assay (Promega), which measured cleavage of a luminescent substrate in the presence and absence of E-64 (**Fig. 4.2D**). Although cathepsins B and L (cysteine proteases) have been suggested to important for rAAV transduction (212), we also observed no decreases in transduction with E-64 treatment. This may be due to a difference in species as the interaction of cathepsins with rAAV was identified in murine cells, whereas we are using human cells. Nevertheless, as PIs inhibition of these proteases would only decrease transduction, cysteine protease inhibition is unlikely to be the mechanism by which PIs enhance rAAV transduction. Taken together, these data suggest enhancement of rAAV transduction by PIs is not due to off target effects on other proteases.

Bortezomib and carfilzomib act on rAAV transduction through the same mechanism. Our results thus far suggest that proteasomal inhibition is the responsible for enhancement of rAAV transduction after PI treatment. To investigate this hypothesis further, we determined whether bortezomib and carfilzomib are both effective on several different AAV serotypes. We treated HeLa cells with 1 μM bortezomib or carfilzomib and 20 000 vg/cell rAAV6, 100 000 vg/cell rAAV8, or 100 000 vg/cell rAAV9 and assayed transduction by flow cytometry at 24 hours. The enhancement of the percentage of cells transduced was similar in all serotypes between bortezomib and carfilzomib, although carfilzomib enhanced fluorescence intensity more for some serotypes (**Fig. 4.3A**), strengthening the hypothesis that bortezomib and carfilzomib act through the same mechanism. Furthermore, to our knowledge, this is the first report rAAV9 enhancement by PIs. To assess directly whether bortezomib and carfilzomib act through the same mechanism, we performed an exchange experiment where we treated cells with bortezomib or carfilzomib in combination, transduced with rAAV2 as before, and assayed transduction at 24 hours. There were no increases or decreases in transduction from combining

these two drugs (**Fig. 4.3B**), suggesting they can be used interchangeably. Combined with our other data, this suggests that bortezomib and carfilzomib both act to enhance rAAV transduction through proteasome inhibition.

Consequently, two hypotheses can be drawn for how proteasome inhibition enhances rAAV transduction: (i) proteasome inhibition prevent the degradation of rAAV capsids, increasing the rAAV pool available to complete transduction; (ii) as misfolded protein responses can enhance rAAV transduction (147), a general misfolded protein response and/or ubiquitination of rAAV capsids facilitates late steps in transduction. To address these hypotheses, we treated HeLa cells with bortezomib or carfilzomib and rAAV2 as before and assayed intracellular vector genome copy number at 24 hours by qPCR (132). The copy number was increased 2.3-fold and 1.8-fold by bortezomib and carfilzomib treatment, respectively (**Fig. 4.3C**); however, this was much smaller than the 28-fold and 23-fold transduction increases observed with bortezomib and carfilzomib (**Fig. 4.1A**). These data suggest the enhancement of transduction observe is unlikely to be directly due to capsid retention (hypothesis (i)). Instead, it is more likely that the buildup of ubiquitinated capsid or a misfolded protein response lead to increased favorability in late transduction steps. This agrees with previous results demonstrating increased nuclear localization of virus following PI treatment (105, 109, 169, 194, 200, 201) and specifically increased nucleolar localization (107). Furthermore, we previously reported that treatment with arsenic trioxide leads to increased transduction through stabilization of perinuclear rAAV capsids and that this effect was distinguishable from PI effects (132). Taken with our current results, this suggests that, while arsenic trioxide is directly influencing transduction through the retention of capsids that would otherwise be degraded, PIs are

influencing transduction through a modification secondary to degradation, explaining their differing effects.

Carfilzomib is less successful at enhancing rAAV transduction *in vivo* than bortezomib. As carfilzomib and bortezomib demonstrate similar rAAV transduction enhancement *in vitro*, we tested carfilzomib's ability to enhance rAAV2 transduction *in vivo* to determine whether proteasome inhibition is sufficient for enhancement of rAAV transduction *in vivo*. We utilized rAAV2, a liver tropic vector, as the majority of AAV biology has been studied with this serotype; however, pharmacokinetic studies with carfilzomib demonstrate low activity in the liver due to drug metabolism (207). Therefore, we expected less enhancement of rAAV transduction in the liver with carfilzomib than with bortezomib. We co-administered either 0.5 mg/kg bortezomib or 1 mg/kg carfilzomib, a similar molar dose, and 1×10^{11} vg/mouse rAAV2 retro-orbitally into age-matched female BALB/c mice (Jackson Laboratories) (109) and assayed transduction through live luciferase imaging (132). No acute liver toxicity occurred with the vehicle or either of the proteasome inhibitors at this dose (**Fig. 4.4A**). We observed enhanced transduction from both bortezomib and carfilzomib treatment at 7 days post-transduction (**Fig. 4.4B**) which quantified as 12.4-fold and 2.7-fold enhancements, respectively (**Fig. 4.4C**). At 14 days, bortezomib mice maintained higher transduction than vehicle mice; however, carfilzomib and vehicle mice demonstrated similar transduction (**Fig. 4.4D**). *Ex vivo* quantification of transduction by luciferase assay and vector genome copy number (132) confirmed the live imaging data (**Fig. 4.4E**). Despite the expected lesser effects of carfilzomib than bortezomib in the liver, these data demonstrate that proteasome inhibition is sufficient for the enhancement of rAAV transduction *in vivo*. In addition, this suggests that, although carfilzomib is not ideal for *in*

vivo rAAV transduction enhancement in the liver, other second-generation, highly specific PIs should be evaluated for this purpose as they become available.

Conclusions

Overall, our data demonstrate proteasome inhibition is sufficient for rAAV transduction enhancement and serine and cysteine protease inhibition is unlikely to contribute to this enhancement. These data will alter the prevailing view in the field that the PIs act on rAAV transduction through off-target effects and instead demonstrate that they act through inhibition of the proteasome. Furthermore, the strategies employed to address these questions could now be applied to other viruses which are thought to be affected by proteasomal activity, such as hepatitis B virus or herpes simplex virus (213, 214). Additionally, the transduction increase seems to be secondary to prevention of rAAV capsid degradation and is instead due to a positive change in late stages of transduction. Furthermore, although carfilzomib is not ideal for enhancing rAAV-mediated liver transduction, our data suggest that other second-generation PIs in development, such as ONX0912, MLN9708, and marizomib (215), should be examined for enhancement of rAAV transduction *in vivo*. As these PIs may have fewer side effects than bortezomib, this may become important for the enhancement of rAAV clinical gene therapy.

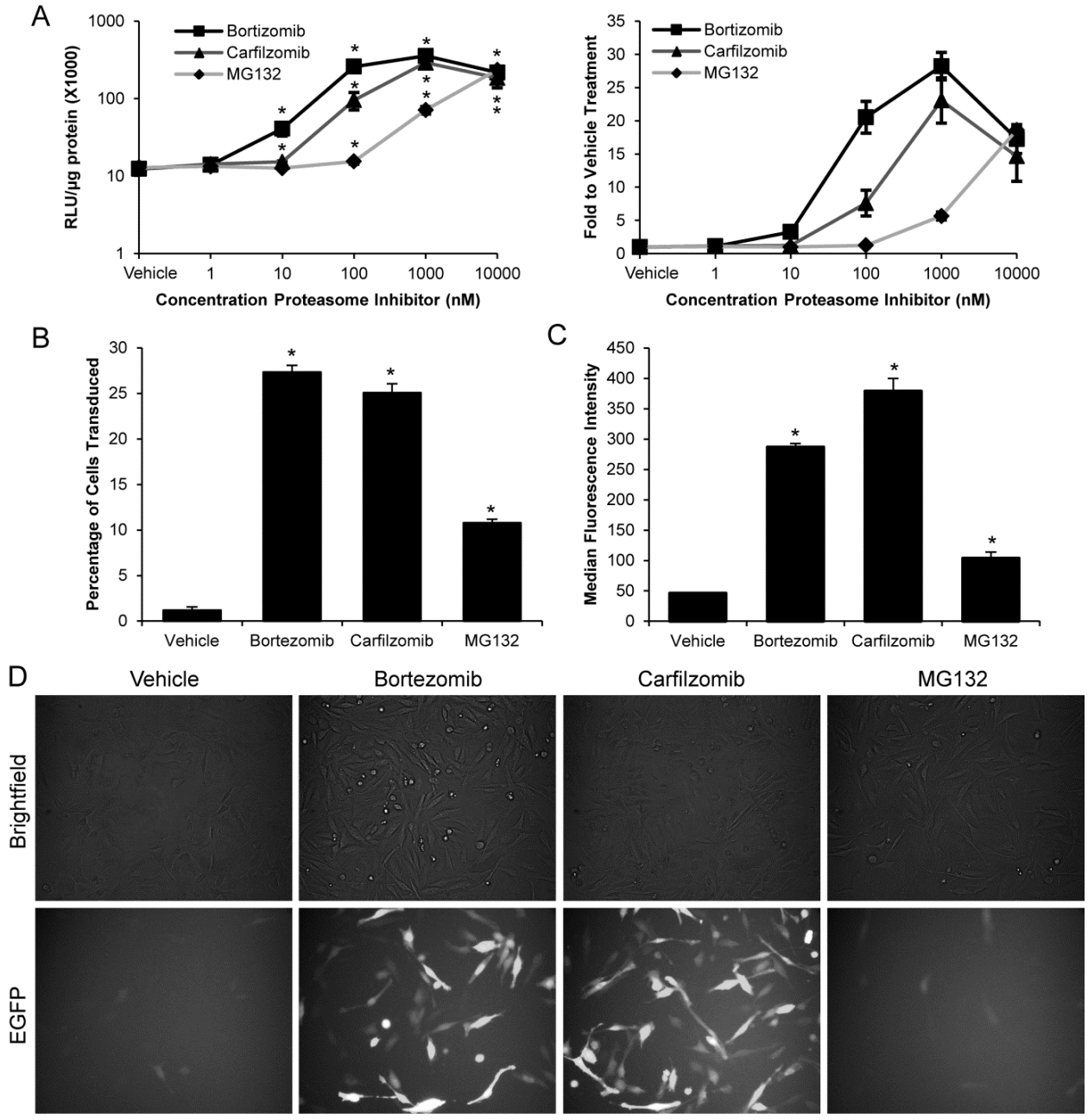

Figure 4.1: Carfilzomib enhances rAAV2 transduction. (A) HeLa cells were co-treated with the indicated does of bortezomib, carfilzomib, MG132 or a DMSO vehicle control and transduced with 1000 vg/cell rAAV2-luciferase. Transduction at 24 hours is indicated as normalized luciferase activity and fold values to vehicle treated group. **(B-C)** HeLa cells were co-treated with 1 µM PI and 500 vg/cell rAAV2-EGFP and transduction was analyzed by flow cytometry at 24 hours. The percentage of cells transduced (B) and median fluorescence intensity of the transduced cells (C) is indicated. **(D)** Brightfield and EGPF fluorescence images at 24 hours post-transduction of cell treated as in (B) and (C) visually indicating transduction. Data shown are representative of three independent experiments. Error bars represent one SD. (*) $p<0.05$ versus the vehicle control based on the Kruskal-Wallis test.

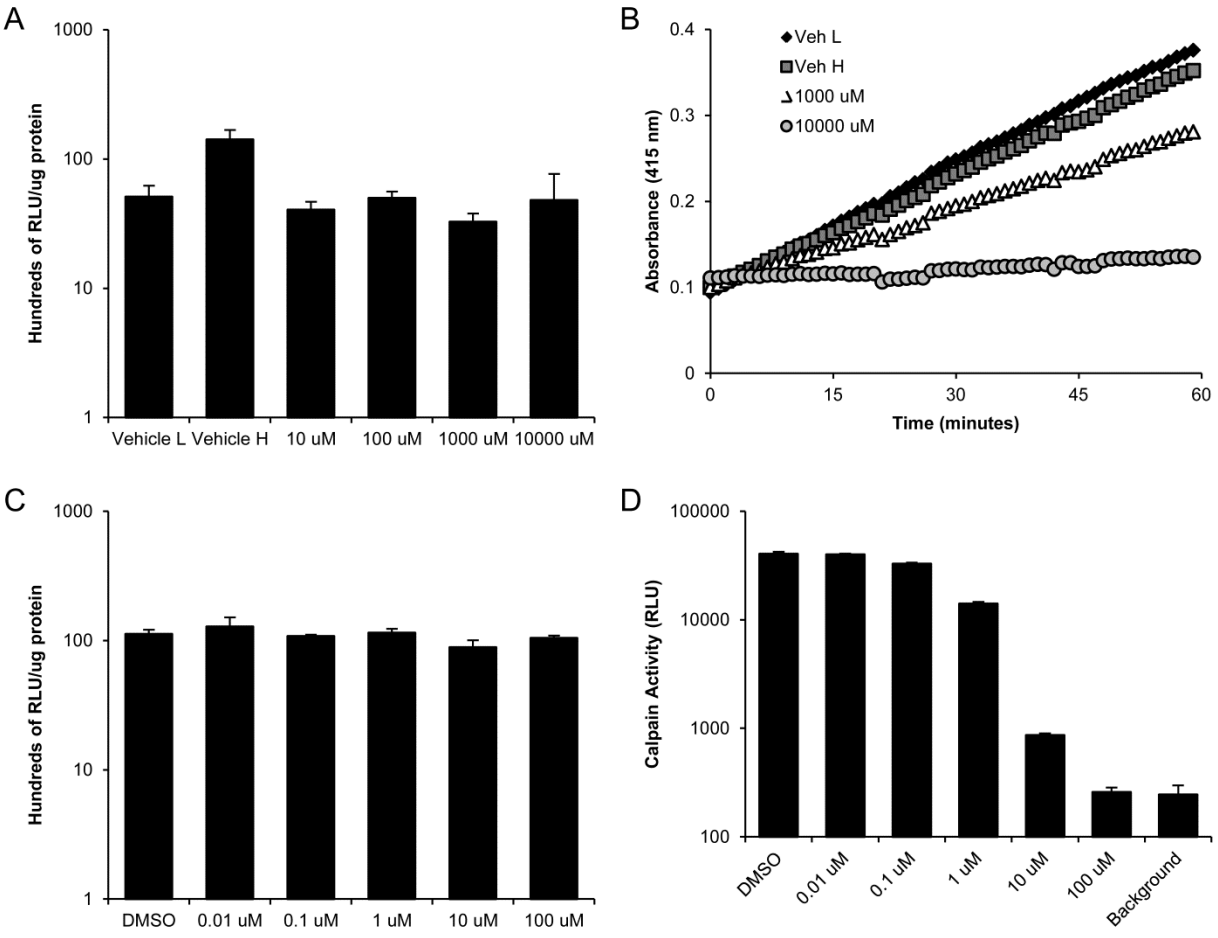

Figure 4.2: Serine and cysteine protease inhibition does not enhance rAAV2 transduction. (A) HeLa cells were treated 3 hours prior to and at the time of transduction with the indicated dose of PMSF, a serine protease inhibitor, or an ethanol vehicle control and transduced with 1000 vg/cell rAAV2-luciferase. Transduction is indicated as normalized luciferase activity. "Vehicle L" group corresponds to 10-1000 μM treatments while "Vehicle H" group corresponds to 10 000 μM treatment. **(B)** Indicated concentrations of PMSF or vehicle were combined with 0.002% trypsin and incubated 30 min at room temperature. Solutions were diluted 1:10 in assay buffer and combined with trypsin substrate in quadruplicate. Average absorbance at 415 nm is shown for 60 readings at 60 s intervals. **(C)** HeLa cells were treated as in (A) with E-64, a cysteine protease inhibitor, or a DMSO vehicle control. Transduction is indicated as normalized luciferase activity. **(D)** Indicated concentrations of E-64 or vehicle control were combined with 20 nM human calpain 1 (BioVision), incubated at room temperature for 10 min, and combined with Calpain-Glo luciferase reagent (Promega) with 2 mM $CaCl_2$. E-64 activity is indicated as relative light units. Data shown are representative of three independent experiments. Error bars represent one SD.

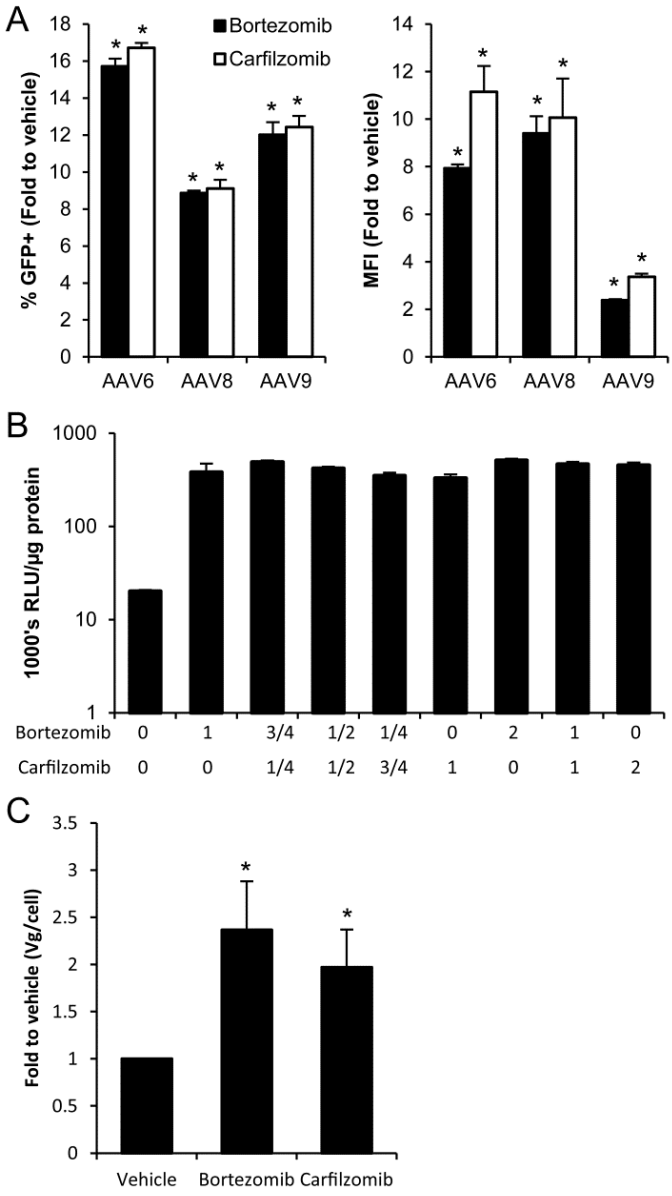

Figure 4.3: Bortezomib and carfilzomib act on rAAV2 transduction through the same mechanism. **(A)** HeLa cells were treated with 1 µM bortezomib, carfilzomib, or vehicle control and 20 000 vg/cell rAAV6-EGFP, 100 000 vg/cell rAAV8-EGFP, or 100 000 vg/cell rAAV9-EGFP and transduction was assayed by flow cytometry at 24 hours post-transduction. Transduction is indicated as fold values to vehicle control groups of percentage of cells transduced and median fluorescence intensity. **(B)** HeLa cells were treated with the indicated µM doses of bortezomib and carfilzomib or a vehicle control and 1000 vg/cell rAAV2-lucifease. Transduction is indicated as normalized luciferase activity. **(C)** HeLa cells were treated as in Fig. 1B and intracellular vector genome copy number was analyzed at 24 hours post-transduction by qPCR. Data is indicated as fold to vehicle control. Data shown in (A) and (B) are representative of three independent experiments. Data shown in (C) is the mean of three independent experiments. Error bars represent one SD. (*) $p<0.05$ versus vehicle control group based on the Kruskal-Wallis test.

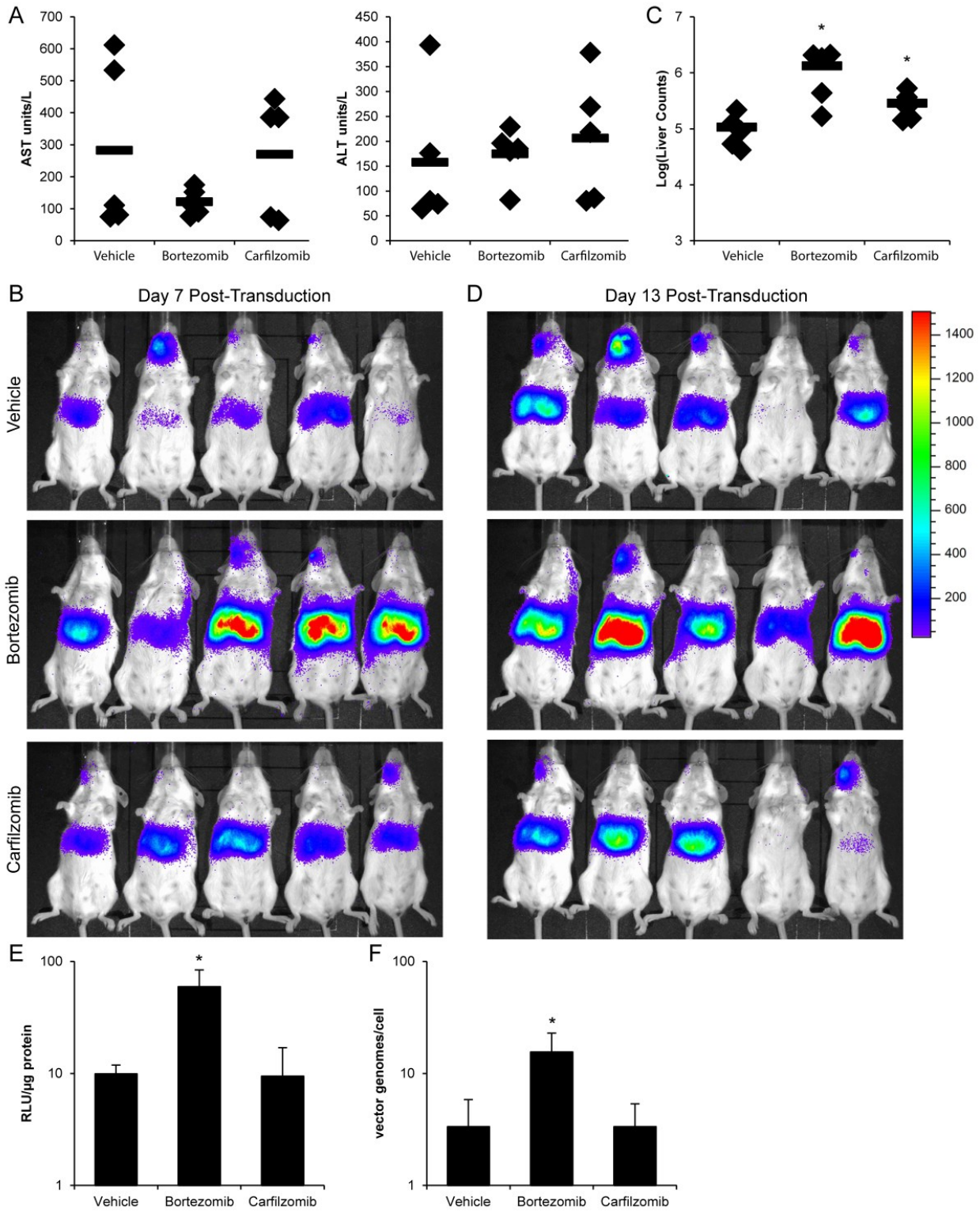

Figure 4.4: Bortezomib is more efficient at enhancing rAAV2 transduction *in vivo* than carfilzomib. Female BALB/c mice were treated with 1E11 vg/mouse rAAV2-luciferase and 0.5 mg/kg bortezomib, 1 mg/kg carfilzomib, or DMSO vehicle control. **(A)** Serum was collected from mice at 24 hours post-treatment and aspartate aminotransferase (AST) and alanine aminotransferase (ALT) were

measured. Individual animals are indicated by diamonds and mean is indicated by bars. **(B)** Transduction was assayed by live imaging at 7 days post-transduction and **(C)** light output from the area of the liver was quantified. **(D)** Transduction at 13 days was assayed by live imaging. **(E)** At 14 days, livers were harvested and transduction is indicated by normalized luciferase activity. **(F)** Vector genome copy number was assayed by qPCR. Error bars represent one SD. (*) $p<0.05$ versus the vehicle control based on the Kruskal-Wallis test.

CHAPTER 5

Conclusions and Future Directions

Summary of Findings

The goal of this dissertation was to determine mechanisms by which the transduction of rAAV can be increased without increasing viral dose. This aim is relevant given the frequent observation of low transgene expression or loss of transgene expression over time in clinical systemic gene therapy applications utilizing rAAV. Towards this aim, we completed three projects. In the first project, we determined that PML inhibited rAAV transduction through prevention of rAAV second-strand synthesis and that knockout of PML led to up to 50-fold increases in transduction (Chapter 2). We then examined the effect of a chemotherapeutic agent, As_2O_3, on AAV transduction. Although this agent was initially examined due to its known effects on a PML fusion protein found in APL patients, we determined that the enhancement of transduction observed with As_2O_3 was unrelated to PML and, in fact, an earlier step in rAAV transduction was altered than is affected by PML. Specifically, we determined that As_2O_3 causes stabilization of perinuclear accumulations of rAAV virions, presumably allowing for increased nuclear trafficking of virions (Chapter 3, (132)). Interestingly, despite the effect of As_2O_3 on rAAV degradation, the effects of As_2O_3 were distinguishable from the effects of PIs on rAAV transduction. Given the lack of consensus on the mechanism of PI effects on rAAV transduction, we then proceeded to investigate whether PIs act on rAAV transduction through proteasome

inhibition or through another mechanism. We determined that proteasome inhibition was sufficient for enhancement of rAAV transduction and that, in contrast to a direct effect of inhibition of degradation, PIs caused an increase in efficiency in a late transduction step (Chapter 4, (216)). The steps in rAAV intracellular trafficking at which these three mechanisms act to increase rAAV transduction are illustrated in **Figure 5.1**. The following sections will specify future directions for these projects relating both to elucidation of rAAV biology and to the application of the results.

Future Perspectives for the Role of PML in Parvovirus Biology and rAAV Gene Therapy

In Chapter 2, we demonstrated that PML causes inhibition of rAAV second-strand DNA synthesis and so inhibits rAAV transduction both *in vitro* and *in vivo*. The method by which PML accomplishes this inhibition and the other cellular factors involved in the process are important outstanding questions relating to these results. Although AAV DNA replication and the cellular factors involved have been investigated, the template DNA utilized in the experiments was plasmid DNA (36, 37); therefore, the specific cellular factors necessary for initial synthesis of the second DNA strand are largely unknown. In addition, although a wide variety of work has examined the interactions of PML with specific cellular proteins (compiled in (217)), the consequences of these interactions is often unknown. Nevertheless, we have not observed a direct interaction between PML and rAAV genomes or capsids (data not shown), suggesting other cellular factors may act as intermediaries in the inhibition of rAAV DNA replication by PML. As a first step in identifying factors that might mediate interactions between PML and rAAV, we utilized a manually curated PML interactome containing more than 150 proteins that interact with PML and more than 750 interactions between them (217) to determine

which of these proteins had known interactions with AAV. In addition, we sorted these proteins with known interactions based on type of protein and role in rAAV transduction (**Fig. 5.2**). Of these proteins, RPA, a single-stranded DNA binding protein, appears of immediate interest due to its role in increasing the processitivity of DNA synthesis during AAV genome replication (36). PML is thought to sequester RPA in cells not undergoing DNA replication and, therefore, we hypothesized that PML inhibits rAAV second-strand synthesis by sequestering RPA. However, we observed no changes in levels of RPA associated with rAAV genomes or the subcellular localization of RPA when PML was overexpressed (data not shown), suggesting RPA does not mediate PML's effect on rAAV transduction. Therefore, the cellular factors mediating the effect of PML on rAAV and the mechanism by which they act remain open questions. Another interesting part of this question is what regions of PML are responsible for its inhibition of rAAV transduction. Our experiments demonstrated that PMLII had the greatest effect on rAAV transduction, while the other isoforms had a lesser 2-fold effect on transduction (**Fig. 2.8**). The inhibition caused by the other isoforms (PMLI, PMLIII, PMLIV, PMLV, and PMLVI) may have been due to either the shared regions of these proteins (exons 1-6a) or the movement of endogenous PMLII into PML bodies due to the overexpression of other isoforms (117, 137). These data demonstrate that the unique region of PMLII (**Fig. 2.12**) plays a significant role in rAAV transduction, while the role of the regions shared between the isoforms remains questionable. Therefore, elucidating the specific regions of PML responsible for its effect on rAAV transduction is an interesting future direction.

We also observed that, in a rAAV production setting, PML overexpression led to a small but significant change in replicated rAAV DNA levels but a much larger change in the capsid and Rep protein levels (**Fig. 2.10**). The large decrease in viral protein levels was also observed

for wild-type AAV. These data raise the question of whether, beyond its role in second-strand synthesis, PML also represses transcription from AAV's promoters. As PML has been demonstrated to inhibit the infection of several other viruses through effects on viral transcription (110, 113) and a large proportion of PML interacting proteins are involved in transcriptional control (217), an effect of PML on AAV transcription would not be unexpected. Furthermore, PML interacts with several factors known to affect AAV transcription (**Fig. 5.2**). Therefore, whether PML causes inhibition of AAV transcription will be interesting to address in the future. Moreover, the role of PML on AAV replication also broaches the question of the effect of helper viruses on PML activity and rAAV replication. Our replication experiments were conducted in the presence of a helper plasmid instead of replicating Ad to avoid changing levels of PML altering proteins during the experiment. Nevertheless, both Ad and HSV encode proteins that alter or inhibit PML activity (115, 116), suggesting that PML's role in AAV replication may differ with helper virus context, which merits further investigation. An additional question raised by the inhibition of wild-type AAV replication by PML is whether this observation can be extended to autonomous parvoviruses. For instance, MVM utilizes many of the same cellular DNA replication factors as AAV and MVM replication centers partially colocalize with PML at specific times during its replication cycle (118, 138). These data suggest that PML may play a role in the replication of autonomous parvoviruses including MVM and this hypothesis should be investigated in the future.

In addition to future directions related to the elucidation of rAAV biology, the inhibitory effect of PML on rAAV suggests directions that could be taken to avoid PML interactions and, therefore, enhance rAAV transduction and production. In production contexts, a shRNA could be incorporated into the helper plasmid (pXX680) in order to lower the levels of PML present

during vector genome replication. Although we examined the effect of PML on rAAV production only in an overexpression context, we hypothesize endogenous levels of PML inhibit rAAV production, and so lowering the levels of endogenous PML during production would lead an increase vector production. Moreover, in transduction settings, incorporating a PML shRNA into the transgene cassette could lower cellular PML levels allowing more vector genomes to become double stranded and so increasing transduction. This would be useful as, although scAAV can avoid the effects of PML on transduction (**Fig. 2.7** & **2.8**), the packaging capacity of scAAV is too small to accommodate the necessary transgene for many applications. In addition, once the cellular factors mediating PML's effect on rAAV transduction are elucidated, it may be possible to target specifically these factors in order to accomplish a similar enhancement of transduction.

Future Perspectives Relating to As_2O_3 Enhancement of rAAV Transduction

In Chapter 3, we determined that As_2O_3 acts to increase rAAV transduction through stabilization of perinuclear accumulations of rAAV virions leading to increased vector genome copy number (**Fig. 3.3** & **Fig. 3.4**). Although this effect was distinguishable from the effect of PIs on rAAV transduction (**Fig. 3.3**), the mostly likely mechanism for this effect is a prevention of rAAV degradation. However, as some portion of virions at the MTOC are retained within endosomes (14), it is not clear whether the degradation process affected is lysosomal, proteasomal, or a combination of both. Therefore, the specific rAAV degradation pathways affected by As_2O_3 remains an interesting question. Furthermore, although we determined as a first step in the cellular mechanism that As_2O_3 acts on rAAV transduction through ROS (**Fig. 3.5**), As_2O_3 influences many cellular pathways (175) and the downstream targets of As_2O_3 and

ROS remain unidentified. In the future, it will be interesting to identify the specific cellular pathways leading to the increase in rAAV transduction. Moreover, we also determined that As_2O_3 increased the transduction of several rAAV serotypes *in vivo* but that the timing of the increase differed between serotypes (**Fig. 3.7**). Specifically, the enhancement of rAAV8 transduction could only be observed at 2 days post-transduction and was not evident at later time points. These data suggest that As_2O_3 affects a rAAV transduction step that is different for rAAV8 than for the other serotypes examined (rAAV2, rAAV6, and rAAV9). The majority of rAAV intracellular trafficking has been elucidated using rAAV2; however, several recent reports compare rAAV serotypes in order to determine the similarities and differences in their trafficking pathways (178, 179). Specifically, rAAV8 and rAAV2 have been demonstrated to traffic through different endosomal compartment and rely on different conditions for endosomal escape (179); therefore, the difference in the kinetics of As_2O_3's effect on rAAV8 transduction may be due to a difference in endosomal trafficking. This will be an interesting question to examine in the future. It will also be interesting to determine what AAV8 capsid motifs are responsible for the differing As_2O_3 effect.

Beyond further elucidations of rAAV biology, the enhancement of rAAV by As_2O_3 can also be evaluated for application. As_2O_3 is approved for use in humans as a chemotherapeutic agent to treat APL and is under evaluation for the treatment of other forms of leukemia (119-121). Indeed, As_2O_3 is often considered a less toxic alternative to traditional chemotherapy (156). The current "gold-standard" for enhancement of rAAV transduction is bortezomib, a PI, which has been tested in large animal models (109). However, bortezomib and other PIs can cause idiopathic liver failure, prohibiting its use to enhance rAAV transduction (109, 155). Therefore, As_2O_3 should be further evaluated for *in vivo* enhancement of rAAV transduction. These

evaluations could include use of As_2O_3 with rAAV carrying therapeutic transgenes, in disease models, and with other routes of rAAV administration. In addition, direct comparisons of the transduction enhancement, risks, and side effects between As_2O_3 and bortezomib would be useful. With this type of evaluation, As_2O_3 may eventually become a good candidate for enhancement of clinical rAAV transduction.

Future Perspectives for the Mechanism of rAAV Transduction Enhancement Following Proteasome Inhibitor Treatment

In Chapter 4, we determined that proteasome inhibition with bortezomib or carfilzomib resulted in an increase in rAAV transduction more than 10-fold higher than the increase in the vector genome copy number (**Fig. 4.3**), demonstrating that the effect of PIs is not a direct effect of prevention of degradation. Instead, these data suggest that proteasome inhibition causes an increase in efficiency in a late stage in transduction. Previous reports have demonstrated increased nuclear and nucleolar localization following proteasome inhibition (105, 107, 109, 201). In the future, it will be interesting to determine what cellular and rAAV changes are responsible for this increase in transduction. For instance, misfolded protein responses have been demonstrated to enhance rAAV transduction (147) and similar cellular conditions may exist with proteasome inhibition. In addition, several studies have demonstrated increased ubiquitination of the rAAV capsid in the presence of PIs (105, 201) and ubiquination may make capsids more efficient at completing their trafficking pathway. Once the virion and cellular changes are elucidated, these data can be used to determine a specific molecular mechanism. Furthermore, more in depth understanding of the mechanism may lead to the identification of factors limiting rAAV transduction that can be targeted to enhance rAAV transduction while avoiding the side

effects of proteasome inhibition. In addition, as we determined that proteasome inhibition was sufficient for the enhancement of rAAV transduction (**Fig. 4.1**), other PIs in development that are more specific than bortezomib and so have less side effects should be evaluated for their ability to enhance rAAV transduction.

Concluding Remarks

rAAV-mediated clinical gene therapy is becoming increasingly successful at reaching efficacy goals but would, nevertheless, benefit from enhanced rAAV transduction. Towards this goal, we have developed several strategies that may eventually allow for rAAV transduction to be safely enhanced and for increased efficacy from clinical gene therapy. These strategies include the identification of a specific cellular factor, PML, that inhibits rAAV transduction, the identification of a pharmacological agent, As_2O_3, that can enhance rAAV transduction, and investigation into the mechanisms involved in a known enhancement of rAAV transduction. Experiments similar to these may lead to important advances in rAAV gene therapy and to the success of gene therapy approaches, as gene therapy treatments become more common and as more commercial gene therapy approaches are approved.

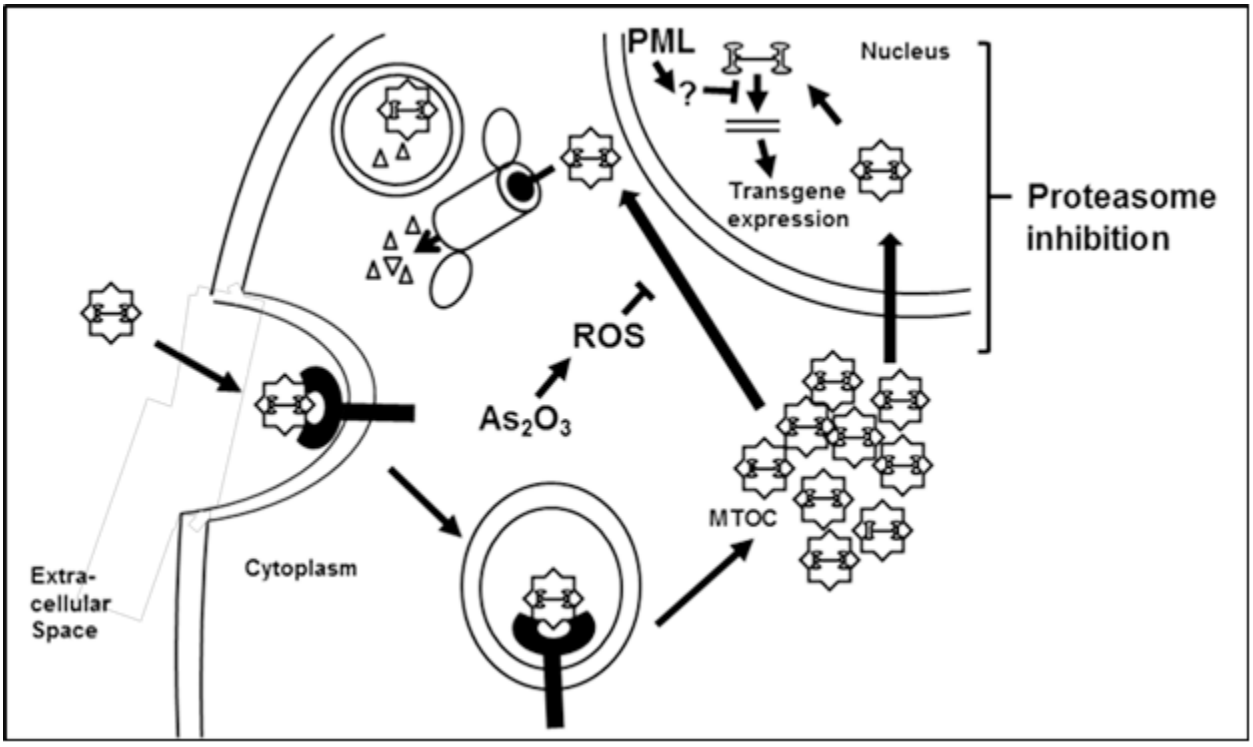

Figure 5.1: rAAV transduction model demonstrating the findings of this dissertation. In this dissertation, we examined three mechanisms by which rAAV transduction can be enhanced. In Chapter 2, we determined that inhibition of PML enhances rAAV transduction. PML acts, presumably through cellular intermediary factors, to inhibit the conversion of the rAAV genome from a single-stranded form to a transcriptionally active double-stranded form. In Chapter 3, we determined that treatment of cells with As_2O_3 enhances rAAV transduction by acting through ROS to inhibit the degradation of perinuclear rAAV virions, allowing for increased nuclear trafficking (132). In Chapter 4, we determined that proteasome inhibition was responsible for the enhancement of transduction from PI treatment and that this enhancement occurs through increasing the efficiency of rAAV transduction at a late step in transduction, not directly through prevention of rAAV degradation (216). This figure compares the steps in transduction affected by these mechanisms. For description of rAAV's general transduction pathway, please see Figure 1.2.

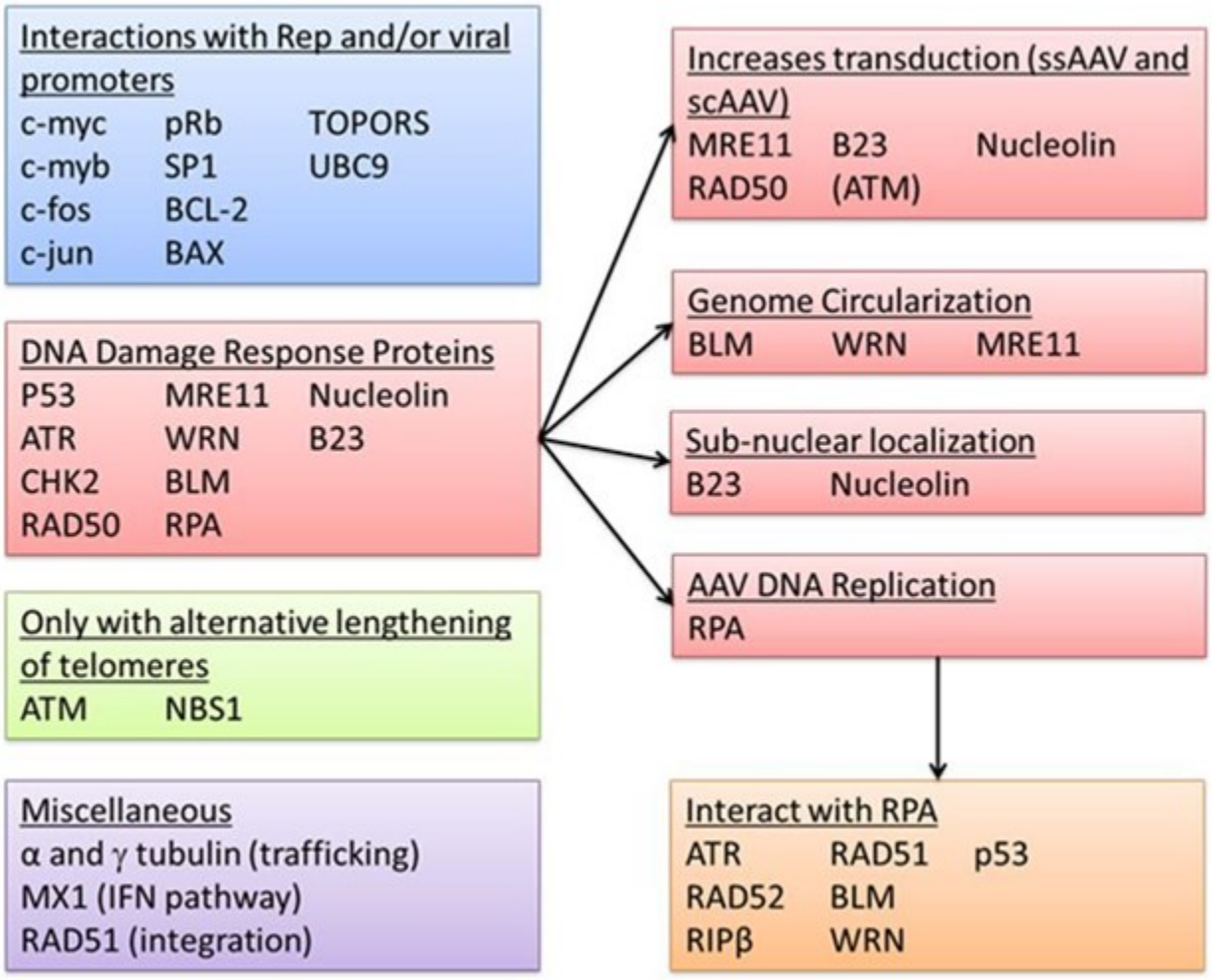

Figure 5.2: Proteins known to interact with both PML and AAV. Using a manually curated PML interactome (217), proteins known to interact with both rAAV and PML were identified. These proteins were grouped based on whether they interact with wild-type AAV specific factors (blue box) (218-225), they were DNA damage response proteins (red boxes) (15, 37, 226-230), only interacted with PML in cell undergoing alternative lengthen of telomeres (green box) (229, 231), or interacted with rAAV in some other way (purple box) (14, 232-234). The DNA damage response proteins were further subdivided in to those known to enhance the transduction of both single-stranded and self-complementary rAAV, those involved in rAAV genome circularization, those affecting sub-nuclear localization, and those involved in rAAV DNA replication (red boxes on right-hand side). Proteins interacting with PML and RPA were also identified (orange box) (217).

REFERENCES

1. **Atchison, R. W., B. C. Casto, and W. M. Hammon.** 1965. Adenovirus-Associated Defective Virus Particles. Science **149:**754-756.

2. **Fields, B. N., D. M. Knipe, P. M. Howley, and Ovid Technologies Inc.** 2007. Fields' virology, p. 2 v. (xix, 3091, 86 p.), 5th ed. Wolters Kluwer Health/Lippincott Williams & Wilkins, Philadelphia.

3. **Berns, K. I., T. C. Pinkerton, G. F. Thomas, and M. D. Hoggan.** 1975. Detection of adeno-associated virus (AAV)-specific nucleotide sequences in DNA isolated from latently infected Detroit 6 cells. Virology **68:**556-560.

4. **Mitchell, A. M., S. C. Nicolson, J. K. Warischalk, and R. J. Samulski.** 2010. AAV's anatomy: roadmap for optimizing vectors for translational success. Curr Gene Ther **10:**319-40.

5. **Xiao, X., W. Xiao, J. Li, and R. J. Samulski.** 1997. A novel 165-base-pair terminal repeat sequence is the sole cis requirement for the adeno-associated virus life cycle. J. Virol. **71:**941-948.

6. **King, J. A., R. Dubielzig, D. Grimm, and J. A. Kleinschmidt.** 2001. DNA helicase-mediated packaging of adeno-associated virus type 2 genomes into preformed capsids. EMBO J **20:**3282-3291.

7. **Kyostio, S. R., R. A. Owens, M. D. Weitzman, B. A. Antoni, N. Chejanovsky, and B. J. Carter.** 1994. Analysis of adeno-associated virus (AAV) wild-type and mutant Rep proteins for their abilities to negatively regulate AAV p5 and p19 mRNA levels. J. Virol. **68:**2947-2957.

8. **Sonntag, F., K. Schmidt, and J. r. A. Kleinschmidt.** 2010. A viral assembly factor promotes AAV2 capsid formation in the nucleolus. Proceedings of the National Academy of Sciences **107:**10220-10225.

9. **Rabinowitz, J. E., and R. J. Samulski.** 2000. Building a Better Vector: The Manipulation of AAV Virions. Virology **278:**301-308.

10. **Popa-Wagner, R., M. Porwal, M. Kann, M. Reuss, M. Weimer, L. Florin, and J. r. A. Kleinschmidt.** 2012. Impact of VP1-Specific Protein Sequence Motifs on Adeno-Associated Virus Type 2 Intracellular Trafficking and Nuclear Entry. Journal of Virology **86:**9163-9174.

11. **Kronenberg, S., J. A. Kleinschmidt, and B. Bottcher.** 2001. Electron cryo-microscopy and image reconstruction of adeno-associated virus type 2 empty capsids. EMBO Rep **2:**997-1002.

12. **Asokan, A., D. V. Schaffer, and R. J. Samulski.** 2012. The AAV vector toolkit: poised at the clinical crossroads. Mol Ther **20:**699-708.

13. **Bartlett, J. S., R. Wilcher, and R. J. Samulski.** 2000. Infectious Entry Pathway of Adeno-Associated Virus and Adeno-Associated Virus Vectors. J. Virol. **74:**2777-2785.

14. **Xiao, P. J., and R. J. Samulski.** 2012. Cytoplasmic trafficking, endosomal escape, and perinuclear accumulation of adeno-associated virus type 2 particles are facilitated by microtubule network. J Virol **86:**10462-73.

15. **Johnson, J. S., and R. J. Samulski.** 2009. Enhancement of adeno-associated virus infection by mobilizing capsids into and out of the nucleolus. J Virol **83:**2632-44.

16. **Ferrari, F. K., T. Samulski, T. Shenk, and R. J. Samulski.** 1996. Second-strand synthesis is a rate-limiting step for efficient transduction by recombinant adeno-associated virus vectors. J. Virol. **70:**3227-3234.

17. **Nakai, H., T. A. Storm, and M. A. Kay.** 2000. Recruitment of Single-Stranded Recombinant Adeno-Associated Virus Vector Genomes and Intermolecular Recombination Are Responsible for Stable Transduction of Liver In Vivo. Journal of Virology **74:**9451-9463.

18. **Beaton, A., P. Palumbo, and K. I. Berns.** 1989. Expression from the adeno-associated virus p5 and p19 promoters is negatively regulated in trans by the rep protein. J Virol **63:**4450-4.

19. **Cheung, A. K., M. D. Hoggan, W. W. Hauswirth, and K. I. Berns.** 1980. Integration of the adeno-associated virus genome into cellular DNA in latently infected human Detroit 6 cells. J. Virol. **33:**739-748.

20. **Kotin, R. M., M. Siniscalco, R. J. Samulski, X. D. Zhu, L. Hunter, C. A. Laughlin, S. McLaughlin, N. Muzyczka, M. Rocchi, and K. I. Berns.** 1990. Site-specific integration by adeno-associated virus. Proceedings of the National Academy of Sciences of the United States of America **87:**2211-2215.

21. **Samulski, R. J., X. Zhu, X. Xiao, J. D. Brook, D. E. Housman, N. Epstein, and L. A. Hunter.** 1991. Targeted integration of adeno-associated virus (AAV) into human chromosome 19. EMBO J **10:**3941-50.

22. **Georg-Fries, B., S. Biederlack, J. Wolf, and H. Zur Hausen.** 1984. Analysis of proteins, helper dependence, and seroepidemiology of a new human parvovirus. Virology **134:**64-71.

23. **Walz, C., A. Deprez, T. Dupressoir, M. Durst, M. Rabreau, and J. R. Schlehofer.** 1997. Interaction of human papillomavirus type 16 and adeno-associated virus type 2 co-infecting human cervical epithelium. J Gen Virol **78:**1441-1452.

24. **Schlehofer, J. R., M. Ehrbar, and H. Z. Hausen.** 1986. Vaccinia virus, herpes simplex virus, and carcinogens induce DNA amplification in a human cell line and support replication of a helpervirus dependent parvovirus. Virology **152:**110-117.

25. **Yakobson, B., T. A. Hrynko, M. J. Peak, and E. Winocour.** 1989. Replication of adeno-associated virus in cells irradiated with UV light at 254 nm. J. Virol. **63:**1023-1030.

26. **Yakobson, B., T. Koch, and E. Winocour.** 1987. Replication of adeno-associated virus in synchronized cells without the addition of a helper virus. J. Virol. **61:**972-981.

27. **Xiao, W., K. H. Warrington, Jr., P. Hearing, J. Hughes, and N. Muzyczka.** 2002. Adenovirus-Facilitated Nuclear Translocation of Adeno-Associated Virus Type 2. J. Virol. **76:**11505-11517.

28. **Duan, D., P. Sharma, L. Dudus, Y. Zhang, S. Sanlioglu, Z. Yan, Y. Yue, Y. Ye, R. Lester, J. Yang, K. J. Fisher, and J. F. Engelhardt.** 1999. Formation of Adeno-Associated Virus Circular Genomes Is Differentially Regulated by Adenovirus E4 ORF6 and E2a Gene Expression. J. Virol. **73:**161-169.

29. **Shi, Y., E. Seto, L. S. Chang, and T. Shenk.** 1991. Transcriptional repression by YY1, a human GLI-Kruppel-related protein, and relief of repression by adenovirus E1A protein. Cell **67:**377-88.

30. **Janik, J. E., M. M. Huston, K. Cho, and J. A. Rose.** 1989. Efficient synthesis of adeno-associated virus structural proteins requires both adenovirus DNA binding protein and VA I RNA. Virology **168:**320-329.

31. **Mouw, M. B., and D. J. Pintel.** 2000. Adeno-Associated Virus RNAs Appear in a Temporal Order and Their Splicing Is Stimulated during Coinfection with Adenovirus. J. Virol. **74:**9878-9888.

32. **Samulski, R. J., and T. Shenk.** 1988. Adenovirus E1B 55-Mr polypeptide facilitates timely cytoplasmic accumulation of adeno-associated virus mRNAs. J. Virol. **62:**206-210.

33. **Huang, M. M., and P. Hearing.** 1989. Adenovirus early region 4 encodes two gene products with redundant effects in lytic infection. J. Virol. **63:**2605-2615.

34. **Ward, P., F. B. Dean, M. E. O'Donnell, and K. I. Berns.** 1998. Role of the Adenovirus DNA-Binding Protein in In Vitro Adeno-Associated Virus DNA Replication. J. Virol. **72:**420-427.

35. **Geoffroy, M.-C., and A. Salvetti.** 2005. Helper Functions Required for Wild Type and Recombinant Adeno- Associated Virus Growth. Current Gene Therapy **5:**265-271.

36. **Nash, K., W. Chen, W. F. McDonald, X. Zhou, and N. Muzyczka.** 2007. Purification of host cell enzymes involved in adeno-associated virus DNA replication. J Virol **81:**5777-87.

37. **Ni, T. H., W. F. McDonald, I. Zolotukhin, T. Melendy, S. Waga, B. Stillman, and N. Muzyczka.** 1998. Cellular proteins required for adeno-associated virus DNA replication in the absence of adenovirus coinfection. J Virol **72:**2777-87.

38. **Gao, G., L. H. Vandenberghe, M. R. Alvira, Y. Lu, R. Calcedo, X. Zhou, and J. M. Wilson.** 2004. Clades of Adeno-Associated Viruses Are Widely Disseminated in Human Tissues. J. Virol. **78:**6381-6388.

39. **Zincarelli, C., S. Soltys, G. Rengo, and J. E. Rabinowitz.** 2008. Analysis of AAV Serotypes 1-9 Mediated Gene Expression and Tropism in Mice After Systemic Injection. Mol Ther **16:**1073-1080.

40. **Kaludov, N., E. Padron, L. Govindasamy, R. McKenna, J. A. Chiorini, and M. Agbandje-McKenna.** 2003. Production, purification and preliminary X-ray crystallographic studies of adeno-associated virus serotype 4. Virology **306:**1-6.

41. **Miller, E. B., B. Gurda-Whitaker, L. Govindasamy, R. McKenna, S. Zolotukhin, N. Muzyczka, and M. Agbandje-McKenna.** 2006. Production, purification and preliminary X-ray crystallographic studies of adeno-associated virus serotype 1. Acta Crystallogr Sect F Struct Biol Cryst Commun **62:**1271-4.

42. **Mitchell, M., H. J. Nam, A. Carter, A. McCall, C. Rence, A. Bennett, B. Gurda, R. McKenna, M. Porter, Y. Sakai, B. J. Byrne, N. Muzyczka, G. Aslanidi, S. Zolotukhin, and M. Agbandje-McKenna.** 2009. Production, purification and preliminary X-ray crystallographic studies of adeno-associated virus serotype 9. Acta Crystallogr Sect F Struct Biol Cryst Commun **65:**715-8.

43. **Nam, H.-J., M. D. Lane, E. Padron, B. Gurda, R. McKenna, E. Kohlbrenner, G. Aslanidi, B. Byrne, N. Muzyczka, S. Zolotukhin, and M. Agbandje-McKenna.** 2007. Structure of Adeno-Associated Virus Serotype 8, a Gene Therapy Vector. J. Virol. **81:**12260-12271.

44. **Quesada, O., B. Gurda, L. Govindasamy, R. McKenna, E. Kohlbrenner, G. Aslanidi, S. Zolotukhin, N. Muzyczka, and M. Agbandje-McKenna.** 2007. Production, purification and preliminary X-ray crystallographic studies of adeno-associated virus serotype 7. Acta Crystallogr Sect F Struct Biol Cryst Commun **63:**1073-6.

45. **Walters, R. W., M. Agbandje-McKenna, V. D. Bowman, T. O. Moninger, N. H. Olson, M. Seiler, J. A. Chiorini, T. S. Baker, and J. Zabner.** 2004. Structure of Adeno-Associated Virus Serotype 5. J. Virol. **78:**3361-3371.

46. **Xie, Q., H. M. Ongley, J. Hare, and M. S. Chapman.** 2008. Crystallization and preliminary X-ray structural studies of adeno-associated virus serotype 6. Acta Crystallogr Sect F Struct Biol Cryst Commun **64:**1074-8.

47. **Mueller, C., and T. R. Flotte.** 2008. Clinical gene therapy using recombinant adeno-associated virus vectors. Gene Ther **15:**858-863.

48. **Podsakoff, G., K. K. Wong, and S. Chatterjee.** 1994. Efficient gene transfer into nondividing cells by adeno-associated virus-based vectors. Journal of Virology **68:**5656-5666.

49. **Xiao, X., J. Li, and R. J. Samulski.** 1996. Efficient long-term gene transfer into muscle tissue of immunocompetent mice by adeno-associated virus vector. Journal of Virology **70:**8098-108.

50. **Rabinowitz, J. E., D. E. Bowles, S. M. Faust, J. G. Ledford, S. E. Cunningham, and R. J. Samulski.** 2004. Cross-dressing the virion: the transcapsidation of adeno-associated virus serotypes functionally defines subgroups. J Virol **78:**4421-32.

51. **Rabinowitz, J. E., F. Rolling, C. Li, H. Conrath, W. Xiao, X. Xiao, and R. J. Samulski.** 2002. Cross-packaging of a single adeno-associated virus (AAV) type 2 vector genome into multiple AAV serotypes enables transduction with broad specificity. J Virol **76:**791-801.

52. **Grieger, J. C., V. W. Choi, and R. J. Samulski.** 2006. Production and characterization of adeno-associated viral vectors. Nat Protoc **1:**1412-28.

53. **McCarty, D. M., H. Fu, P. E. Monahan, C. E. Toulson, P. Naik, and R. J. Samulski.** 2003. Adeno-associated virus terminal repeat (TR) mutant generates self-complementary vectors to overcome the rate-limiting step to transduction in vivo. Gene Ther **10:**2112-2118.

54. **McCarty, D. M., P. E. Monahan, and R. J. Samulski.** 2001. Self-complementary recombinant adeno-associated virus (scAAV) vectors promote efficient transduction independently of DNA synthesis. Gene Ther **8:**1248-54.

55. **Deyle, D. R., and D. W. Russell.** 2009. Adeno-associated virus vector integration. Curr Opin Mol Ther **11:**442-7.

56. **McCarty, D. M., S. M. Young, Jr., and R. J. Samulski.** 2004. Integration of adeno-associated virus (AAV) and recombinant AAV vectors. Annu Rev Genet **38:**819-45.

57. **Rosas, L. E., J. L. Grieves, K. Zaraspe, K. M. D. La Perle, H. Fu, and D. M. McCarty.** 2012. Patterns of scAAV Vector Insertion Associated With Oncogenic Events in a Mouse Model for Genotoxicity. Mol Ther **20:**2098-2110.

58. **Miao, C. H., R. O. Snyder, D. B. Schowalter, G. A. Patijn, B. Donahue, B. Winther, and M. A. Kay.** 1998. The kinetics of rAAV integration in the liver. Nat Genet **19:**13-5.

59. **Miller, D. G., G. D. Trobridge, L. M. Petek, M. A. Jacobs, R. Kaul, and D. W. Russell.** 2005. Large-Scale Analysis of Adeno-Associated Virus Vector Integration Sites in Normal Human Cells. J. Virol. **79:**11434-11442.

60. **Gaudet, D., J. Methot, and J. Kastelein.** 2012. Gene therapy for lipoprotein lipase deficiency. Curr Opin Lipidol **23:**310-20.

61. **Colella, P., and A. Auricchio.** 2012. Gene therapy of inherited retinopathies: a long and successful road from viral vectors to patients. Hum Gene Ther **23:**796-807.

62. **Gray, S. J.** 2013. Gene therapy and neurodevelopmental disorders. Neuropharmacology **68:**136-42.

63. **Zouein, F. A., and G. W. Booz.** 2013. AAV-mediated gene therapy for heart failure: enhancing contractility and calcium handling. F1000Prime Rep **5:**27.

64. **Excoffon, K. J., G. Liu, L. Miao, J. E. Wilson, B. M. McManus, C. F. Semenkovich, T. Coleman, P. Benoit, N. Duverger, D. Branellec, P. Denefle, M. R. Hayden, and M. E. Lewis.** 1997. Correction of hypertriglyceridemia and impaired fat tolerance in lipoprotein lipase-deficient mice by adenovirus-mediated expression of human lipoprotein lipase. Arterioscler Thromb Vasc Biol **17:**2532-9.

65. **Liu, G., K. J. Ashbourne Excoffon, J. E. Wilson, B. M. McManus, Q. R. Rogers, L. Miao, J. J. Kastelein, M. E. Lewis, and M. R. Hayden.** 2000. Phenotypic correction of feline lipoprotein lipase deficiency by adenoviral gene transfer. Hum Gene Ther **11:**21-32.

66. **Rip, J., M. C. Nierman, C. J. Ross, J. W. Jukema, M. R. Hayden, J. J. Kastelein, E. S. Stroes, and J. A. Kuivenhoven.** 2006. Lipoprotein lipase S447X: a naturally occurring gain-of-function mutation. Arterioscler Thromb Vasc Biol **26:**1236-45.

67. **Ross, C. J., J. Twisk, J. M. Meulenberg, G. Liu, K. van den Oever, E. Moraal, W. T. Hermens, J. Rip, J. J. Kastelein, J. A. Kuivenhoven, and M. R. Hayden.** 2004. Long-term correction of murine lipoprotein lipase deficiency with AAV1-mediated gene transfer of the naturally occurring LPL(S447X) beneficial mutation. Hum Gene Ther **15:**906-19.

68. **Ross, C. J., J. Twisk, A. C. Bakker, F. Miao, D. Verbart, J. Rip, T. Godbey, P. Dijkhuizen, W. T. Hermens, J. J. Kastelein, J. A. Kuivenhoven, J. M. Meulenberg, and M. R. Hayden.** 2006. Correction of feline lipoprotein lipase deficiency with adeno-associated virus serotype 1-mediated gene transfer of the lipoprotein lipase S447X beneficial mutation. Hum Gene Ther **17:**487-99.

69. **Stroes, E. S., M. C. Nierman, J. J. Meulenberg, R. Franssen, J. Twisk, C. P. Henny, M. M. Maas, A. H. Zwinderman, C. Ross, E. Aronica, K. A. High, M. M. Levi, M. R. Hayden, J. J. Kastelein, and J. A. Kuivenhoven.** 2008. Intramuscular administration of AAV1-lipoprotein lipase S447X lowers triglycerides in lipoprotein lipase-deficient patients. Arterioscler Thromb Vasc Biol **28:**2303-4.

70. **Gaudet, D., J. Methot, S. Dery, D. Brisson, C. Essiembre, G. Tremblay, K. Tremblay, J. de Wal, J. Twisk, N. van den Bulk, V. Sier-Ferreira, and S. van Deventer.** 2013. Efficacy and long-term safety of alipogene tiparvovec (AAV1-LPLS447X) gene therapy for lipoprotein lipase deficiency: an open-label trial. Gene Ther **20:**361-9.

71. **Carpentier, A. C., F. Frisch, S. M. Labbe, R. Gagnon, J. de Wal, S. Greentree, H. Petry, J. Twisk, D. Brisson, and D. Gaudet.** 2012. Effect of alipogene tiparvovec (AAV1-LPL(S447X)) on postprandial chylomicron metabolism in lipoprotein lipase-deficient patients. J Clin Endocrinol Metab **97:**1635-44.

72. **Jacobson, S. G., A. V. Cideciyan, R. Ratnakaram, E. Heon, S. B. Schwartz, A. J. Roman, M. C. Peden, T. S. Aleman, S. L. Boye, A. Sumaroka, T. J. Conlon, R. Calcedo, J. J. Pang, K. E. Erger, M. B. Olivares, C. L. Mullins, M. Swider, S. Kaushal, W. J. Feuer, A. Iannaccone, G. A. Fishman, E. M. Stone, B. J. Byrne, and W. W. Hauswirth.** 2012. Gene therapy for leber congenital amaurosis caused by RPE65 mutations: safety and efficacy in 15 children and adults followed up to 3 years. Arch Ophthalmol **130:**9-24.

73. **Ali, R. R., M. B. Reichel, A. J. Thrasher, R. J. Levinsky, C. Kinnon, N. Kanuga, D. M. Hunt, and S. S. Bhattacharya.** 1996. Gene transfer into the mouse retina mediated by an adeno-associated viral vector. Hum Mol Genet **5:**591-4.

74. **Barker, S. E., C. A. Broderick, S. J. Robbie, Y. Duran, M. Natkunarajah, P. Buch, K. S. Balaggan, R. E. MacLaren, J. W. B. Bainbridge, A. J. Smith, and R. R. Ali.** 2009. Subretinal delivery of adeno-associated virus serotype 2 results in minimal immune responses that allow repeat vector administration in immunocompetent mice. The Journal of Gene Medicine **11:**486-497.

75. **McClements, M. E., and R. E. MacLaren.** 2013. Gene therapy for retinal disease. Transl Res **161:**241-54.

76. **Chung, D. C., and E. I. Traboulsi.** 2009. Leber congenital amaurosis: clinical correlations with genotypes, gene therapy trials update, and future directions. J AAPOS **13:**587-92.

77. **Maguire, A. M., K. A. High, A. Auricchio, J. F. Wright, E. A. Pierce, F. Testa, F. Mingozzi, J. L. Bennicelli, G. S. Ying, S. Rossi, A. Fulton, K. A. Marshall, S. Banfi, D. C. Chung, J. I. Morgan, B. Hauck, O. Zelenaia, X. Zhu, L. Raffini, F. Coppieters, E. De Baere, K. S. Shindler, N. J. Volpe, E. M. Surace, C. Acerra, A. Lyubarsky, T. M. Redmond, E. Stone, J. Sun, J. W. McDonnell, B. P. Leroy, F. Simonelli, and J. Bennett.** 2009. Age-dependent effects of RPE65 gene therapy for Leber's congenital amaurosis: a phase 1 dose-escalation trial. Lancet **374:**1597-605.

78. **Testa, F., A. M. Maguire, S. Rossi, E. A. Pierce, P. Melillo, K. Marshall, S. Banfi, E. M. Surace, J. Sun, C. Acerra, J. F. Wright, J. Wellman, K. A. High, A. Auricchio, J. Bennett, and F. Simonelli.** 2013. Three-year follow-up after unilateral subretinal

delivery of adeno-associated virus in patients with Leber congenital Amaurosis type 2. Ophthalmology **120:**1283-91.

79. **Cai, X., S. M. Conley, and M. I. Naash.** 2009. RPE65: role in the visual cycle, human retinal disease, and gene therapy. Ophthalmic Genet **30:**57-62.

80. **Bainbridge, J. W., A. J. Smith, S. S. Barker, S. Robbie, R. Henderson, K. Balaggan, A. Viswanathan, G. E. Holder, A. Stockman, N. Tyler, S. Petersen-Jones, S. S. Bhattacharya, A. J. Thrasher, F. W. Fitzke, B. J. Carter, G. S. Rubin, A. T. Moore, and R. R. Ali.** 2008. Effect of gene therapy on visual function in Leber's congenital amaurosis. N Engl J Med **358:**2231-9.

81. **Maguire, A. M., F. Simonelli, E. A. Pierce, E. N. Pugh, Jr., F. Mingozzi, J. Bennicelli, S. Banfi, K. A. Marshall, F. Testa, E. M. Surace, S. Rossi, A. Lyubarsky, V. R. Arruda, B. Konkle, E. Stone, J. Sun, J. Jacobs, L. Dell'Osso, R. Hertle, J. X. Ma, T. M. Redmond, X. Zhu, B. Hauck, O. Zelenaia, K. S. Shindler, M. G. Maguire, J. F. Wright, N. J. Volpe, J. W. McDonnell, A. Auricchio, K. A. High, and J. Bennett.** 2008. Safety and efficacy of gene transfer for Leber's congenital amaurosis. N Engl J Med **358:**2240-8.

82. **Hauswirth, W. W., T. S. Aleman, S. Kaushal, A. V. Cideciyan, S. B. Schwartz, L. Wang, T. J. Conlon, S. L. Boye, T. R. Flotte, B. J. Byrne, and S. G. Jacobson.** 2008. Treatment of leber congenital amaurosis due to RPE65 mutations by ocular subretinal injection of adeno-associated virus gene vector: short-term results of a phase I trial. Hum Gene Ther **19:**979-90.

83. **Bennett, J., M. Ashtari, J. Wellman, K. A. Marshall, L. L. Cyckowski, D. C. Chung, S. McCague, E. A. Pierce, Y. Chen, J. L. Bennicelli, X. Zhu, G.-s. Ying, J. Sun, J. F. Wright, A. Auricchio, F. Simonelli, K. S. Shindler, F. Mingozzi, K. A. High, and A. M. Maguire.** 2012. AAV2 Gene Therapy Readministration in Three Adults with Congenital Blindness. Science Translational Medicine **4:**120ra15.

84. **Walsh, C. E., and K. M. Batt.** 2013. Hemophilia clinical gene therapy: brief review. Translational Research **161:**307-312.

85. **Fabb, S. A., and J. G. Dickson.** 2000. Technology evaluation: AAV factor IX gene therapy, Avigen Inc. Curr Opin Mol Ther **2:**601-6.

86. **Manno, C. S., G. F. Pierce, V. R. Arruda, B. Glader, M. Ragni, J. J. Rasko, M. C. Ozelo, K. Hoots, P. Blatt, B. Konkle, M. Dake, R. Kaye, M. Razavi, A. Zajko, J. Zehnder, P. K. Rustagi, H. Nakai, A. Chew, D. Leonard, J. F. Wright, R. R. Lessard, J. M. Sommer, M. Tigges, D. Sabatino, A. Luk, H. Jiang, F. Mingozzi, L. Couto, H. C. Ertl, K. A. High, and M. A. Kay.** 2006. Successful transduction of liver in hemophilia by AAV-Factor IX and limitations imposed by the host immune response. Nat Med **12:**342-7.

87. **Schuettrumpf, J., J. H. Liu, L. B. Couto, K. Addya, D. G. Leonard, Z. Zhen, J. Sommer, and V. R. Arruda.** 2006. Inadvertent germline transmission of AAV2 vector:

findings in a rabbit model correlate with those in a human clinical trial. Mol Ther **13:**1064-73.

88. **Nathwani, A. C., E. G. Tuddenham, S. Rangarajan, C. Rosales, J. McIntosh, D. C. Linch, P. Chowdary, A. Riddell, A. J. Pie, C. Harrington, J. O'Beirne, K. Smith, J. Pasi, B. Glader, P. Rustagi, C. Y. Ng, M. A. Kay, J. Zhou, Y. Spence, C. L. Morton, J. Allay, J. Coleman, S. Sleep, J. M. Cunningham, D. Srivastava, E. Basner-Tschakarjan, F. Mingozzi, K. A. High, J. T. Gray, U. M. Reiss, A. W. Nienhuis, and A. M. Davidoff.** 2011. Adenovirus-associated virus vector-mediated gene transfer in hemophilia B. N Engl J Med **365:**2357-65.

89. **Jiang, H., G. F. Pierce, M. C. Ozelo, E. V. de Paula, J. A. Vargas, P. Smith, J. Sommer, A. Luk, C. S. Manno, K. A. High, and V. R. Arruda.** 2006. Evidence of multiyear factor IX expression by AAV-mediated gene transfer to skeletal muscle in an individual with severe hemophilia B. Mol Ther **14:**452-5.

90. **Manno, C. S., A. J. Chew, S. Hutchison, P. J. Larson, R. W. Herzog, V. R. Arruda, S. J. Tai, M. V. Ragni, A. Thompson, M. Ozelo, L. B. Couto, D. G. B. Leonard, F. A. Johnson, A. McClelland, C. Scallan, E. Skarsgard, A. W. Flake, M. A. Kay, K. A. High, and B. Glader.** 2003. AAV-mediated factor IX gene transfer to skeletal muscle in patients with severe hemophilia B. Blood **101:**2963-2972.

91. **Bartel, M. A., J. R. Weinstein, and D. V. Schaffer.** 2012. Directed evolution of novel adeno-associated viruses for therapeutic gene delivery. Gene Ther **19:**694-700.

92. **Maheshri, N., J. T. Koerber, B. K. Kaspar, and D. V. Schaffer.** 2006. Directed evolution of adeno-associated virus yields enhanced gene delivery vectors. Nat Biotech **24:**198-204.

93. **Perabo, L., J. Endell, S. King, K. Lux, D. Goldnau, M. Hallek, and H. Büning.** 2006. Combinatorial engineering of a gene therapy vector: directed evolution of adeno-associated virus. The Journal of Gene Medicine **8:**155-162.

94. **Gray, S. J., B. L. Blake, H. E. Criswell, S. C. Nicolson, R. J. Samulski, and T. J. McCown.** 2010. Directed Evolution of a Novel Adeno-associated Virus (AAV) Vector That Crosses the Seizure-compromised Blood-Brain Barrier (BBB). Mol Ther **18:**570-578.

95. **Koerber, J. T., R. Klimczak, J.-H. Jang, D. Dalkara, J. G. Flannery, and D. V. Schaffer.** 2009. Molecular Evolution of Adeno-associated Virus for Enhanced Glial Gene Delivery. Mol Ther **17:**2088-2095.

96. **Li, W., A. Asokan, Z. Wu, T. Van Dyke, N. DiPrimio, J. S Johnson, L. Govindaswamy, M. Agbandje-McKenna, S. Leichtle, D. Eugene Redmond Jr, T. J. McCown, K. B. Petermann, N. E. Sharpless, and R. J. Samulski.** 2008. Engineering and Selection of Shuffled AAV Genomes: A New Strategy for Producing Targeted Biological Nanoparticles. Mol Ther **16:**1252-1260.

97. **Li, W., L. Zhang, J. S. Johnson, W. Zhijian, J. C. Grieger, X. Ping-Jie, L. M. Drouin, M. Agbandje-McKenna, R. J. Pickles, and R. J. Samulski.** 2009. Generation of Novel AAV Variants by Directed Evolution for Improved CFTR Delivery to Human Ciliated Airway Epithelium. Mol Ther **17:**2067-2077.

98. **Miao, C. H., H. Nakai, A. R. Thompson, T. A. Storm, W. Chiu, R. O. Snyder, and M. A. Kay.** 2000. Nonrandom Transduction of Recombinant Adeno-Associated Virus Vectors in Mouse Hepatocytes In Vivo: Cell Cycling Does Not Influence Hepatocyte Transduction. Journal of Virology **74:**3793-3803.

99. **Wu, Z., A. Asokan, J. C. Grieger, L. Govindasamy, M. Agbandje-McKenna, and R. J. Samulski.** 2006. Single Amino Acid Changes Can Influence Titer, Heparin Binding, and Tissue Tropism in Different Adeno-Associated Virus Serotypes. Journal of Virology **80:**11393-11397.

100. **Shen, S., K. D. Bryant, S. M. Brown, S. H. Randell, and A. Asokan.** 2011. Terminal N-linked galactose is the primary receptor for adeno-associated virus 9. Journal of Biological Chemistry **286:**13532-13540.

101. **Bell, C. L., B. L. Gurda, K. Van Vliet, M. Agbandje-McKenna, and J. M. Wilson.** 2012. Identification of the Galactose Binding Domain of the Adeno-Associated Virus Serotype 9 Capsid. Journal of Virology **86:**7326-7333.

102. **Shen, S., E. D. Horowitz, A. N. Troupes, S. M. Brown, N. Pulicherla, R. J. Samulski, M. Agbandje-McKenna, and A. Asokan.** 2013. Engraftment of a Galactose Receptor Footprint onto Adeno-associated Viral Capsids Improves Transduction Efficiency. Journal of Biological Chemistry **288:**28814-28823.

103. **Alexander, I. E., D. W. Russell, and A. D. Miller.** 1994. DNA-damaging agents greatly increase the transduction of nondividing cells by adeno-associated virus vectors. Journal of Virology **68:**8282-8287.

104. **Russell, D. W., I. E. Alexander, and A. D. Miller.** 1995. DNA synthesis and topoisomerase inhibitors increase transduction by adeno-associated virus vectors. Proc Natl Acad Sci U S A **92:**5719-23.

105. **Duan, D., Y. Yue, Z. Yan, J. Yang, and J. F. Engelhardt.** 2000. Endosomal processing limits gene transfer to polarized airway epithelia by adeno-associated virus. J Clin Invest **105:**1573-87.

106. **Douar, A. M., K. Poulard, D. Stockholm, and O. Danos.** 2001. Intracellular trafficking of adeno-associated virus vectors: routing to the late endosomal compartment and proteasome degradation. J Virol **75:**1824-33.

107. **Johnson, J. S., and R. J. Samulski.** 2009. Enhancement of Adeno-Associated Virus Infection by Mobilizing Capsids into and Out of the Nucleolus. J. Virol. **83:**2632-2644.

108. **Nathwani, A. C., M. Cochrane, J. McIntosh, C. Y. Ng, J. Zhou, J. T. Gray, and A. M. Davidoff.** 2009. Enhancing transduction of the liver by adeno-associated viral vectors. Gene Ther **16:**60-9.

109. **Monahan, P. E., C. D. Lothrop, J. Sun, M. L. Hirsch, T. Kafri, B. Kantor, R. Sarkar, D. M. Tillson, J. R. Elia, and R. J. Samulski.** 2010. Proteasome inhibitors enhance gene delivery by AAV virus vectors expressing large genomes in hemophilia mouse and dog models: a strategy for broad clinical application. Mol Ther **18:**1907-16.

110. **Chelbi-Alix, M. K., F. Quignon, L. Pelicano, M. H. Koken, and H. de The.** 1998. Resistance to virus infection conferred by the interferon-induced promyelocytic leukemia protein. J Virol **72:**1043-51.

111. **McNally, B. A., J. Trgovcich, G. G. Maul, Y. Liu, and P. Zheng.** 2008. A role for cytoplasmic PML in cellular resistance to viral infection. PLoS One **3:**e2277.

112. **Pampin, M., Y. Simonin, B. Blondel, Y. Percherancier, and M. K. Chelbi-Alix.** 2006. Cross talk between PML and p53 during poliovirus infection: implications for antiviral defense. J Virol **80:**8582-92.

113. **Regad, T., A. Saib, V. Lallemand-Breitenbach, P. P. Pandolfi, H. de The, and M. K. Chelbi-Alix.** 2001. PML mediates the interferon-induced antiviral state against a complex retrovirus via its association with the viral transactivator. EMBO J **20:**3495-505.

114. **Reichelt, M., L. Wang, M. Sommer, J. Perrino, A. M. Nour, N. Sen, A. Baiker, L. Zerboni, and A. M. Arvin.** 2011. Entrapment of viral capsids in nuclear PML cages is an intrinsic antiviral host defense against varicella-zoster virus. PLoS Pathog **7:**e1001266.

115. **Everett, R. D., C. Parada, P. Gripon, H. Sirma, and A. Orr.** 2008. Replication of ICP0-null mutant herpes simplex virus type 1 is restricted by both PML and Sp100. J Virol **82:**2661-72.

116. **Leppard, K. N., E. Emmott, M. S. Cortese, and T. Rich.** 2009. Adenovirus type 5 E4 Orf3 protein targets promyelocytic leukaemia (PML) protein nuclear domains for disruption via a sequence in PML isoform II that is predicted as a protein interaction site by bioinformatic analysis. J Gen Virol **90:**95-104.

117. **Fraefel, C., A. G. Bittermann, H. Bueler, I. Heid, T. Bachi, and M. Ackermann.** 2004. Spatial and temporal organization of adeno-associated virus DNA replication in live cells. J Virol **78:**389-98.

118. **Young, P. J., K. T. Jensen, L. R. Burger, D. J. Pintel, and C. L. Lorson.** 2002. Minute Virus of Mice NS1 Interacts with the SMN Protein, and They Colocalize in Novel Nuclear Bodies Induced by Parvovirus Infection. Journal of Virology **76:**3892-3904.

119. **Au, W. Y., C. R. Kumana, H. K. Lee, S. Y. Lin, H. Liu, D. Y. Yeung, J. S. Lau, and Y. L. Kwong.** 2011. Oral arsenic trioxide-based maintenance regimens for first complete

remission of acute promyelocytic leukemia: a 10-year follow-up study. Blood **118:**6535-43.

120. **List, A., M. Beran, J. DiPersio, J. Slack, N. Vey, C. S. Rosenfeld, and P. Greenberg.** 2003. Opportunities for Trisenox (arsenic trioxide) in the treatment of myelodysplastic syndromes. Leukemia **17:**1499-507.

121. **Park, W. H., J. G. Seol, E. S. Kim, J. M. Hyun, C. W. Jung, C. C. Lee, B. K. Kim, and Y. Y. Lee.** 2000. Arsenic trioxide-mediated growth inhibition in MC/CAR myeloma cells via cell cycle arrest in association with induction of cyclin-dependent kinase inhibitor, p21, and apoptosis. Cancer Res **60:**3065-71.

122. **Emadi, A., and S. D. Gore.** 2010. Arsenic trioxide - An old drug rediscovered. Blood Rev **24:**191-9.

123. **Bogyo, M., and E. W. Wang.** 2002. Proteasome inhibitors: complex tools for a complex enzyme. Curr Top Microbiol Immunol **268:**185-208.

124. **Simonelli, F., A. M. Maguire, F. Testa, E. A. Pierce, F. Mingozzi, J. L. Bennicelli, S. Rossi, K. Marshall, S. Banfi, E. M. Surace, J. Sun, T. M. Redmond, X. Zhu, K. S. Shindler, G.-S. Ying, C. Ziviello, C. Acerra, J. F. Wright, J. W. McDonnell, K. A. High, J. Bennett, and A. Auricchio.** 2010. Gene Therapy for Leber's Congenital Amaurosis is Safe and Effective Through 1.5 Years After Vector Administration. Mol Ther **18:**643-650.

125. **Xiao, W., K. H. Warrington, Jr., P. Hearing, J. Hughes, and N. Muzyczka.** 2002. Adenovirus-facilitated nuclear translocation of adeno-associated virus type 2. J Virol **76:**11505-17.

126. **Geoffroy, M. C., and M. K. Chelbi-Alix.** 2011. Role of promyelocytic leukemia protein in host antiviral defense. J Interferon Cytokine Res **31:**145-58.

127. **Diaz-Griffero, F., X. R. Qin, F. Hayashi, T. Kigawa, A. Finzi, Z. Sarnak, M. Lienlaf, S. Yokoyama, and J. Sodroski.** 2009. A B-box 2 surface patch important for TRIM5alpha self-association, capsid binding avidity, and retrovirus restriction. J Virol **83:**10737-51.

128. **Mallery, D. L., W. A. McEwan, S. R. Bidgood, G. J. Towers, C. M. Johnson, and L. C. James.** 2010. Antibodies mediate intracellular immunity through tripartite motif-containing 21 (TRIM21). Proc Natl Acad Sci U S A **107:**19985-90.

129. **McNab, F. W., R. Rajsbaum, J. P. Stoye, and A. O'Garra.** 2010. Tripartite-motif proteins and innate immune regulation. Curr Opin Immunol **23:**46-56.

130. **Condemine, W., Y. Takahashi, J. Zhu, F. Puvion-Dutilleul, S. Guegan, A. Janin, and H. de The.** 2006. Characterization of endogenous human promyelocytic leukemia isoforms. Cancer Res **66:**6192-8.

131. **Lang, M., T. Jegou, I. Chung, K. Richter, S. Munch, A. Udvarhelyi, C. Cremer, P. Hemmerich, J. Engelhardt, S. W. Hell, and K. Rippe.** 2010. Three-dimensional organization of promyelocytic leukemia nuclear bodies. J Cell Sci **123:**392-400.

132. **Mitchell, A. M., C. Li, and R. J. Samulski.** 2013. Arsenic trioxide stabilizes accumulations of adeno-associated virus virions at the perinuclear region, increasing transduction in vitro and in vivo. J Virol **87:**4571-83.

133. **Wang, Z. G., L. Delva, M. Gaboli, R. Rivi, M. Giorgio, C. Cordon-Cardo, F. Grosveld, and P. P. Pandolfi.** 1998. Role of PML in cell growth and the retinoic acid pathway. Science **279:**1547-51.

134. **Thomas, C. E., T. A. Storm, Z. Huang, and M. A. Kay.** 2004. Rapid Uncoating of Vector Genomes Is the Key to Efficient Liver Transduction with Pseudotyped Adeno-Associated Virus Vectors. Journal of Virology **78:**3110-3122.

135. **Arad, U.** 1998. Modified Hirt procedure for rapid purification of extrachromosomal DNA from mammalian cells. Biotechniques **24:**760-2.

136. **Davidoff, A. M., C. Y. Ng, J. Zhou, Y. Spence, and A. C. Nathwani.** 2003. Sex significantly influences transduction of murine liver by recombinant adeno-associated viral vectors through an androgen-dependent pathway. Blood **102:**480-8.

137. **Weidtkamp-Peters, S., T. Lenser, D. Negorev, N. Gerstner, T. G. Hofmann, G. Schwanitz, C. Hoischen, G. Maul, P. Dittrich, and P. Hemmerich.** 2008. Dynamics of component exchange at PML nuclear bodies. J Cell Sci **121:**2731-43.

138. **Christensen, J., and P. Tattersall.** 2002. Parvovirus initiator protein NS1 and RPA coordinate replication fork progression in a reconstituted DNA replication system. J Virol **76:**6518-31.

139. **Berscheminski, J., P. Groitl, T. Dobner, P. Wimmer, and S. Schreiner.** 2013. The adenoviral oncogene E1A-13S interacts with a specific isoform of the tumor suppressor PML to enhance viral transcription. J Virol **87:**965-77.

140. **Nojima, T., T. Oshiro-Ideue, H. Nakanoya, H. Kawamura, T. Morimoto, Y. Kawaguchi, N. Kataoka, and M. Hagiwara.** 2009. Herpesvirus protein ICP27 switches PML isoform by altering mRNA splicing. Nucleic Acids Res **37:**6515-27.

141. **Cuchet, D., A. Sykes, A. Nicolas, A. Orr, J. Murray, H. Sirma, J. Heeren, A. Bartelt, and R. D. Everett.** 2011. PML isoforms I and II participate in PML-dependent restriction of HSV-1 replication. J Cell Sci **124:**280-91.

142. **Chang, L. S., Y. Shi, and T. Shenk.** 1989. Adeno-associated virus P5 promoter contains an adenovirus E1A-inducible element and a binding site for the major late transcription factor. J. Virol. **63:**3479-3488.

143. **Hermonat, P. L., A. D. Santin, R. B. Batchu, and D. Zhan.** 1998. The adeno-associated virus Rep78 major regulatory protein binds the cellular TATA-binding protein in vitro and in vivo. Virology **245:**120-7.

144. **Pereira, D. J., D. M. McCarty, and N. Muzyczka.** 1997. The adeno-associated virus (AAV) Rep protein acts as both a repressor and an activator to regulate AAV transcription during a productive infection. J Virol **71:**1079-88.

145. **Weger, S., M. Wendland, J. A. Kleinschmidt, and R. Heilbronn.** 1999. The adeno-associated virus type 2 regulatory proteins rep78 and rep68 interact with the transcriptional coactivator PC4. J Virol **73:**260-9.

146. **Nakai, H., S. R. Yant, T. A. Storm, S. Fuess, L. Meuse, and M. A. Kay.** 2001. Extrachromosomal Recombinant Adeno-Associated Virus Vector Genomes Are Primarily Responsible for Stable Liver Transduction In Vivo. J. Virol. **75:**6969-6976.

147. **Johnson, J. S., M. Gentzsch, L. Zhang, C. M. Ribeiro, B. Kantor, T. Kafri, R. J. Pickles, and R. J. Samulski.** 2011. AAV exploits subcellular stress associated with inflammation, endoplasmic reticulum expansion, and misfolded proteins in models of cystic fibrosis. PLoS Pathog **7:**e1002053.

148. **Zhong, L., K. Qing, Y. Si, L. Chen, M. Tan, and A. Srivastava.** 2004. Heat-shock treatment-mediated increase in transduction by recombinant adeno-associated virus 2 vectors is independent of the cellular heat-shock protein 90. J Biol Chem **279:**12714-23.

149. **Yalkinoglu, A. O., R. Heilbronn, A. Burkle, J. R. Schlehofer, and H. zur Hausen.** 1988. DNA amplification of adeno-associated virus as a response to cellular genotoxic stress. Cancer Res **48:**3123-9.

150. **Golding, I.** 2011. Decision making in living cells: lessons from a simple system. Annu Rev Biophys **40:**63-80.

151. **van der Ven, A., R. van Diest, K. Hamulyak, M. Maes, C. Bruggeman, and A. Appels.** 2003. Herpes viruses, cytokines, and altered hemostasis in vital exhaustion. Psychosom Med **65:**194-200.

152. **Huang, W., P. Xie, M. Xu, P. Li, and G. Zao.** 2011. The influence of stress factors on the reactivation of latent herpes simplex virus type 1 in infected mice. Cell Biochem Biophys **61:**115-22.

153. **Ju, X. D., S. Q. Lou, W. G. Wang, J. Q. Peng, and H. Tian.** 2004. Effect of hydroxyurea and etoposide on transduction of human bone marrow mesenchymal stem and progenitor cell by adeno-associated virus vectors. Acta Pharmacol Sin **25:**196-202.

154. **Prasad, K. M., Y. Xu, Z. Yang, M. C. Toufektsian, S. S. Berr, and B. A. French.** 2007. Topoisomerase inhibition accelerates gene expression after adeno-associated virus-mediated gene transfer to the mammalian heart. Mol Ther **15:**764-71.

155. **Cornelis, T., E. A. Beckers, A. L. Driessen, F. M. van der Sande, and G. H. Koek.** 2012. Bortezomib-associated fatal liver failure in a haemodialysis patient with multiple myeloma. Clin Toxicol (Phila) **50:**444-5.

156. **Baljevic, M., J. H. Park, E. Stein, D. Douer, J. K. Altman, and M. S. Tallman.** 2011. Curing all patients with acute promyelocytic leukemia: are we there yet? Hematol Oncol Clin North Am **25:**1215-33, viii.

157. **Spuches, A. M., H. G. Kruszyna, A. M. Rich, and D. E. Wilcox.** 2005. Thermodynamics of the As(III)-thiol interaction: arsenite and monomethylarsenite complexes with glutathione, dihydrolipoic acid, and other thiol ligands. Inorg Chem **44:**2964-72.

158. **Dai, J., R. S. Weinberg, S. Waxman, and Y. Jing.** 1999. Malignant cells can be sensitized to undergo growth inhibition and apoptosis by arsenic trioxide through modulation of the glutathione redox system. Blood **93:**268-77.

159. **Kapahi, P., T. Takahashi, G. Natoli, S. R. Adams, Y. Chen, R. Y. Tsien, and M. Karin.** 2000. Inhibition of NF-kappa B activation by arsenite through reaction with a critical cysteine in the activation loop of Ikappa B kinase. J Biol Chem **275:**36062-6.

160. **Jeanne, M., V. Lallemand-Breitenbach, O. Ferhi, M. Koken, M. Le Bras, S. Duffort, L. Peres, C. Berthier, H. Soilihi, B. Raught, and H. de The.** 2010. PML/RARA oxidation and arsenic binding initiate the antileukemia response of As2O3. Cancer Cell **18:**88-98.

161. **Larochette, N., D. Decaudin, E. Jacotot, C. Brenner, I. Marzo, S. A. Susin, N. Zamzami, Z. Xie, J. Reed, and G. Kroemer.** 1999. Arsenite induces apoptosis via a direct effect on the mitochondrial permeability transition pore. Exp Cell Res **249:**413-21.

162. **Hong, S. H., Z. Yang, and M. L. Privalsky.** 2001. Arsenic trioxide is a potent inhibitor of the interaction of SMRT corepressor with Its transcription factor partners, including the PML-retinoic acid receptor alpha oncoprotein found in human acute promyelocytic leukemia. Mol Cell Biol **21:**7172-82.

163. **Park, J. W., Y. J. Choi, M. A. Jang, S. H. Baek, J. H. Lim, T. Passaniti, and T. K. Kwon.** 2001. Arsenic trioxide induces G2/M growth arrest and apoptosis after caspase-3 activation and bcl-2 phosphorylation in promonocytic U937 cells. Biochem Biophys Res Commun **286:**726-34.

164. **Malbec, M., Q. T. Pham, M. B. Plourde, A. Letourneau-Hogan, M. E. Nepveu-Traversy, and L. Berthoux.** 2010. Murine double minute 2 as a modulator of retroviral restrictions mediated by TRIM5alpha. Virology **405:**414-23.

165. **Sebastian, S., E. Sokolskaja, and J. Luban.** 2006. Arsenic counteracts human immunodeficiency virus type 1 restriction by various TRIM5 orthologues in a cell type-dependent manner. J Virol **80:**2051-4.

166. **Stalder, R., F. Blanchet, B. Mangeat, and V. Piguet.** 2010. Arsenic modulates APOBEC3G-mediated restriction to HIV-1 infection in myeloid dendritic cells. J Leukoc Biol **88:**1251-8.

167. **Au, W. Y., and Y. L. Kwong.** 2005. Frequent varicella zoster reactivation associated with therapeutic use of arsenic trioxide: portents of an old scourge. J Am Acad Dermatol **53:**890-2.

168. **Nouri, K., C. A. Ricotti, Jr., N. Bouzari, H. Chen, E. Ahn, and A. Bach.** 2006. The incidence of recurrent herpes simplex and herpes zoster infection during treatment with arsenic trioxide. J Drugs Dermatol **5:**182-5.

169. **Jennings, K., T. Miyamae, R. Traister, A. Marinov, S. Katakura, D. Sowders, B. Trapnell, J. M. Wilson, G. Gao, and R. Hirsch.** 2005. Proteasome inhibition enhances AAV-mediated transgene expression in human synoviocytes in vitro and in vivo. Mol Ther **11:**600-7.

170. **Zhang, W., K. Ohnishi, K. Shigeno, S. Fujisawa, K. Naito, S. Nakamura, K. Takeshita, A. Takeshita, and R. Ohno.** 1998. The induction of apoptosis and cell cycle arrest by arsenic trioxide in lymphoid neoplasms. Leukemia **12:**1383-91.

171. **Xiao, P. J., C. Li, A. Neumann, and R. J. Samulski.** 2011. Quantitative 3D tracing of gene-delivery viral vectors in human cells and animal tissues. Mol Ther **20:**317-28.

172. **Gu, Y., D. F. Lewis, Y. Zhang, L. J. Groome, and Y. Wang.** 2006. Increased superoxide generation and decreased stress protein Hsp90 expression in human umbilical cord vein endothelial cells (HUVECs) from pregnancies complicated by preeclampsia. Hypertens Pregnancy **25:**169-82.

173. **Li, C., N. Diprimio, D. E. Bowles, M. L. Hirsch, P. E. Monahan, A. Asokan, J. Rabinowitz, M. Agbandje-McKenna, and R. J. Samulski.** 2012. Single amino acid modification of adeno-associated virus capsid changes transduction and humoral immune profiles. J Virol **86:**7752-9.

174. **Sanlioglu, S., P. K. Benson, J. Yang, E. M. Atkinson, T. Reynolds, and J. F. Engelhardt.** 2000. Endocytosis and nuclear trafficking of adeno-associated virus type 2 are controlled by rac1 and phosphatidylinositol-3 kinase activation. J Virol **74:**9184-96.

175. **Miller, W. H., Jr., H. M. Schipper, J. S. Lee, J. Singer, and S. Waxman.** 2002. Mechanisms of action of arsenic trioxide. Cancer Res **62:**3893-903.

176. **Lallemand-Breitenbach, V., M. C. Guillemin, A. Janin, M. T. Daniel, L. Degos, S. C. Kogan, J. M. Bishop, and H. de The.** 1999. Retinoic acid and arsenic synergize to eradicate leukemic cells in a mouse model of acute promyelocytic leukemia. J Exp Med **189:**1043-52.

177. **Shen, Z. X., G. Q. Chen, J. H. Ni, X. S. Li, S. M. Xiong, Q. Y. Qiu, J. Zhu, W. Tang, G. L. Sun, K. Q. Yang, Y. Chen, L. Zhou, Z. W. Fang, Y. T. Wang, J. Ma, P. Zhang,**

T. D. Zhang, S. J. Chen, Z. Chen, and Z. Y. Wang. 1997. Use of arsenic trioxide (As2O3) in the treatment of acute promyelocytic leukemia (APL): II. Clinical efficacy and pharmacokinetics in relapsed patients. Blood **89:**3354-60.

178. **Keiser, N. W., Z. Yan, Y. Zhang, D. C. Lei-Butters, and J. F. Engelhardt.** 2011. Unique characteristics of AAV1, 2, and 5 viral entry, intracellular trafficking, and nuclear import define transduction efficiency in HeLa cells. Hum Gene Ther **22:**1433-44.

179. **Liu, Y., K. I. Joo, and P. Wang.** 2012. Endocytic processing of adeno-associated virus type 8 vectors for transduction of target cells. Gene Ther.

180. **Sanlioglu, S., and J. F. Engelhardt.** 1999. Cellular redox state alters recombinant adeno-associated virus transduction through tyrosine phosphatase pathways. Gene Ther **6:**1427-37.

181. **Wheeler, M. D., H. Kono, I. Rusyn, G. E. Arteel, D. McCarty, R. J. Samulski, and R. G. Thurman.** 2000. Chronic ethanol increases adeno-associated viral transgene expression in rat liver via oxidant and NFkappaB-dependent mechanisms. Hepatology **32:**1050-9.

182. **Jayandharan, G. R., G. Aslanidi, A. T. Martino, S. C. Jahn, G. Q. Perrin, R. W. Herzog, and A. Srivastava.** 2011. Activation of the NF-kappaB pathway by adeno-associated virus (AAV) vectors and its implications in immune response and gene therapy. Proc Natl Acad Sci U S A **108:**3743-8.

183. **Hwang, D. R., Y. C. Tsai, J. C. Lee, K. K. Huang, R. K. Lin, C. H. Ho, J. M. Chiou, Y. T. Lin, J. T. Hsu, and C. T. Yeh.** 2004. Inhibition of hepatitis C virus replication by arsenic trioxide. Antimicrob Agents Chemother **48:**2876-82.

184. **Kuroki, M., Y. Ariumi, M. Ikeda, H. Dansako, T. Wakita, and N. Kato.** 2009. Arsenic trioxide inhibits hepatitis C virus RNA replication through modulation of the glutathione redox system and oxidative stress. J Virol **83:**2338-48.

185. **Bulliard, Y., I. Narvaiza, A. Bertero, S. Peddi, U. F. Rohrig, M. Ortiz, V. Zoete, N. Castro-Diaz, P. Turelli, A. Telenti, O. Michielin, M. D. Weitzman, and D. Trono.** 2011. Structure-function analyses point to a polynucleotide-accommodating groove essential for APOBEC3A restriction activities. J Virol **85:**1765-76.

186. **Geelen, J. L., R. Boom, G. P. Klaver, R. P. Minnaar, M. C. Feltkamp, F. J. van Milligen, C. J. Sol, and J. van der Noordaa.** 1987. Transcriptional activation of the major immediate early transcription unit of human cytomegalovirus by heat-shock, arsenite and protein synthesis inhibitors. J Gen Virol **68 (Pt 11):**2925-31.

187. **Sides, M. D., G. J. Block, B. Shan, K. C. Esteves, Z. Lin, E. K. Flemington, and J. A. Lasky.** 2011. Arsenic mediated disruption of promyelocytic leukemia protein nuclear bodies induces ganciclovir susceptibility in Epstein-Barr positive epithelial cells. Virology **416:**86-97.

188. **Binny, C., J. McIntosh, M. Della Peruta, H. Kymalainen, E. G. Tuddenham, S. M. Buckley, S. N. Waddington, J. H. McVey, Y. Spence, C. L. Morton, A. J. Thrasher, J. T. Gray, F. J. Castellino, A. F. Tarantal, A. M. Davidoff, and A. C. Nathwani.** 2012. AAV-mediated gene transfer in the perinatal period results in expression of FVII at levels that protect against fatal spontaneous hemorrhage. Blood **119:**957-66.

189. **Goodrich, L. R., J. N. Phillips, C. W. McIlwraith, S. B. Foti, J. C. Grieger, S. J. Gray, and R. J. Samulski.** 2013. Optimization of scAAVIL-1ra In Vitro and In Vivo to Deliver High Levels of Therapeutic Protein for Treatment of Osteoarthritis. Mol Ther Nucleic Acids **2:**e70.

190. **Markusic, D. M., and R. W. Herzog.** 2012. Liver-Directed Adeno-Associated Viral Gene Therapy for Hemophilia. J Genet Syndr Gene Ther **1:**1-9.

191. **Yan, Z., R. Zak, G. W. Luxton, T. C. Ritchie, U. Bantel-Schaal, and J. F. Engelhardt.** 2002. Ubiquitination of both adeno-associated virus type 2 and 5 capsid proteins affects the transduction efficiency of recombinant vectors. J Virol **76:**2043-53.

192. **Ding, W., Z. Yan, R. Zak, M. Saavedra, D. M. Rodman, and J. F. Engelhardt.** 2003. Second-strand genome conversion of adeno-associated virus type 2 (AAV-2) and AAV-5 is not rate limiting following apical infection of polarized human airway epithelia. J Virol **77:**7361-6.

193. **Yan, Z., R. Zak, Y. Zhang, W. Ding, S. Godwin, K. Munson, R. Peluso, and J. F. Engelhardt.** 2004. Distinct Classes of Proteasome-Modulating Agents Cooperatively Augment Recombinant Adeno-Associated Virus Type 2 and Type 5-Mediated Transduction from the Apical Surfaces of Human Airway Epithelia. Journal of Virology **78:**2863-2874.

194. **Denby, L., S. A. Nicklin, and A. H. Baker.** 2005. Adeno-associated virus (AAV)-7 and -8 poorly transduce vascular endothelial cells and are sensitive to proteasomal degradation. Gene Ther **12:**1534-8.

195. **Grieger, J. C., and R. J. Samulski.** 2005. Packaging capacity of adeno-associated virus serotypes: impact of larger genomes on infectivity and postentry steps. J Virol **79:**9933-44.

196. **Li, W., L. Zhang, Z. Wu, R. J. Pickles, and R. J. Samulski.** 2011. AAV-6 mediated efficient transduction of mouse lower airways. Virology **417:**327-33.

197. **Pajusola, K., M. Gruchala, H. Joch, T. F. Luscher, S. Yla-Herttuala, and H. Bueler.** 2002. Cell-type-specific characteristics modulate the transduction efficiency of adeno-associated virus type 2 and restrain infection of endothelial cells. J Virol **76:**11530-40.

198. **Hacker, U. T., L. Wingenfeld, D. M. Kofler, N. K. Schuhmann, S. Lutz, T. Herold, S. B. King, F. M. Gerner, L. Perabo, J. Rabinowitz, D. M. McCarty, R. J. Samulski, M. Hallek, and H. Buning.** 2005. Adeno-associated virus serotypes 1 to 5 mediated

tumor cell directed gene transfer and improvement of transduction efficiency. J Gene Med **7:**1429-38.

199. **Cheng, B., C. Ling, Y. Dai, Y. Lu, L. G. Glushakova, S. W. Gee, K. E. McGoogan, G. V. Aslanidi, M. Park, P. W. Stacpoole, D. Siemann, C. Liu, and A. Srivastava.** 2012. Development of optimized AAV3 serotype vectors: mechanism of high-efficiency transduction of human liver cancer cells. Gene Ther **19:**375-84.

200. **Zhang, F. L., S. Q. Jia, S. P. Zheng, and W. Ding.** 2011. Celastrol enhances AAV1-mediated gene expression in mice adipose tissues. Gene Ther **18:**128-34.

201. **Zhong, L., W. Zhao, J. Wu, B. Li, S. Zolotukhin, L. Govindasamy, M. Agbandje-McKenna, and A. Srivastava.** 2007. A dual role of EGFR protein tyrosine kinase signaling in ubiquitination of AAV2 capsids and viral second-strand DNA synthesis. Mol Ther **15:**1323-30.

202. **Zhong, L., B. Li, G. Jayandharan, C. S. Mah, L. Govindasamy, M. Agbandje-McKenna, R. W. Herzog, K. A. Weigel-Van Aken, J. A. Hobbs, S. Zolotukhin, N. Muzyczka, and A. Srivastava.** 2008. Tyrosine-phosphorylation of AAV2 vectors and its consequences on viral intracellular trafficking and transgene expression. Virology **381:**194-202.

203. **Arastu-Kapur, S., J. L. Anderl, M. Kraus, F. Parlati, K. D. Shenk, S. J. Lee, T. Muchamuel, M. K. Bennett, C. Driessen, A. J. Ball, and C. J. Kirk.** 2011. Nonproteasomal Targets of the Proteasome Inhibitors Bortezomib and Carfilzomib: a Link to Clinical Adverse Events. Clinical Cancer Research **17:**2734-2743.

204. **Puente, X. S., L. M. Sanchez, C. M. Overall, and C. Lopez-Otin.** 2003. Human and mouse proteases: a comparative genomic approach. Nat Rev Genet **4:**544-558.

205. **Groll, M., K. B. Kim, N. Kairies, R. Huber, and C. M. Crews.** 2000. Crystal structure of epoxomicin:20s proteasome reveals a molecular basis for selectivity of alpha,beta-epoxyketone proteasome inhibitors. J.Am.Chem.Soc. **122:**1237-1238.

206. **Sin, N., K. B. Kim, M. Elofsson, L. Meng, H. Auth, B. H. Kwok, and C. M. Crews.** 1999. Total synthesis of the potent proteasome inhibitor epoxomicin: a useful tool for understanding proteasome biology. Bioorg Med Chem Lett **9:**2283-8.

207. **Demo, S. D., C. J. Kirk, M. A. Aujay, T. J. Buchholz, M. Dajee, M. N. Ho, J. Jiang, G. J. Laidig, E. R. Lewis, F. Parlati, K. D. Shenk, M. S. Smyth, C. M. Sun, M. K. Vallone, T. M. Woo, C. J. Molineaux, and M. K. Bennett.** 2007. Antitumor activity of PR-171, a novel irreversible inhibitor of the proteasome. Cancer Res **67:**6383-91.

208. **Adams, J., V. J. Palombella, E. A. Sausville, J. Johnson, A. Destree, D. D. Lazarus, J. Maas, C. S. Pien, S. Prakash, and P. J. Elliott.** 1999. Proteasome inhibitors: a novel class of potent and effective antitumor agents. Cancer Res **59:**2615-22.

209. **Kuhn, D. J., Q. Chen, P. M. Voorhees, J. S. Strader, K. D. Shenk, C. M. Sun, S. D. Demo, M. K. Bennett, F. W. van Leeuwen, A. A. Chanan-Khan, and R. Z. Orlowski.** 2007. Potent activity of carfilzomib, a novel, irreversible inhibitor of the ubiquitin-proteasome pathway, against preclinical models of multiple myeloma. Blood **110:**3281-90.

210. **Tsubuki, S., Y. Saito, M. Tomioka, H. Ito, and S. Kawashima.** 1996. Differential inhibition of calpain and proteasome activities by peptidyl aldehydes of di-leucine and tri-leucine. J Biochem **119:**572-6.

211. **Anwar, A., D. Siegel, J. K. Kepa, and D. Ross.** 2002. Interaction of the Molecular Chaperone Hsp70 with Human NAD(P)H:Quinone Oxidoreductase 1. Journal of Biological Chemistry **277:**14060-14067.

212. **Akache, B., D. Grimm, X. Shen, S. Fuess, S. R. Yant, D. S. Glazer, J. Park, and M. A. Kay.** 2007. A Two-hybrid Screen Identifies Cathepsins B and L as Uncoating Factors for Adeno-associated Virus 2 and 8. Mol Ther **15:**330-339.

213. **Qiu, M., Y. Chen, L. Cheng, Y. Chu, H.-Y. Song, and Z.-W. Wu.** 2013. Pyrrolidine Dithiocarbamate Inhibits Herpes Simplex Virus 1 and 2 Replication, and Its Activity May Be Mediated through Dysregulation of the Ubiquitin-Proteasome System. Journal of Virology **87:**8675-8686.

214. **Wang, Y., X. L. Li, Y. S. Yu, Z. H. Tang, and G. Q. Zang.** 2013. Inhibition of Hepatitis B Virus Production In Vitro by Proteasome Inhibitor MG132. Hepato-gastroenterology **60:**837-841.

215. **Gentile, M., A. G. Recchia, C. Mazzone, E. Lucia, E. Vigna, and F. Morabito.** 2013. Perspectives in the treatment of multiple myeloma. Expert Opin Biol Ther.

216. **Mitchell, A. M., and R. J. Samulski.** 2013. Mechanistic insights into the enhancement of adeno-associated virus transduction by proteasome inhibitors. J Virol **DOI: 10.1128/JVI.01826-13**.

217. **Van Damme, E., K. Laukens, T. H. Dang, and X. Van Ostade.** 2010. A manually curated network of the PML nuclear body interactome reveals an important role for PML-NBs in SUMOylation dynamics. Int J Biol Sci **6:**51-67.

218. **Hermonat, P. L.** 1994. Down-regulation of the human c-fos and c-myc proto-oncogene promoters by adeno-associated virus Rep78. Cancer Lett **81:**129-36.

219. **Hermonat, P. L., A. D. Santin, and R. B. Batchu.** 1996. The adeno-associated virus Rep78 major regulatory/transformation suppressor protein binds cellular Sp1 in vitro and evidence of a biological effect. Cancer Res **56:**5299-304.

220. **Klein-Bauernschmitt, P., H. zur Hausen, and J. R. Schlehofer.** 1992. Induction of differentiation-associated changes in established human cells by infection with adeno-associated virus type 2. J Virol **66:**4191-200.

221. **Lin, L., T. Ozaki, Y. Takada, H. Kageyama, Y. Nakamura, A. Hata, J. H. Zhang, W. F. Simonds, A. Nakagawara, and H. Koseki.** 2005. topors, a p53 and topoisomerase I-binding RING finger protein, is a coactivator of p53 in growth suppression induced by DNA damage. Oncogene **24:**3385-96.

222. **Prasad, C. K., C. Meyers, D. J. Zhan, H. You, M. Chiriva-Internati, J. L. Mehta, Y. Liu, and P. L. Hermonat.** 2003. The adeno-associated virus major regulatory protein Rep78-c-Jun-DNA motif complex modulates AP-1 activity. Virology **314:**423-31.

223. **Saudan, P., J. Vlach, and P. Beard.** 2000. Inhibition of S-phase progression by adeno-associated virus Rep78 protein is mediated by hypophosphorylated pRb. EMBO J **19:**4351-61.

224. **Weger, S., E. Hammer, and R. Heilbronn.** 2004. SUMO-1 modification regulates the protein stability of the large regulatory protein Rep78 of adeno associated virus type 2 (AAV-2). Virology **330:**284-94.

225. **Zhou, C., Q. Yang, and J. P. Trempe.** 1999. Enhancement of UV-induced cytotoxicity by the adeno-associated virus replication proteins. Biochim Biophys Acta **1444:**371-83.

226. **Weger, S., E. Hammer, and R. Heilbronn.** 2002. Topors, a p53 and topoisomerase I binding protein, interacts with the adeno-associated virus (AAV-2) Rep78/68 proteins and enhances AAV-2 gene expression. J Gen Virol **83:**511-6.

227. **Cataldi, M. P., and D. M. McCarty.** 2010. Differential effects of DNA double-strand break repair pathways on single-strand and self-complementary adeno-associated virus vector genomes. J Virol **84:**8673-82.

228. **Schwartz, R. A., C. T. Carson, C. Schuberth, and M. D. Weitzman.** 2009. Adeno-associated virus replication induces a DNA damage response coordinated by DNA-dependent protein kinase. J Virol **83:**6269-78.

229. **Schwartz, R. A., J. A. Palacios, G. D. Cassell, S. Adam, M. Giacca, and M. D. Weitzman.** 2007. The Mre11/Rad50/Nbs1 complex limits adeno-associated virus transduction and replication. J Virol **81:**12936-45.

230. **Choi, V. W., D. M. McCarty, and R. J. Samulski.** 2006. Host cell DNA repair pathways in adeno-associated viral genome processing. J Virol **80:**10346-56.

231. **Sanlioglu, S., P. Benson, and J. F. Engelhardt.** 2000. Loss of ATM function enhances recombinant adeno-associated virus transduction and integration through pathways similar to UV irradiation. Virology **268:**68-78.

232. **Hirosue, S., K. Senn, N. Clement, M. Nonnenmacher, L. Gigout, R. M. Linden, and T. Weber.** 2007. Effect of inhibition of dynein function and microtubule-altering drugs on AAV2 transduction. Virology **367:**10-8.

233. **Vasileva, A., R. M. Linden, and R. Jessberger.** 2006. Homologous recombination is required for AAV-mediated gene targeting. Nucleic Acids Res **34:**3345-60.

234. **Wallen, A. J., G. A. Barker, D. E. Fein, H. Jing, and S. L. Diamond.** 2011. Enhancers of adeno-associated virus AAV2 transduction via high throughput siRNA screening. Mol Ther **19:**1152-60.